



Theses and Dissertations

2019-08-01

Mechanoreceptor Activation in the Treatment of Drug-Use Disorders: Mechanism and Outcome

Kyle Bills
Brigham Young University

Follow this and additional works at: <https://scholarsarchive.byu.edu/etd>

BYU ScholarsArchive Citation

Bills, Kyle, "Mechanoreceptor Activation in the Treatment of Drug-Use Disorders: Mechanism and Outcome" (2019). *Theses and Dissertations*. 8627.
<https://scholarsarchive.byu.edu/etd/8627>

This Dissertation is brought to you for free and open access by BYU ScholarsArchive. It has been accepted for inclusion in Theses and Dissertations by an authorized administrator of BYU ScholarsArchive. For more information, please contact ellen_amatangelo@byu.edu.

Mechanoreceptor Activation in the Treatment of Drug-Use Disorders:
Mechanism and Outcome

Kyle Bills

A dissertation submitted to the faculty of
Brigham Young University
in partial fulfillment of the requirements for the degree of

Doctor of Philosophy

Scott C. Steffensen, Chair
Ulrike Hildegard Mitchell
Sterling N. Sudweeks
David Morley Thomson
Jonathan Jayme Wisco

Neuroscience Center
Brigham Young University

Copyright © 2019 Kyle Bills

All Rights Reserved

ABSTRACT

Mechanoreceptor Activation in the Treatment of Drug-Use Disorders: Mechanism and Outcome

Kyle Bills
Neuroscience Center, BYU
Doctor of Philosophy

The therapeutic benefits attributed to activation of peripheral mechanoreceptors are poorly understood. There is growing evidence that mechanical stimulation modulates substrates in the supraspinal central nervous system (CNS) that are outside the canonical somatosensory circuits. This work demonstrates that activation of peripheral mechanoreceptors via mechanical stimulation (MStim) is sufficient to increase dopamine release in the nucleus accumbens (NAc), alter neuron firing rate in the ventral tegmental area (VTA) and increase membrane translocation of delta opioid receptors (DORs) in the NAc. Further, we demonstrate that these effects are dependent on DORs and acetylcholine receptors. Additionally, MStim can block neuronal markers of chronic ethanol dependence including ethanol-induced changes to VTA GABA neuron firing during withdrawal, and DA release profiles after reinstatement ethanol during withdrawal. These are presented in tandem with evidence that MStim also ameliorates behavioral indices of ethanol withdrawal. Finally, exercise, a modality that includes a mechanosensory component, is shown to alter expression of kappa opioid receptors (KORs) in the NAc. This change substantively depresses KORs influence over evoked DA release in direct contravention to the effects of chronic ethanol. These changes translate into reduced drinking behavior.

Keywords: mechanoreceptors, dopamine, GABA, nucleus accumbens, ventral tegmental area, delta-opioid receptors, kappa-opioid receptors, exercise, alcohol, cholinergic interneurons, whole-body vibration

ACKNOWLEDGEMENTS

Thanks are owed first and foremost to God for the allowance of life, liberty and means to pursue greater understanding and outcome for those trapped in the grips of addiction. I am ever grateful for my wife Stephanie who, for reasons known only to her, has always shown great confidence in my ability to discharge the duties at hand. She is selfless, loving, thoughtful, beautiful and a myriad of other superlative things that cannot be listed in a reasonable volume. I owe much to my parents and sisters who cared for business interests during this educational sabbatical. I am thankful for the guidance and mentoring I received from Scott Steffensen, upon whom my training and support rested. Without his generosity and willingness to take risks on unproven theories, I would not have been able to perform these experiments. I could not have imagined a better man to work for. I offer my thanks to Jordan Yorgason, who was critical in my learning to perform experiments and reason as a scientist should. I am additionally grateful to Andrew Payne and Daniel O Bray and James Brundage, wonderful colleagues who are kind, patient and wonderful examples of what I want to be. Finally, to countless undergraduate students without whom our laboratory would come to a halt.

TABLE OF CONTENTS

ABSTRACT.....	ii
ACKNOWLEDGEMENTS	iii
LIST OF FIGURES	xii
CHAPTER 1: Introduction	1
Scope of the Problem.....	1
Mesolimbic Dopamine System and Dependence	1
Dopamine Receptors.....	3
Opioid Receptors	5
Kappa Opioid Receptors.....	5
Mu (MOR) and Delta (DOR) Opioid Receptors	6
Mechanoreceptors as possible therapeutic targets for drug-use disorders.....	7
Scope of the Work Performed in This Dissertation.....	8
References	11
CHAPTER 2: Targeted Subcutaneous Vibration with Single-Neuron Electrophysiology as a Novel Method for Understanding the Central Effects of Peripheral Vibrational Therapy in a Rodent Model.....	21
Abstract	22
Introduction	23
Materials and Methods	26

Vibrational Motors	26
Surgical Procedure and In Vivo Single Cell Electrophysiology.....	27
Characterization of VTA GABA Neurons in vivo and Recordings	28
Grass Stimulator and Vibration Stimulation.....	29
Micro Controller Driver.....	29
Statistical Analysis	30
Results	31
Discussion	33
Future Direction.....	34
Declaration of Conflicting Interests	35
Funding.....	35
References	36
Figure Legends.....	39
Figure 2.1: Vibrational motor.....	39
Figure 2.2: Motor displacement and acceleration by frequency.....	39
Figure 2.3: Circuit for micro controller driving motor.....	39
Figure 2.4: Effects of variable frequency and locale subcutaneous vibrational stimulus on GABA neuron firing rate in the VTA.....	39
Figure 2.5 Group data showing average GABA neuron firing rate depression from baseline and maximum depression	39

CHAPTER 3: Mechanical stimulation of cervical vertebrae modulates the discharge activity of ventral tegmental area neurons and dopamine release in the nucleus accumbens	40
Abstract	41
Significance Statement.....	42
Introduction	43
Materials and Methods	45
Vibrational Motors	45
Animals and MStim Motor Implantation	45
Single Cell Electrophysiology	45
Characterization of VTA GABA and DA Neurons In vivo.....	46
Grass Stimulator and MStim for In-vivo Recordings.....	46
Fast-Scan Cyclic Voltammetry.....	47
Microdialysis and High Performance Liquid Chromatography	47
Preparation of Brain Slices for Imaging and Confocal Microscopy.....	48
Data Collection and Statistical Analysis.....	49
Results	51
MStim Modulation of VTA Neurons	51
MStim Modulation of VTA Neurons: Role of NAc Projections and Endogenous Opioids..	52
MStim Enhancement of Dopamine Release: Role of Endogenous Opioids.....	53
MStim Activation of NAc Neurons	54

Discussion	55
References	59
Figure Legends	63
Figure 3.1 – Frequency and duration-dependent effects of MStim on VTA GABA neuron firing rate	63
Figure 3.2 – Spatiotemporal variation in MStim-induced effects on VTA GABA neuron firing rate	63
Figure 3.3 – Dopamine neuron response to MStim	63
Figure 3.4 – Role of NAc inputs to the VTA and endogenous opioids in MStim-induced inhibition of VTA GABA neuron firing rate	64
Figure 3.5 – MStim effects on basal and evoked DA release in the NAc.	64
Figure 3.6 – Role of DORs and CINs in MStim-induced enhancement of DA release in the NAc.....	64
Figure 3.7 – MStim activates neurons and induces translocation of DORs in the NAc.....	64
Figures	66
Figure 3.1	66
Figure 3.2.....	67
Figure 3.3.....	68
Figure 3.4.....	69
Figure 3.5.....	70
Figure 3.6.....	71

Figure 3.7.....	72
CHAPTER 4: Mechanical stimulation alters chronic ethanol-induced changes to VTA GABA	
neurons, NAc DA release and measures of withdrawal.....	73
Abstract	74
Introduction	75
Materials and Methods	77
Animals and MStim Motor Implantation	77
Single Cell Electrophysiology	78
Characterization of VTA GABA.....	79
Grass Stimulator and MStim for in-vivo Recordings	79
Microdialysis and High Performance Liquid Chromatography	79
Behavioral Measures of Withdrawal	80
Data Collection and Statistical Analysis.....	81
Results	82
Amelioration of chronic ethanol-induced changes to VTA GABA neurons by MStim.....	82
MStim effects on chronic ethanol-induced changes to NAc DA release	82
MStim blocks withdrawal symptoms in rats exposed to chronic EtOH.....	84
Discussion	85
References	88
Figure Legends.....	91

Figure 4.1 – Effects of MStim on VTA GABA neuron firing rate after reinstatement ethanol during withdrawal.....	91
Figure 4.2 – Basal dopamine release in the NAc following EtOH injection (2.5g/kg IP)	91
Figure 4.3 – Blocking of EtOH-induced behavioral measures of withdrawal by MStim	91
Figures.....	91
Figure 4.1	92
Figure 4.2.....	93
Figure 4.3.....	94
CHAPTER 5: Exercise Blocks Ethanol-Induced sensitization of Kappa Opioid Receptors	95
Abstract	96
Introduction.....	97
Kappa Opioid Receptors.....	97
Exercise and the Mesolimbic Dopamine System	97
Material and Methods.....	98
Animals.....	98
Brain Slice Preparation.....	99
Fast Scan Cyclic Voltammetry	99
Preparation of Brain Slices for Imaging and Confocal Microscopy.....	100
Statistical Analysis	101
Results	102

KOR effects on Dopamine Release in the Context of Exercise and Ethanol	102
Immunohistochemical Analysis of KORs in the NAc and VTA.....	102
Effects of Exercise and Ethanol on Drink-in-the-Dark Behavior.....	103
Discussion	104
Figure Legends.....	108
Figure 5.1: Exercise blocks ethanol-induced sensitivity of KORs in the NAc.....	108
Figure 5.2: Exercise alters ethanol-induced KOR expression in the NAc and VTA.....	108
Figure 5.3: Exercise decreases drinking in dependent but not naïve mice	108
Figures.....	109
Figure 5.1.....	109
Figure 5.2.....	110
Figure 5.3.....	111
CHAPTER 6: Discussion and Conclusions	112
Somatosensory Pathways Involved in Acupuncture-mediated Alterations to Mesolimbic Structures	112
Mechanoreceptor Activation as the Primary Driver of Mesolimbic Alterations without Mechanoacupuncture.....	113
Specificity of Effects relate to Mechanoreceptor Density and Type	113
MStim Effects on NAc DA Levels are Locally Mediated by DORs and Acetylcholine Release.....	114
A Working Model of MStim Effects in the Mesolimbic Circuitry.....	116

MStim Blockage of Markers of Chronic Ethanol Dependence	117
Exercise and Ethanol Dependence	118
Conclusions and Future Directions.....	119
References	120
Curriculum Vitae.....	123

LIST OF FIGURES

Figure 1.1: Simplified Diagram of the Mesolimbic Circuitry.....	2
Figure 1.2: Description of D2 Receptors Mechanism of Auto-Inhibition of DA Release.....	4
Figure 1.3: Location of Mesolimbic Opioid Receptors	6
Figure 2.1: Vibrational Motor.....	26
Figure 2.2: Motor Displacement and Acceleration by Frequency	27
Figure 2.3: Circuit for Microcontroller	30
Figure 2.4: Effects of Variable Frequency and Local Subcutaneous Vibrational Stimulus on GABA Neuron Firing Rate in the VTA	31
Figure 2.5: Group Data Showing Average and Maximal GABA Neuron Firing Rate Depression from Baseline	32
Figure 3.1: Frequency and Duration-Dependent Effects of MStim on VTA GABA Neurons Firing Rate	66
Figure 3.2: Spatiotemporal Variation in MStim-Induced Effects on VTA GABA Neuron Firing Rate	67
Figure 3.3: Dopamine Neuron Response to MStim.....	68
Figure 3.4: Role of NAc Inputs to the VTA and Endogenous Opioids in MStim-Induced Inhibition of VTA GABA Neuron Firing Rate.....	69
Figure 3.5: MStim Effects on Basal and Evoked DA Release in the NAc	70

Figure 3.6: Role of DORs and CINs in MStim-Induced Enhancement of DA Release in the NAc	71
Figure 3.7: MStim Activates Neurons and Induces Translocation of DORs in the NAc	72
Figure 4.1: Effects of MStim on VTA GABA Neuron Firing Rate after Reinstatement Ethanol During Withdrawal	92
Figure 4.2: Basal Dopamine Release in the NAc Following EtOH Injection (2.5g/kg IP)	93
Figure 4.3: Blocking of EtOH-Induced Behavioral Measures of Withdrawal by MStim	94
Figure 5.1: Exercise Blocks Ethanol-Induced Sensitivity of KORs in the NAc.....	109
Figure 5.2: Exercise Alters Ethanol-Induced KOR Expression in the NAc and VTA	110
Figure 5.3: Exercise Decreases Drinking in Dependent but not Naïve Mice	111
Figure 6.1: A Working Model Explaining MStim Effects on the Mesolimbic Circuitry	116

CHAPTER 1: Introduction

Scope of the Problem

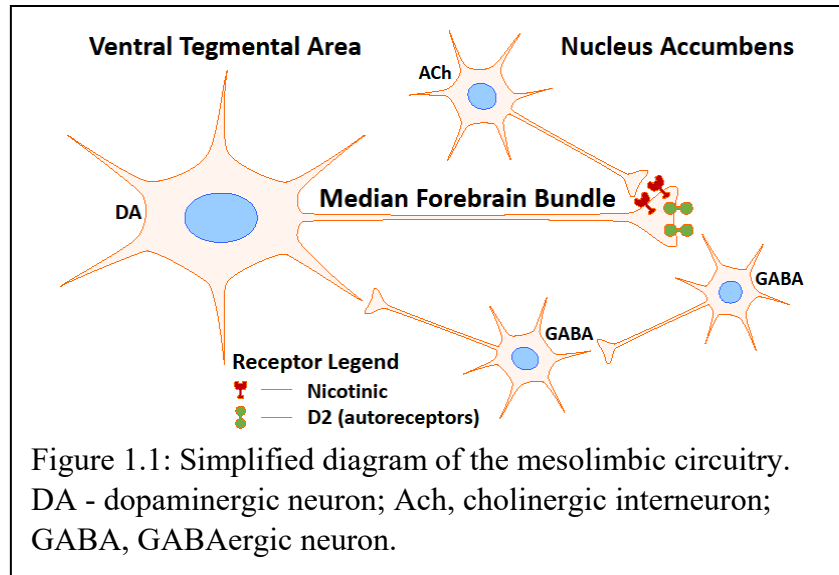
Alcohol addiction is a chronic relapsing disease that affects more Americans than all forms of cancer combined (SAMHSA, 2016). It leads to destructive psychological, physical, social, and economic consequences. It is estimated that over 28 million Americans are currently in need of treatment for alcohol abuse, resulting in over \$249 billion in direct costs (Sacks, Gonzales, Bouchery, Tomedi, & Brewer, 2015). Making matters worse, only 13% of those needing intervention actually receive it. Further, in spite of the wonderful advances in our understanding of the neuropathophysiology of addiction, the success rate of treatment has not substantively changed over the last hundred years, with around 50% of those treated relapsing (Moos & Moos, 2006; SAMHSA, 2016; White, 2012) within a year. This represents approximately 6% of those suffering from the disease receiving effective treatment. A report ranking the different conditions relative to the “global burden of disease” found that alcohol ranked 3rd out of the 25 major contributors (Lim et al., 2012). Developing new treatments looms seismically as a determinant quest for addiction researchers until, at the least, outcomes are markedly improved.

Mesolimbic Dopamine System and Dependence

The primary form of alcohol abused by humans is ethanol. It is clear that ethanol’s rewarding and addictive properties are mediated, in large part, by dopamine (DA)

neurotransmission in the mesolimbic system.

Projections originate in the ventral tegmental area (VTA) of the midbrain and travel to the nucleus accumbens (NAc) in the ventral striatum (**Fig. 1.1**).

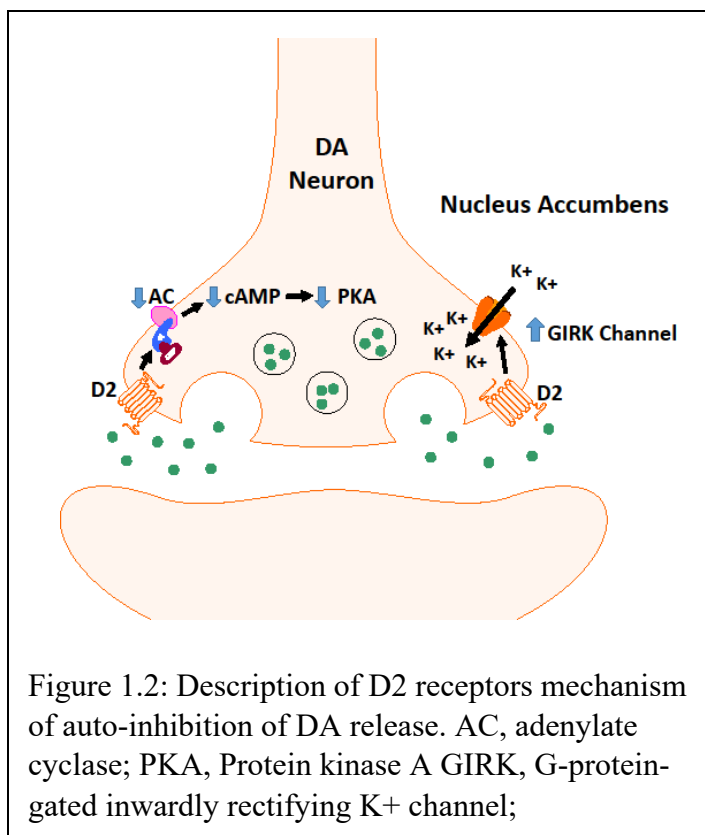


Dopamine release in the NAc represents a scalar index of reward (Wise, 2008), with increased levels associated with increased reward. Levels of DA increase with acute consumption of drugs of abuse, providing a reinforcing stimulus for further use (Carboni, Imperato, Perezzani, & Di Chiara, 1989; Yoshimoto, McBride, Lumeng, & Li, 1992). During the withdrawal state, neuroplastic alterations occur in the mesolimbic DA circuit leading to hypofunction (Karkhanis, Huggins, Rose, & Jones, 2016; Koeltzow & White, 2003; Maisonneuve, Ho, & Kreek, 1995; Rose et al., 2016). This reduction in DA is theorized to be the primary driver of relapse as blocking or ablating this pathway leads to dramatic decreases in drug self-administration (Lyness & Smith, 1992). Although the prevailing dogma is that DA neurons projecting from the VTA to the NAc mediate the rewarding and addictive properties of drugs of abuse (Wise, 2008), GABA neurons in the VTA have garnered much interest of late for their role in modulating DA release and as independent substrates mediating drug reward. Acute administration of cocaine, ethanol and methamphetamine have been shown to cause inhibition of VTA GABA neurons (Gallegos, Criado, Lee, Henriksen, & Steffensen, 1999; Ludlow et al., 2009; Steffensen et al., 2008;

Steffensen et al., 2009; Stobbs et al., 2004), producing a net disinhibition of VTA DA neurons (Bocklisch et al., 2013; Carboni et al., 1989; Yoshimoto et al., 1992). In contrast, in a state of withdrawal, VTA GABA neurons undergo plasticity and become hyperactive (Bonci & Williams, 1997; Gallegos et al., 1999; Hopf et al., 2007) leading to decreased mesolimbic DA release in the NAc (Karkhanis et al., 2016; Koeltzow & White, 2003; Maisonneuve et al., 1995; Rose et al., 2016). Understanding ethanol's effects on the mesolimbic system is a singular challenge. This difficulty stems, in part, from the fact that there is no known ethanol receptor, rather a myriad of interactions between cell subtypes that change from acute to chronic exposure and again in the withdrawal state.

Dopamine Receptors

Two distinct sub classifications of DA receptors are commonly described. These are the D1 and D2 classes. Though the two families share a high degree of homology in their respective transmembrane domains, pharmacologically, they are distinct. D1 family receptors, including D1 and D5, are thought to be found on both pre- and postsynaptic membranes. In the ventral striatum they can be found on GABA-ergic medium spiny neurons (Beaulieu & Gainetdinov, 2011). These receptors are coupled to $G_{\alpha s}$ G-proteins which ultimately increase the likelihood of postsynaptic depolarization (Rankin & Sibley, 2010). The D2-like family of DA receptors include D2, D3, and D4 receptor subtypes. The D2 subtype can be broken down further into two



distinct isoforms, the long form (D2Lh) and the short form (D2Sh). There is currently much debate regarding their relative locations and contributions. It has been reported that the D2Sh subtype are predominately presynaptic, though this matter is not settled (Usiello et al., 2000). D2 receptors, broadly, are coupled to G_{αi} G-proteins. They cause a decrease in cAMP levels and subsequent reduction in DA release (**Fig. 1.2**). D2 receptors produce an auto-inhibitory

feedback mechanism that is particularly important when studying ethanol, which acutely increases DA levels and D2 receptor activity, and chronically, decreases DA levels and D2 activity. Dopamine 2 receptors are reportedly in flux as the mesolimbic system progresses from acute ethanol exposure to a state of dependence. It is reported that ethanol preferring rats demonstrate a reduction in D2 receptor density (McBride, Chernet, Dyr, Lumeng, & Li, 1993; Stefanini et al., 1992; Strother, Lumeng, Li, & McBride, 2003). Further, ethanol preferring rats show a reduction in D2 receptor efficacy (Hietala et al., 1994). These receptors are expressed on cell bodies, dendrites and axons of cholinergic interneurons (CINs) in the NAc (Alcantara, Chen, Herring, Mendenhall, & Berlanga, 2003). Accumbal CINs activate nicotinic acetylcholine (ACh) receptors on DA terminals and increase DA neurotransmission (Yorgason, Zeppenfeld, & Williams, 2017).

Opioid Receptors

There are three well described classical opioid receptor (OR) types, kappa (KOR), mu (MOR), and delta (DOR). Others types have been described and debated (ORL1, sigma, epsilon, orphinan, etc...). We will focus on the three classical opioid receptors with implications to the mesolimbic DA system. These receptors are coupled to Gi-proteins and produce inhibition through several means, including inhibition of adenylate cyclase, reduction of calcium currents, and activation of inwardly rectifying potassium channels (Attali, Saya, & Vogel, 1989; Henry, Grandy, Lester, Davidson, & Chavkin, 1995; Konkoy & Childers, 1989; Prather et al., 1995; Tallent, Dichter, Bell, & Reisine, 1994). They also activate a number of kinase cascades such as the mitogen-activated protein kinase cascade (Fukuda, Kato, Morikawa, Shoda, & Mori, 1996). Many ligands activate these receptors with most cross-activating between the three; though they exhibit differing preferences. The main endogenous ligands involved in their activation are of three classes, dynorphins, which are derived from the precursor protein pro-dynorphin and are preferential for KORs (Aldrich & McLaughlin, 2009); enkephalins, which are derived from pro-opiomelanocortin and are preferential to MORs and DORs; and endorphins, which are also derived from pro-opiomelanocortin and have a preference for MORs. These receptors are similar in structure and have some overlap in ligand binding. Though activation of all receptor types is associated with analgesia, MORs and DORs produce euphoria and increased risk for dependence while KORs, conversely, when activated elicit dysphoria.

Kappa Opioid Receptors

KORs are expressed extensively in the NAc, both in the core and the shell (Mansour, Burke, Pavlic, Akil, & Watson, 1996; Mansour, Khachaturian, Lewis, Akil, & Watson, 1987; Spanagel, Herz, & Shippenberg, 1992), where their activation inhibits DA release (Spanagel et al., 1992). Data suggests that they are synthesized in the cell bodies of DA neurons in the VTA

where they are expressed and also subsequently transported to terminals in the NAc where they are integrated into the presynaptic membrane (**Fig. 1.3**) (Mansour, Fox, Akil, & Watson, 1995). Activation of KORs is associated with dysphoria (Shippenberg, Zapata, & Chefer, 2007). Evidence suggests that there is an upregulation of KORs in alcohol-dependent animals that may play a role in the increased seeking behavior seen with dependence (Sirohi, Bakalkin, & Walker, 2012). This is demonstrated by a decrease in dependent-state seeking behavior when the KOR antagonist nor-BNI is administered while having no effect on non-dependent animals (Walker & Koob, 2008). Further chronic intermittent ethanol exposure has been shown to increase the effect of KORs in the NAc. These data suggest a role for KORs in the synaptic adaptations that accrue to alcohol dependence (Shippenberg et al., 2007).

Mu (MOR) and Delta (DOR) Opioid Receptors

In contrast to KORs, MORs and DORs are associated with euphoria, imparting to agonists of these receptors a high potential for abuse (Devine & Wise, 1994). Activation facilitates DA release in the NAc by two mechanisms. First, MORs and DORs act on local GABA interneurons in the NAc increasing DA release, presumably, through disinhibition of DA terminals, cholinergic interneurons, and glutamatergic projections to the NAc

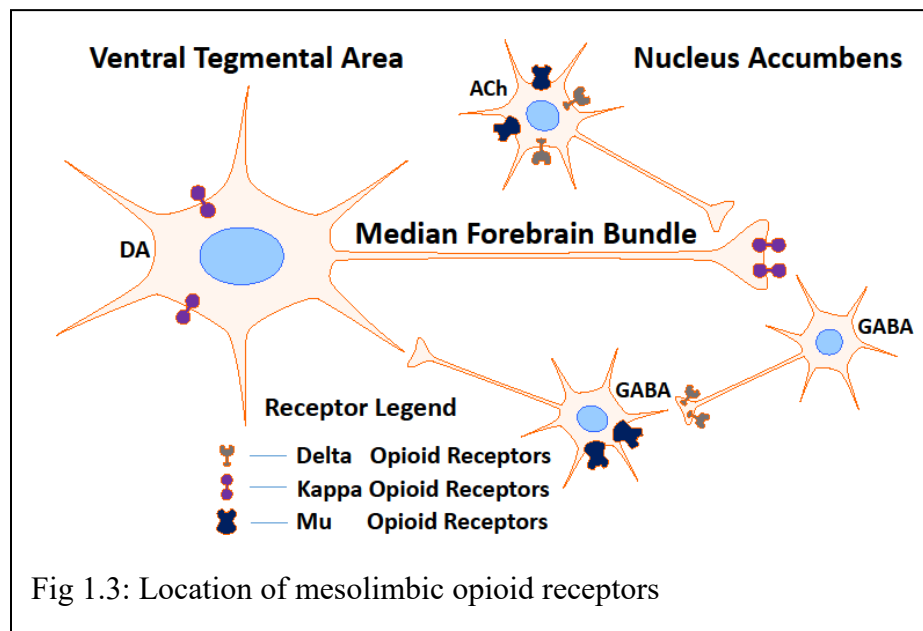


(Fig. 1.3)(Hirose et al., 2005; Murakawa et al., 2004; Okutsu et al., 2006; Yoshida et al., 1999).

Second, MORs on GABA interneurons in the VTA disinhibit DA projections to the NAc (Bonci & Williams, 1997; Johnson & North, 1992; Steffensen et al., 2006). Though some aspects of MOR and DOR activity is similar, there are profound differences in their respective contributions to ethanol dependence. Non-selective MOR and DOR antagonists have been shown to decrease ethanol's enhancement of DA release in the NAc in rats (Acquas, Meloni, & Di Chiara, 1993; Benjamin, Grant, & Pohorecky, 1993; Lee et al., 2005). Interestingly, while mice that lack MORs, or have them selectively blocked, appear immune to the reinforcing effects of ethanol (Job et al., 2007; Roberts et al., 2000), those that lack DORs demonstrate an increase in ethanol seeking behavior (Roberts et al., 2001).

Recently, evidence has emerged implicating DORs in the mesolimbic effects of a targeted mechano-acupuncture treatment when given at the HT7 acupoint, located medial to the flexor carpi ulnaris tendon at the wrist. This mechanically-based treatment activates peripheral mechanoreceptors and excites the traditional somatosensory pathway from spine to nucleus cuneatus to thalamus (Chang et al., 2017). Interestingly, it has been shown to influence VTA GABA neurons, producing a transient inhibition in their firing and reducing ethanol-seeking behavior in rodents (Chang et al., 2017; Yang et al., 2010).

Mechanoreceptors as possible therapeutic targets for drug-use disorders

Previously, low and medium (2-100 Hz) frequency electroacupuncture, which activates peripheral mechanoreceptors, has been shown to activate enkephalinergic and beta-endorphinergic neurons in the arcuate nucleus (Wang, Mao, & Han, 1990a, 1990b), which in turn inhibit GABA neurons, likely, via activation of mu- and delta-opioid receptors (MORs and DORs) (Mansour, Khachaturian, Lewis, Akil, & Watson, 1988; Yang et al., 2010). Further

acupuncture modulates VTA GABA neurons via somatosensory pathways and reduces ethanol and cocaine psychomotor effects and drug-seeking behavior (Chang et al., 2017; Jin et al., 2017; Kim et al., 2013; Yang et al., 2010; Yoon et al., 2012). Stimulation at HT7 (Shenmen acupoint) activates the dorsal column medial lemniscal (DCML) pathway, synapses in the nucleus cuneatus (CN) and subsequently relays through the thalamus and lateral habenula before finally modulating the excitability of VTA GABA neurons (Chang et al., 2017), presumably through DORs that are expressed on GABA neurons in the NAc core greater than the shell (Hipolito, Sanchez-Catalan, Zanolini, Polache, & Granero, 2008). We hypothesize that activation begins with peripheral mechanoreceptors, such as Meissner's, Pacinian corpuscles, and Merkel cells and ends with DORs in the NAc. It is generally accepted that these receptors possess "optimal" frequency ranges in which they are most active. Merkel cells become more responsive with increased frequency and amplitude of stimulation in a near linear relationship from approximately 1-100 Hz and 1-1500 μ m respectively (Rowe, Tracey, Mahns, Sahai, & Ivanusic, 2005). Meissner's corpuscles are considered to become optimally activated at frequencies around 50 Hz (Macefield, 2005), while Pacinian corpuscles optimally respond to higher frequencies beginning as low as 100 Hz, but optimally in the range of 200-400 Hz (Biswas, Manivannan, & Srinivasan, 2015). The clarification of the neurological pathway underlying HT7's mesolimbic effects suggests that activation of the pathway generally will be sufficient to produce the same effect.

Scope of the Work Performed in This Dissertation

To this point, several important factors underlying the use of mechanoreceptor stimulation in the treatment of drug abuse remain to be elucidated, including, determining whether mechanoreceptor activation alone is sufficient to alter mesolimbic function, critical

neuronal substrates activated, regional specificity of receptor activation, optimal vibrational frequency of mechanical stimulus, optimal duration of treatment and behavioral efficacy of the treatments in question. To this end, we originally proposed 2 specific aims to address these questions.

Aim 1: To define the mechanism underlying the effects upon VTA GABA, DA neurons and NAc DA release elicited by subcutaneous vibration at the C7-T1 laminae and HT7. The previously published literature combined with our preliminary data suggest that stimulation of the DCML neurological pathway will be sufficient to produce changes in the mesolimbic system. This aim sets out to show these effects, define the DCML and opioid receptors as mechanistically involved and describe the optimal vibrational frequency and duration for maximal effect. **The hypothesis** is that subcutaneous vibration will: 1) Produce a transient increase followed by a longer decrease in VTA GABA neuron firing rate and that vibration at HT7 and the C7-T1 laminae will produce the same changes; 2) Cause an increase in VTA DA neuron firing rate; 3) Increase evoked DA release in the NAc; 5) Exhibit a dose dependent response; and 6) Be reversed by ablation of the DCML or administration of naltrindole. These hypotheses will be tested with in vivo electrophysiology, and in situ NAc fast-scan cyclic voltammetry to evaluate phasic and spontaneous DA release, respectively.

Aim 2: Evaluate the effects of subcutaneous vibration as an attenuator of cocaine psychomotor-activating effects, self-administration and ultrasonic vocalizations.

Acute cocaine exposure has been shown to increase 50 KHz ultrasonic vocalizations and locomotor activity in rats. HT7 acupuncture has been shown to effectively decrease these psychomotor activities as well as self-administration. **The hypothesis** is that subcutaneous vibration or optogenetic stimulation will: 1) Decrease 50 KHz ultrasonic vocalizations and

locomotor activity in rats after acute cocaine exposure; 2) Decrease cocaine self-administration; and 3) Reduce the effects of acute cocaine exposure on VTA GABA and DA neurons and DA release in the NAc via their activation of DCML neurological pathway. These hypotheses will be tested with behavioral assays, in vivo electrophysiology, and voltammetry.

Originally, the aims were narrowly focused on acupuncture as a modality. As our understanding increased, so did our scope, with expansion to mechanical stimulation of the cervical vertebrae at the C7-T1 level (MStim). After completing the studies outlined in Aim 1, it became clear that the effects elicited by MStim were robust and carried translational potential as a treatment for drug-use disorders. Our aims changed to accommodate a more complete understanding of the mechanistic nature of MStim-induced effects on the mesolimbic circuitry. In addition to the studies proposed we evaluated DA release in the NAc via microdialysis and pharmacologically studied the importance of DORs both systemically and locally in the VTA and NAc. Further, we looked at the importance of acetylcholine release in the NAc as a mediator of terminal DA release and the preeminence of the NAc as the mesolimbic entry point of MStim and the driver of VTA changes. Through immunohistological (IHC) methods, we examined the expression patterns of DORs in the VTA and NAc in response to MStim. These findings are described in **Chapter 3**. Aim 2 was changed substantively as well. Again, because of the translational potential of this treatment, we felt it more relevant to examine its effects on the withdrawal state rather than the acutely intoxicated state. Therefore, we studied MStim effects on chronic ethanol withdrawal. We examined VTA GABA neurons and DA release patterns in the NAc. We also measured behavioral metrics of withdrawal (**Chapter 4**). Finally, because of the broadened impact of MStim as opposed to acupuncture alone. We performed a study to investigate exercise induced alterations to chronic ethanol exposure. We examined these effects in the context of

KORs using fast-scan cyclic voltammetry and IHC staining. We also measured ethanol drinking behavior via a drink-in-the-dark paradigm (**Chapter 5**).

References

- Acquas, E., Meloni, M., & Di Chiara, G. (1993). Blockade of delta-opioid receptors in the nucleus accumbens prevents ethanol-induced stimulation of dopamine release. *Eur J Pharmacol*, 230(2), 239-241.
- Alcantara, A. A., Chen, V., Herring, B. E., Mendenhall, J. M., & Berlanga, M. L. (2003). Localization of dopamine D2 receptors on cholinergic interneurons of the dorsal striatum and nucleus accumbens of the rat. *Brain Res*, 986(1-2), 22-29. doi:10.1016/s0006-8993(03)03165-2
- Aldrich, J. V., & McLaughlin, J. P. (2009). Peptide kappa opioid receptor ligands: potential for drug development. *AAPS J*, 11(2), 312-322. doi:10.1208/s12248-009-9105-4
- Attali, B., Saya, D., & Vogel, Z. (1989). Kappa-opiate agonists inhibit adenylate cyclase and produce heterologous desensitization in rat spinal cord. *J Neurochem*, 52(2), 360-369.
- Beaulieu, J. M., & Gainetdinov, R. R. (2011). The physiology, signaling, and pharmacology of dopamine receptors. *Pharmacol Rev*, 63(1), 182-217. doi:10.1124/pr.110.002642
- Benjamin, D., Grant, E. R., & Pohorecky, L. A. (1993). Naltrexone reverses ethanol-induced dopamine release in the nucleus accumbens in awake, freely moving rats. *Brain Res*, 621(1), 137-140.
- Biswas, A., Manivannan, M., & Srinivasan, M. A. (2015). Vibrotactile sensitivity threshold: nonlinear stochastic mechanotransduction model of the Pacinian Corpuscle. *IEEE Trans Haptics*, 8(1), 102-113. doi:10.1109/TOH.2014.2369422

- Bocklisch, C., Pascoli, V., Wong, J. C., House, D. R., Yvon, C., de Roo, M., Luscher, C. (2013). Cocaine disinhibits dopamine neurons by potentiation of GABA transmission in the ventral tegmental area. *Science*, 341(6153), 1521-1525. doi:10.1126/science.1237059
- Bonci, A., & Williams, J. T. (1997). Increased probability of GABA release during withdrawal from morphine. *J Neurosci*, 17(2), 796-803.
- Carboni, E., Imperato, A., Perezzi, L., & Di Chiara, G. (1989). Amphetamine, cocaine, phencyclidine and nomifensine increase extracellular dopamine concentrations preferentially in the nucleus accumbens of freely moving rats. *Neuroscience*, 28(3), 653-661.
- Chang, S., Ryu, Y., Gwak, Y. S., Kim, N. J., Kim, J. M., Lee, J. Y., . . . Kim, H. Y. (2017). Spinal pathways involved in somatosensory inhibition of the psychomotor actions of cocaine. *Sci Rep*, 7(1), 5359. doi:10.1038/s41598-017-05681-7
- Devine, D. P., & Wise, R. A. (1994). Self-administration of morphine, DAMGO, and DPDPE into the ventral tegmental area of rats. *J Neurosci*, 14(4), 1978-1984.
- Fukuda, K., Kato, S., Morikawa, H., Shoda, T., & Mori, K. (1996). Functional coupling of the delta-, mu-, and kappa-opioid receptors to mitogen-activated protein kinase and arachidonate release in Chinese hamster ovary cells. *J Neurochem*, 67(3), 1309-1316.
- Gallegos, R. A., Criado, J. R., Lee, R. S., Henriksen, S. J., & Steffensen, S. C. (1999). Adaptive responses of GABAergic neurons in the ventral tegmental area to chronic ethanol. *J. Pharmacol. Exp. Ther.*, 291, 1045-1053.

- Henry, D. J., Grandy, D. K., Lester, H. A., Davidson, N., & Chavkin, C. (1995). Kappa-opioid receptors couple to inwardly rectifying potassium channels when coexpressed by *Xenopus* oocytes. *Mol Pharmacol*, 47(3), 551-557.
- Hietala, J., West, C., Syvalahti, E., Nagren, K., Lehtikainen, P., Sonninen, P., & Ruotsalainen, U. (1994). Striatal D2 dopamine receptor binding characteristics in vivo in patients with alcohol dependence. *Psychopharmacology (Berl)*, 116(3), 285-290.
- Hipolito, L., Sanchez-Catalan, M. J., Zanolini, I., Polache, A., & Granero, L. (2008). Shell/core differences in mu- and delta-opioid receptor modulation of dopamine efflux in nucleus accumbens. *Neuropharmacology*, 55(2), 183-189. doi:10.1016/j.neuropharm.2008.05.012
- Hirose, N., Murakawa, K., Takada, K., Oi, Y., Suzuki, T., Nagase, H., . . . Koshikawa, N. (2005). Interactions among mu- and delta-opioid receptors, especially putative delta1- and delta2-opioid receptors, promote dopamine release in the nucleus accumbens. *Neuroscience*, 135(1), 213-225. doi:10.1016/j.neuroscience.2005.03.065
- Hopf, F. W., Martin, M., Chen, B. T., Bowers, M. S., Mohamedi, M. M., & Bonci, A. (2007). Withdrawal from intermittent ethanol exposure increases probability of burst firing in VTA neurons in vitro. *J Neurophysiol*, 98(4), 2297-2310. doi:00824.2007 [pii]
- Jin, W., Kim, M. S., Jang, E. Y., Lee, J. Y., Lee, J. G., Kim, H. Y., . . . Yang, C. H. (2017). Acupuncture reduces relapse to cocaine-seeking behavior via activation of GABA neurons in the ventral tegmental area. *Addict Biol*. doi:10.1111/adb.12499
- Job, M. O., Tang, A., Hall, F. S., Sora, I., Uhl, G. R., Bergeson, S. E., & Gonzales, R. A. (2007). Mu (mu) opioid receptor regulation of ethanol-induced dopamine response in the ventral

- striatum: evidence of genotype specific sexual dimorphic epistasis. *Biol Psychiatry*, 62(6), 627-634. doi:10.1016/j.biopsych.2006.11.016
- Johnson, S. W., & North, R. A. (1992). Opioids excite dopamine neurons by hyperpolarization of local interneurons. *J Neurosci*, 12(2), 483-488.
- Karkhanis, A. N., Huggins, K. N., Rose, J. H., & Jones, S. R. (2016). Switch from excitatory to inhibitory actions of ethanol on dopamine levels after chronic exposure: Role of kappa opioid receptors. *Neuropharmacology*, 110, 190-197. doi:10.1016/j.neuropharm.2016.07.022
- Kim, S. A., Lee, B. H., Bae, J. H., Kim, K. J., Steffensen, S. C., Ryu, Y. H., . . . Kim, H. Y. (2013). Peripheral afferent mechanisms underlying acupuncture inhibition of cocaine behavioral effects in rats. *Plos One*, 8(11), e81018. doi:10.1371/journal.pone.0081018
- Koeltzow, T. E., & White, F. J. (2003). Behavioral depression during cocaine withdrawal is associated with decreased spontaneous activity of ventral tegmental area dopamine neurons. *Behav Neurosci*, 117(4), 860-865.
- Konkoy, C. S., & Childers, S. R. (1989). Dynorphin-selective inhibition of adenylyl cyclase in guinea pig cerebellum membranes. *Mol Pharmacol*, 36(4), 627-633.
- Lee, Y. K., Park, S. W., Kim, Y. K., Kim, D. J., Jeong, J., Myrick, H., & Kim, Y. H. (2005). Effects of naltrexone on the ethanol-induced changes in the rat central dopaminergic system. *Alcohol Alcohol*, 40(4), 297-301. doi:10.1093/alcalc/agh163
- Lim, S. S., Vos, T., Flaxman, A. D., Danaei, G., Shibuya, K., Adair-Rohani, H., . . . Memish, Z. A. (2012). A comparative risk assessment of burden of disease and injury attributable to 67 risk factors and risk factor clusters in 21 regions, 1990-2010: a systematic analysis for

- the Global Burden of Disease Study 2010. *Lancet*, 380(9859), 2224-2260.
doi:10.1016/S0140-6736(12)61766-8
- Ludlow, K. H., Bradley, K. D., Allison, D. W., Taylor, S. R., Yorgason, J. T., Hansen, D. M., . . . Steffensen, S. C. (2009). Acute and chronic ethanol modulate dopamine D2-subtype receptor responses in ventral tegmental area GABA neurons. *Alcohol Clin Exp Res*, 33(5), 804-811. doi:10.1111/j.1530-0277.2009.00899.x
- Lyness, W. H., & Smith, F. L. (1992). Influence of dopaminergic and serotonergic neurons on intravenous ethanol self-administration in the rat. *Pharmacol Biochem Behav*, 42(1), 187-192.
- Macefield, V. G. (2005). Physiological characteristics of low-threshold mechanoreceptors in joints, muscle and skin in human subjects. *Clin Exp Pharmacol Physiol*, 32(1-2), 135-144. doi:10.1111/j.1440-1681.2005.04143.x
- Maisonneuve, I. M., Ho, A., & Kreek, M. J. (1995). Chronic administration of a cocaine "binge" alters basal extracellular levels in male rats: an in vivo microdialysis study. *J Pharmacol Exp Ther*, 272(2), 652-657.
- Mansour, A., Burke, S., Pavlic, R. J., Akil, H., & Watson, S. J. (1996). Immunohistochemical localization of the cloned kappa 1 receptor in the rat CNS and pituitary. *Neuroscience*, 71(3), 671-690.
- Mansour, A., Fox, C. A., Akil, H., & Watson, S. J. (1995). Opioid-receptor mRNA expression in the rat CNS: anatomical and functional implications. *Trends Neurosci*, 18(1), 22-29.
- Mansour, A., Khachaturian, H., Lewis, M. E., Akil, H., & Watson, S. J. (1987). Autoradiographic differentiation of mu, delta, and kappa opioid receptors in the rat forebrain and midbrain. *J Neurosci*, 7(8), 2445-2464.

- Mansour, A., Khachaturian, H., Lewis, M. E., Akil, H., & Watson, S. J. (1988). Anatomy of CNS opioid receptors. *Trends Neurosci*, 11(7), 308-314.
- McBride, W. J., Chernet, E., Dyr, W., Lumeng, L., & Li, T. K. (1993). Densities of dopamine D2 receptors are reduced in CNS regions of alcohol-preferring P rats. *Alcohol*, 10(5), 387-390.
- Moos, R. H., & Moos, B. S. (2006). Rates and predictors of relapse after natural and treated remission from alcohol use disorders. *Addiction*, 101(2), 212-222. doi:10.1111/j.1360-0443.2006.01310.x
- Murakawa, K., Hirose, N., Takada, K., Suzuki, T., Nagase, H., Cools, A. R., & Koshikawa, N. (2004). Deltorphin II enhances extracellular levels of dopamine in the nucleus accumbens via opioid receptor-independent mechanisms. *Eur J Pharmacol*, 491(1), 31-36. doi:10.1016/j.ejphar.2004.03.028
- Okutsu, H., Watanabe, S., Takahashi, I., Aono, Y., Saigusa, T., Koshikawa, N., & Cools, A. R. (2006). Endomorphin-2 and endomorphin-1 promote the extracellular amount of accumbal dopamine via nonopioid and mu-opioid receptors, respectively. *Neuropsychopharmacology*, 31(2), 375-383. doi:10.1038/sj.npp.1300804
- Prather, P. L., McGinn, T. M., Claude, P. A., Liu-Chen, L. Y., Loh, H. H., & Law, P. Y. (1995). Properties of a kappa-opioid receptor expressed in CHO cells: interaction with multiple G-proteins is not specific for any individual G alpha subunit and is similar to that of other opioid receptors. *Brain Res Mol Brain Res*, 29(2), 336-346.
- Rankin, M. L., & Sibley, D. R. (2010). Constitutive phosphorylation by protein kinase C regulates D1 dopamine receptor signaling. *J Neurochem*, 115(6), 1655-1667. doi:10.1111/j.1471-4159.2010.07074.x

- Roberts, A. J., Gold, L. H., Polis, I., McDonald, J. S., Filliol, D., Kieffer, B. L., & Koob, G. F. (2001). Increased ethanol self-administration in delta-opioid receptor knockout mice. *Alcohol Clin Exp Res*, 25(9), 1249-1256.
- Roberts, A. J., McDonald, J. S., Heyser, C. J., Kieffer, B. L., Matthes, H. W., Koob, G. F., & Gold, L. H. (2000). mu-Opioid receptor knockout mice do not self-administer alcohol. *J Pharmacol Exp Ther*, 293(3), 1002-1008.
- Rose, J. H., Karkhanis, A. N., Chen, R., Gioia, D., Lopez, M. F., Becker, H. C., . . . Jones, S. R. (2016). Supersensitive Kappa Opioid Receptors Promotes Ethanol Withdrawal-Related Behaviors and Reduce Dopamine Signaling in the Nucleus Accumbens. *Int J Neuropsychopharmacol*, 19(5). doi:10.1093/ijnp/pyv127
- Rowe, M. J., Tracey, D. J., Mahns, D. A., Sahai, V., & Ivanusic, J. J. (2005). Mechanosensory perception: are there contributions from bone-associated receptors? *Clin Exp Pharmacol Physiol*, 32(1-2), 100-108. doi:10.1111/j.1440-1681.2005.04136.x
- Sacks, J. J., Gonzales, K. R., Bouchery, E. E., Tomedi, L. E., & Brewer, R. D. (2015). 2010 National and State Costs of Excessive Alcohol Consumption. *Am J Prev Med*, 49(5), e73-79. doi:10.1016/j.amepre.2015.05.031
- SAMHSA. (2016). *Facing Addicton in America: The Surgeon Gernal's Report on Alcohol, Drugs, and Health*. Retrieved from
- Shippenberg, T. S., Zapata, A., & Chefer, V. I. (2007). Dynorphin and the pathophysiology of drug addiction. *Pharmacol Ther*, 116(2), 306-321. doi:10.1016/j.pharmthera.2007.06.011
- Sirohi, S., Bakalkin, G., & Walker, B. M. (2012). Alcohol-induced plasticity in the dynorphin/kappa-opioid receptor system. *Front Mol Neurosci*, 5, 95. doi:10.3389/fnmol.2012.00095

- Spanagel, R., Herz, A., & Shippenberg, T. S. (1992). Opposing tonically active endogenous opioid systems modulate the mesolimbic dopaminergic pathway. *Proc Natl Acad Sci U S A*, 89(6), 2046-2050.
- Stefanini, E., Frau, M., Garau, M. G., Garau, B., Fadda, F., & Gessa, G. L. (1992). Alcohol-preferring rats have fewer dopamine D2 receptors in the limbic system. *Alcohol Alcohol*, 27(2), 127-130.
- Steffensen, S. C., Stobbs, S. H., Colago, E. E., Lee, R. S., Koob, G. F., Gallegos, R. A., & Henriksen, S. J. (2006). Contingent and non-contingent effects of heroin on mu-opioid receptor-containing ventral tegmental area GABA neurons. *Exp Neurol*, 202(1), 139-151. doi:10.1016/j.expneurol.2006.05.023
- Steffensen, S. C., Taylor, S. R., Horton, M. L., Barber, E. N., Lyle, L. T., Stobbs, S. H., & Allison, D. W. (2008). Cocaine disinhibits dopamine neurons in the ventral tegmental area via use-dependent blockade of GABA neuron voltage-sensitive sodium channels. *Eur J Neurosci*, 28(10), 2028-2040. doi:10.1111/j.1460-9568.2008.06479.x
- Steffensen, S. C., Walton, C. H., Hansen, D. M., Yorgason, J. T., Gallegos, R. A., & Criado, J. R. (2009). Contingent and non-contingent effects of low-dose ethanol on GABA neuron activity in the ventral tegmental area. *Pharmacol Biochem Behav*, 92(1), 68-75. doi:S0091-3057(08)00354-7 [pii]
- Stobbs, S. H., Ohran, A. J., Lassen, M. B., Allison, D. W., Brown, J. E., & Steffensen, S. C. (2004). Ethanol suppression of ventral tegmental area GABA neuron electrical transmission involves NMDA receptors. *J Pharmacol Exp Ther*, 311(1), 282-289.

- Strother, W. N., Lumeng, L., Li, T. K., & McBride, W. J. (2003). Regional CNS densities of serotonin 1A and dopamine D2 receptors in periadolescent alcohol-preferring P and alcohol-nonpreferring NP rat pups. *Pharmacol Biochem Behav*, 74(2), 335-342.
- Tallent, M., Dichter, M. A., Bell, G. I., & Reisine, T. (1994). The cloned kappa opioid receptor couples to an N-type calcium current in undifferentiated PC-12 cells. *Neuroscience*, 63(4), 1033-1040.
- Usiello, A., Baik, J. H., Rouge-Pont, F., Picetti, R., Dierich, A., LeMeur, M., . . . Borrelli, E. (2000). Distinct functions of the two isoforms of dopamine D2 receptors. *Nature*, 408(6809), 199-203. doi:10.1038/35041572
- Walker, B. M., & Koob, G. F. (2008). Pharmacological evidence for a motivational role of kappa-opioid systems in ethanol dependence. *Neuropsychopharmacology*, 33(3), 643-652. doi:10.1038/sj.npp.1301438
- Wang, Q., Mao, L., & Han, J. (1990a). Analgesic electrical stimulation of the hypothalamic arcuate nucleus: tolerance and its cross-tolerance to 2 Hz or 100 Hz electroacupuncture. *Brain Res*, 518(1-2), 40-46.
- Wang, Q., Mao, L., & Han, J. (1990b). The arcuate nucleus of hypothalamus mediates low but not high frequency electroacupuncture analgesia in rats. *Brain Res*, 513(1), 60-66.
- White, W. L. (2012). *Recovery/Remission from Substance Use Disorders*. Retrieved from
- Wise, R. A. (2008). Dopamine and reward: the anhedonia hypothesis 30 years on. *Neurotox Res*, 14(2-3), 169-183. doi:10.1007/BF03033808
- Yang, C. H., Yoon, S. S., Hansen, D. M., Wilcox, J. D., Blumell, B. R., Park, J. J., & Steffensen, S. C. (2010). Acupuncture inhibits GABA neuron activity in the ventral tegmental area

- and reduces ethanol self-administration. *Alcohol Clin Exp Res*, 34(12), 2137-2146.
doi:10.1111/j.1530-0277.2010.01310.x
- Yoon, S. S., Yang, E. J., Lee, B. H., Jang, E. Y., Kim, H. Y., Choi, S. M., . . . Yang, C. H.
(2012). Effects of acupuncture on stress-induced relapse to cocaine-seeking in rats.
Psychopharmacology (Berl), 222(2), 303-311. doi:10.1007/s00213-012-2683-3
- Yorgason, J. T., Zeppenfeld, D. M., & Williams, J. T. (2017). Cholinergic Interneurons Underlie
Spontaneous Dopamine Release in Nucleus Accumbens. *J Neurosci*, 37(8), 2086-2096.
doi:10.1523/JNEUROSCI.3064-16.2017
- Yoshida, Y., Koide, S., Hirose, N., Takada, K., Tomiyama, K., Koshikawa, N., & Cools, A. R.
(1999). Fentanyl increases dopamine release in rat nucleus accumbens: involvement of
mesolimbic mu- and delta-2-opioid receptors. *Neuroscience*, 92(4), 1357-1365.
- Yoshimoto, K., McBride, W. J., Lumeng, L., & Li, T. K. (1992). Alcohol stimulates the release
of dopamine and serotonin in the nucleus accumbens. *Alcohol*, 9(1), 17-22. doi:0741-
8329(92)90004-T [pii]

CHAPTER 2: Targeted Subcutaneous Vibration with Single-Neuron Electrophysiology as a
Novel Method for Understanding the Central Effects of Peripheral Vibrational Therapy in a
Rodent Model

**Targeted Subcutaneous Vibration with Single-Neuron Electrophysiology as a
Novel Method for Understanding the Central Effects of Peripheral
Vibrational Therapy in a Rodent Model**

Kyle B Bills, DC ¹, Travis Clarke, MS¹, George H Major, BS⁴, Cecil B Jacobson³, Jonathan D. Blotter, PhD³, J Brent Feland, PhD, PT², and Scott C Steffensen, PhD.^{1*}

¹ Brigham Young University, Department of Psychology/Neuroscience; Provo, Utah

² Brigham Young University, Department of Exercise Sciences; Provo, Utah

³ Brigham Young University, Department of Engineering; Provo, Utah

⁴ University of California at Los Angeles, Department of Chemistry and Biochemistry

*Corresponding Author

Scott C. Steffensen

1050 SWKT

Brigham Young University

Provo UT, 84602

Tel: 801-422-9499

Fax: 801-422-0602

Email: scott_steffensen@byu.edu

Formatted for the journal *Dose Response*

Abstract

Very little is known about the effects of whole body vibration on the supraspinal central nervous system. Though much clinical outcome data and mechanistic data about peripheral neural and musculoskeletal mechanisms have been explored, the lack of central understanding is a barrier to evidence-based, best practice guidelines in the use of vibrational therapy. Disparate methods of administration render study to study comparisons difficult. To address this lack of uniformity, we present the use of targeted subcutaneous vibration combined with simultaneous *in vivo* electrophysiological recordings as a method of exploring the central effects of peripheral vibration therapy. We used implanted motors driven by both Grass stimulators and programmed micro controllers to vary frequency and location of stimulation in an anesthetized *in vivo* rat model while simultaneously recording firing rate from GABA neurons in the ventral tegmental area. We show peripheral vibration can alter GABA neuron firing rate in a location and frequency dependent manner. We include detailed schematics and code to aid others in the replication of this technique. This method allows for control of previous weaknesses in the literature including variability in body position, vibrational intensity, node and anti-node interactions with areas of differing mechanoreceptor densities, and prefrontal cortex influence.

Introduction

Vibrational therapy, through the use of whole body vibration (WBV) platforms or localized peripheral vibration (LPV), is increasing in popularity. Early investigations looked at vibration-induced enhancement of physical performance such as power and strength¹, and this body of literature is now extensive. Over the last 15 years, the vibration literature has rapidly expanded to include studies on a variety of responses ranging from flexibility^{2,3} and balance⁴, to bone metabolism⁵, hormone release⁶, and aging and loss of balance⁷. The application of vibration stimulates mechanoreceptors in the skin, muscle, and joint which influence monosynaptic and polysynaptic pathways in the peripheral and central nervous systems (PNS and CNS). Much of the initial explanation regarding the functional efficacy of WBV or LPV has focused on peripheral neuromechanical alterations.

Early work utilizing LPV directly to a tendon or muscle helped establish peripheral neuromechanical responses to vibration. Vibration can invoke the stretch reflex by exciting group Ia afferents⁸, while secondary afferents and Golgi tendon organs (GTO) show a decreased response to vibration input⁹. However, the firing rate of both afferents and the GTO response increase with muscle contraction^{9,10}. Other studies suggest that both the H-reflex and stretch reflex are suppressed during vibration due to pre-synaptic inhibition¹¹, and that this suppression is sustained following application of WBV^{12,13}. Weight bearing activities and exercise application of WBV on reflex responses appears more controversial with load-bearing movement and complexity of tasks possibly interfering with assumed neuromechanisms¹². More recently, however, the variability in results of similar studies and the broadening of vibration application for study has suggested a more important role of central or supraspinal influence. Reflex

contraction appears dependent on efferent fusimotor input, which suggests supraspinal control is involved¹⁴. Current research observing the effects of vibration on symptoms of various medical conditions including stroke¹⁵ and Parkinson's disease¹⁶, amongst others¹⁷, suggests that WBV is a safe and beneficial method for improving these symptoms, as well as general movement patterns, gait, and balance. Evaluation of such conditions offers further evidence that supraspinal and central mechanisms are involved in the body's responses to vibration input. Reports of enhanced corticospinal excitability concomitant with spinal inhibition¹⁸ and facilitated motor evoked potentials¹⁹ further highlight the enhanced role of the central nervous system in modulating responses to vibration. The concomitant increased cortical excitability seems to compensate for lower excitability at the spinal level²⁰.

Touch (both fine and crude) pathways such as the dorsal column/medial lemniscal pathways (DCML) and pain/temperature pathways (anterolateral columns) are well defined in both texts and research literature regarding their structures and regions crossed as information is relayed from a peripheral receptor to the somatosensory cortex. However, activation of specific mechanoreceptor responses within a defined area and their effects on central neuron activity remains largely unknown. Mechanical stimulation of the DCML pathway via mechanoacupuncture at the wrist has been shown to produce modulatory effects in γ -aminobutyric acid (GABA)-containing neurons in the midbrain ventral tegmental area (VTA)²¹. Further these effects have been traced through synapses in the nucleus cuneatus (CN) and subsequent relays through the thalamus and lateral habenula before finally producing inhibition of VTA GABA neurons²¹. Thus, groundwork has been laid demonstrating, indirectly, that peripheral mechanoreceptor activation affects higher order functions of the CNS (e.g., limbic), beyond simple somatosensory processing. There is also

compelling evidence demonstrating central changes in response to mechanical vibration as measured with fMRI, EEG, heart rate variability and evoked potentials^{18,22-24}. Unfortunately, the lack of better detail to supraspinal responses is still an impediment to the development of evidence-based therapeutic guidelines and consensus on vibration's therapeutic value and mechanism of action. The use of fMRI lacks temporal and spatial resolution and primarily gives regional specificity and indirect information about neuron activity. Conversely, the use of EEG offers improved temporal resolution but lacks regional specificity. Evoked potentials give information about a change in the facilitation/inhibition of the entire pathway with limitations similar to EEG. Heart rate variability also lacks spatiotemporal resolution and is, at best, a generalized indirect measure of autonomic nervous activity. These deficiencies underpin the need for novel methods of investigation to determine how peripheral mechanical vibration affects central activity. These previous methods leave a gap in the ability to understand how individual neurons within a targeted area respond to LPV.

In this paper, we lay out the application of localized subcutaneous vibration with simultaneous *in-vivo* single neuron electrophysiology. This technology has been a long-standing and commonly used technique to measure changes in neuron firing rate in response to various experimental conditions. However, to date, it has not been applied to the field of clinically applied vibration. Use of this technique can further our understanding of the non-canonical effects of LPV. Not only does this method give us the ability to understand the individual neuron response to LPV, but it also allows us to control the application of the peripheral vibration (region, frequency, and amplitude). To demonstrate the utility of this technique, we aimed to test regional and frequency-based differences in LPV on GABA neuron firing rate in the VTA. To test this, we implanted

subcutaneous vibrating motors in two different regions (posterior neck C7-T1 and the biceps femoris of the posterior hindlimb) of wistar rats. Further, we tested the difference between 50 Hz and 115 Hz at the C7-T1 level of the spinal column. We hypothesized that regional and frequency-based differences would produce disparate changes in GABA neuron firing rate due to differences in both mechanoreceptor density and specificity.

Materials and Methods

Vibrational Motors

The vibration excitation source used in this research was a 3 volt, DC coin vibration motor (10 mm x 2.7 mm, DC 3V/0.1A, Uxcell, Hong Kong, CN). This motor induces vibration due to a rotating unbalance. The motor is encased in a small circular disc with a 10 mm diameter and 2.7 mm length. The weight of the motor was 6 g. A photograph of the motor is shown in **Figure 2.1**.



Figure 2.1: Vibrational Motor.

To ensure proper excitation to the system through predictable output, the vibration output of the motor was evaluated. The procedure consisted of configuring the motor input voltage and then randomly selecting one of the predetermined frequencies. The motor output velocity was measured 10 times at each frequency and voltage setting using a laser Doppler vibrometer (LDV). The LDV provided a non-intrusive measurement without adding any mass to the motor. The displacement and acceleration were computed from the velocity measurements. Two input voltage settings of 1 volt and 2 volts were used. The frequencies tested were at every 10 Hz ranging from 40 Hz to 160 Hz.

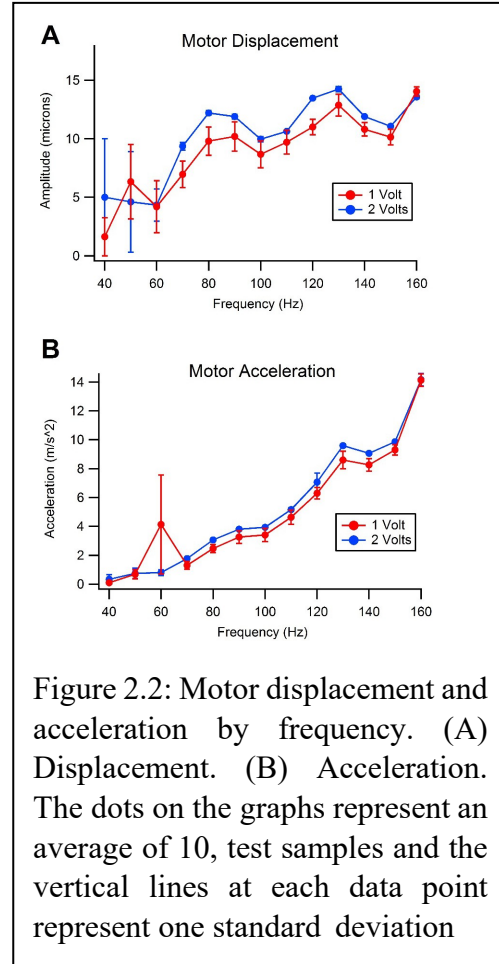


Figure 2.2: Motor displacement and acceleration by frequency. (A) Displacement. (B) Acceleration. The dots on the graphs represent an average of 10, test samples and the vertical lines at each data point represent one standard deviation

The motor characterization results are shown in Figure

2.2. **Figure 2.2A** shows the amplitude of the motor output displacement as a function of frequency. The displacement data show a relatively flat frequency response from 80 Hz to 150 Hz. **Figure 2.2B** shows the acceleration versus frequency data for the motor. As expected, the acceleration output increases quadratically with frequency. From these data, it was determined that this motor had a fairly flat frequency response across the frequencies of interest and was sufficiently characterized to produce sufficiently repeatable results for the experiments described below.

Surgical Procedure and In Vivo Single Cell Electrophysiology

Wistar rats, weighing 250-320 g, from our breeding colony at Brigham Young University were used. Rats were housed in groups of 2-3 at a fixed temperature (21-23°C) and humidity (55-65%) on a reverse light/dark cycle with *ad libitum* food and water. Rats were anesthetized using isoflurane and placed in a stereotaxic apparatus. Anesthesia was then maintained at 1%. Body temperature was maintained at $37.4^{\circ} \pm 0.4^{\circ}\text{C}$ by a feedback regulated heating pad. A 10 mm incision was made either at the C7-T1 levels posteriorly at midline or at the ipsilateral biceps femoris muscle. The Fascia was dissected and muscle tissue was left intact. A 10 mm x 2.7 mm, DC 3V/.1A micro coin vibration motor (Uxcell, Hong Kong, CN), was then implanted subcutaneously (to the right of midline for cervical implant) and the incision was closed adhesively. Extracellular potentials were recorded by a single 3.0 M KCl-filled micropipette (2 to 4 Mohms; 1-2 μm inside diameter). With the skull exposed, a hole was drilled for placement of the pipette which was driven into the VTA with a piezoelectric microdrive (EXFO Burleigh 8200 controller and Inchworm, Victor, NY) via stereotaxic coordinates [from bregma: 5.6 to 6.5 posterior (P), 0.5 to 1.0 lateral (L), 6.5 to 7.8 ventral (V)]. Potentials were displayed on a digital oscilloscope and amplified with an Axon Instruments Multiclamp 700A amplifier (Union City, CA). Single-cell activity was filtered at 0.3 to 10 kHz (3 dB) with Multiclamp 700A and sampled at 20 kHz (12 bit resolution) with National Instruments acquisition boards. Extracellularly recorded action potentials were discriminated with a WPI, WP-121 Spike Discriminator (Sarasota, FL). Single-unit potentials, discriminated spikes, and stimulation events were captured by National Instruments NB-MIO-16 digital I/O and counter/timer acquisition boards (Austin, TX) in Mac computers.

Characterization of VTA GABA Neurons in vivo and Recordings

VTA GABA neurons were identified by previously-established stereotaxic coordinates and by spontaneous and stimulus-evoked electrophysiological criteria. They included: relatively fast firing rate ($>10\text{Hz}$), ON-OFF phasic non-bursting activity, and spike duration less than $200\text{ }\mu\text{sec}$. We evaluated only those spikes that had greater than 5:1 signal-to-noise ratio. After positive GABA neuron identification, baseline firing rate was measured for 5-minutes to ensure stability prior to vibratory stimulus.

Grass Stimulator and Vibration Stimulation

Following measurement of the GABA neuron baseline firing rate, a 60-second vibration stimulus was introduced. The vibrating motor was connected to the S44 Grass Stimulator (Grass Medical Instruments, West Warwick, RI). For electrophysiological recordings, the stimulator was set at 2 volts for 0.1 msec duration and 0 msec delay. Pulses per second were varied to produce variations in vibrational frequency. All vibratory stimuli were 60 sec in duration and followed by 15-min of recording the GABA neuron firing rate. Experimental groups included 50 Hz ($n=4$) and 115 Hz ($n=4$) given subcutaneously at the C7/T1 level and 50 Hz ($n=4$) given subcutaneously at the right biceps femoris muscle.

Micro Controller Driver

In order to facilitate the replication of this technique we include an alternative method for generating the vibratory stimulus using a PIC24F16KA301 micro controller to generate a pulse width modulation (PWM) signal. This PWM can be modified to emulate multiple signals of varying

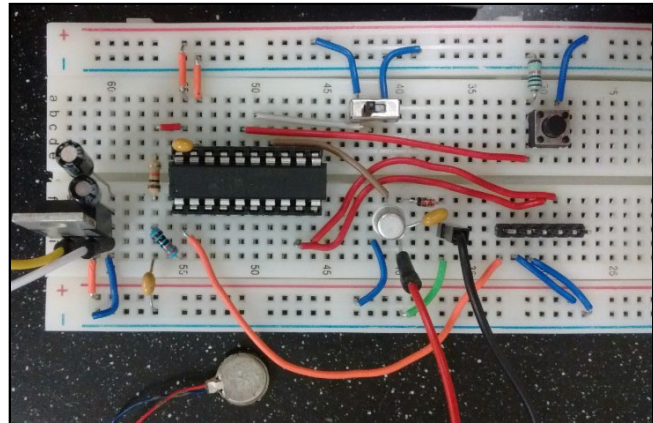


Figure 2.3 – Circuit for micro controller

frequency and amplitude. The PWM is then passed through a transistor that provides the needed current to the motor. The full circuit is pictured in **Figure 2.3** and the schematic and code to drive the micro controller can be found at <http://github.com/steffensenlab>.

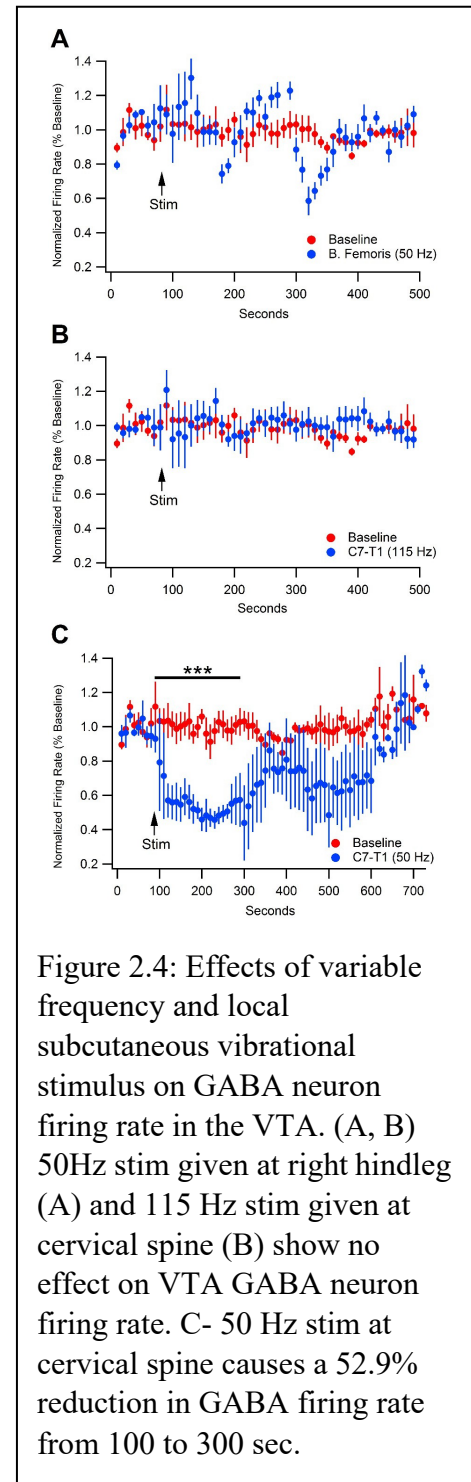
Statistical Analysis

Single-unit, discriminated spikes were processed with IGOR Pro software (Wavemetrics, Lake Oswego, OR). Extracellularly recorded single-unit action potentials were discriminated by a peak detector digital processing LabVIEW algorithm. After 5-min of recording, the final 60 sec of firing rate data before vibrational stimulus were averaged to establish a baseline for comparison. The results for control, 50 Hz and 115 Hz vibrational groups were derived from calculations performed on ratemeter records and expressed as means \pm SEM. All statistical tests were performed in JMP13. Data from each recording were normalized and combined and binned in 100 sec intervals for comparison across time. All comparisons were initially made using a one-way ANOVA. Following the ANOVA, all groups and bins were compared to corresponding controls using a Dunnett's analysis. The control group was established by taking firing rate data from GABA neurons in rats that received no vibratory stimulation but did receive subcutaneous implants of

vibrating motors which were placed near the cervical spine as described previously. Baseline recordings (n=4) were normalized and combined prior to comparison with experimental groups. Figures were compiled using IGOR Pro Software.

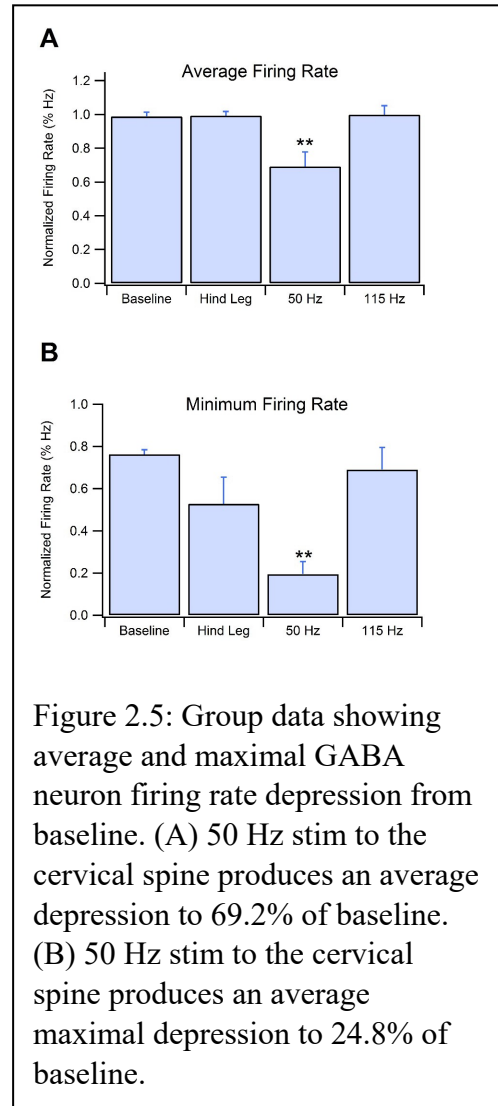
Results

Figure 2.4 demonstrates the three LPV experimental conditions that were tested and compared to unstimulated baseline. **Figure 2.4A** shows stimulation at the right hind leg. A vibrational stimulus at this location of 50 Hz for 60 sec showed no significant change in GABA firing rate over any time frame. **Figure 2.4B** demonstrates the effects of a 115 Hz stimulation at C7-T1 for 60 sec. As with stimulation to the hind leg, 115 Hz did not show a change in GABA firing rate across any time. In contrast, **Figure 2.4C** reveals a depression in GABA neuron firing rate resultant from a 50 Hz vibration at C7-T1 for 60 sec. Initial ANOVA revealed differences between bins at 101-200 [$F_{(3,11)} = 16.7675$, $p=0.0002$] and 201-300 sec [$F_{(3,11)} = 19.51$, $p = 0.0001$]. After 50 Hz stimulus was given at 100 sec, from time 100 to 200 sec, GABA neuron firing rate depressed to 48.3% ($\pm 3.2\%$, $n=4$, $p<.0001$) of baseline and to 45.9% ($\pm 7.3\%$,



n=4, $p < .0001$) of baseline from 200 to 300 sec. No other time frame or experimental condition produced a significant change in firing rate.

Figure 2.5A shows group data comparing firing rate averages of all locations and frequencies from time of vibrational stimulus to 400 sec post-stimulation. Analysis revealed significant differences between average vibration-induced firing rate depression between groups [$F_{(3,11)} = 7.14$, $p = 0.006$]. 50 Hz stimulation at the right C1-T1 laminae produced an average depression to 69.2% ($\pm 3.0\%$, n=4, $p = 0.0002$) of baseline and was the only stimulus to produce a significant reduction in firing rate over time. Panel B compares the greatest firing rate depression produced in each experimental group. Because VTA GABA neurons exhibit a natural cyclical ebb and flow some variation is expected even within the unstimulated group. There was a significant difference between the minimum firing



rates of the four experimental groups [$F_{(3,11)} = 7.8545$, $p = 0.0044$]. Unstimulated baseline recordings produce a maximal drop to 78.1% ($\pm 0.4\%$, n=4) of averaged baseline. All other maximal depressions were compared to the variation in the baseline group. 50 Hz vibration to the cervical spine produced an average maximal drop in firing rate to 24.8% ($\pm 1.4\%$, n=4, $p = 0.003$) of baseline. No other group produced a significant inhibition to firing rate.

Discussion

These findings are suggestive that LPV produces transient changes to cellular excitability in the VTA. Further, that vibrational frequency and location of stimulus are important factors in peripheral vibration-induced changes. The sites of stimulation were chosen due to their disparate relative levels of mechanoreceptor expression in the subcutaneous tissue and adjacent joint capsules. In humans, high levels of cutaneous and joint mechanoreceptors have been identified in the intervertebral disc and facet joints of the spine, with greater relative levels in the cervical spine than thoracic or lumbar^{25,26}. The control stimulation was chosen due to its distance from joint mechanoreceptors. The motor implant site provided at least 20 mm of distance between the motor and the nearest joint. Further, there is a lack of cutaneous Pacinian corpuscle expression in rodents enhancing the effect of increased distance from joint²⁷. The two frequencies of vibration were chosen to more selectively activate either Meissner's corpuscles or Pacinian corpuscles; the former having a lower intensity dynamic range of around 5-100 Hz and the latter a higher range of around 100-300 Hz²⁸⁻³¹. However, it is noted that these ranges are commonly thought to be approximate and some overlap certainly exists. A small population of lanceolate endings exist that have been shown to respond to vibration in a range around 5-200 Hz, though this population of endings has only been demonstrated in recordings of cat whisker hair³². Other common cutaneous and joint mechanoreceptors are thought to be more specific to light touch (Merkel Cells) and stretch (Ruffini corpuscles) and thus are less likely to be significant in the presence of prolonged vibrational input³³. 50 and 115 Hz vibrational frequencies were chosen to more selectively target Meissner's and Pacinian Corpuscles respectively.

VTA GABA neuron activity transiently and significantly decreased after targeted subcutaneous vibration at the C7-T1 level when stimulation occurred at 50 Hz. These changes were not present when stimulation was given at 115 Hz or when stimulation was given at the muscle belly of the biceps femoris muscle of the upper hind leg. Additionally, they suggest that targeted, anatomically-specific and frequency-variable vibration, coupled with single-unit extracellular electrophysiology is an effective method for measuring direct alterations in neuronal firing rate resultant from peripheral vibration. A previous study recording GABA neuron firing rate changes in the VTA due to acupuncture treatment suggested that receptor sensitivities might be responsible for the reported frequency dependent effects on these neurons³⁴. GABA neurons in the VTA were chosen due to internal preliminary data indicating their responsiveness to peripheral vibration and because of their relevance in addiction research³⁴⁻³⁶. This method can be employed to further clarify regional and frequency based sensitivities, mechanoreceptors subtypes, and tractology involved in alterations of central neuronal function. To our knowledge this method has not been applied to the field of therapeutic vibration. It can provide a framework for ongoing description of the central pathways involved in this emerging field of physical medicine.

Future Direction

It is unknown the extent to which higher order neuronal processing affects the currently observed effects of WBV such as improvement in gait, movement patterns and balance. By extension, even less is understood about the changes that occur primarily in these higher circuits. This lack of understanding is a major impediment to our ability to develop optimized, evidence-based care protocols and could contribute to the mixed outcome data surrounding both WBV and LPV, and their therapeutic applications. The diversity of vibrational testing protocols divergent in

frequency, duration, type, amplitude, resonant location and subject positioning render inference about precise neural mechanisms difficult. The lack of homogenous testing protocols could contribute to the mixed reports of the efficacy of WBV in the treatment of various conditions^{37,38}. Indeed, it has been shown that slight variations in a subject's posture or weight distribution can greatly affect the transmission of vibratory stimuli through the body³⁹. Future studies should focus on addressing these issues, specifically tracking the cellular and circuitry changes that contribute to current therapeutic applications and outcomes from WBV. Frequency and regional specificity along with duration or treatment must be addressed in order to maximize patient outcomes. These answers will be difficult to ascertain without directly measuring circuitry of interest in animal models and human subjects for each condition for which WBV is a potential therapy. An understanding of cellular and circuitry changes could provide insight into applications not currently being considered, including methods such as deep brain stimulation or genetic therapies. Localized subcutaneous vibration with simultaneous *in vivo* single-unit electrophysiology can provide heretofore lacking information about individual neuronal changes in the central nervous system. Filling this gap may help provide a more complete picture of the central effects of vibratory therapeutics and lead to improved continuity of application and outcome in the future.

Declaration of Conflicting Interests

The author(s) declared no potential conflicts of interest with respect to the research, authorship, and/or publication of this article.

Funding

This work was supported by PHS NIH grants AA020919 and DA035958 to SCS.

References

1. Bosco C, Cardinale M, Tsarpela O. Influence of vibration on mechanical power and electromyogram activity in human arm flexor muscles. *Eur J Appl Physiol Occup Physiol*. 1999;79(4):306-311.
2. Feland JB, Hawks M, Hopkins JT, Hunter I, Johnson AW, Eggett DL. Whole body vibration as an adjunct to static stretching. *Int J Sports Med*. 2010;31(8):584-589.
3. Houston MN, Hodson VE, Adams KK, Hoch JM. The effectiveness of whole-body-vibration training in improving hamstring flexibility in physically active adults. *J Sport Rehabil*. 2015;24(1):77-82.
4. Tseng SY, Hsu PS, Lai CL, Liao WC, Lee MC, Wang CH. Effect of two frequencies of whole-body vibration training on balance and flexibility of the elderly: a randomized controlled trial. *Am J Phys Med Rehabil*. 2016;95(10):730-737.
5. Dionello CF, Sa-Caputo D, Pereira HV, et al. Effects of whole body vibration exercises on bone mineral density of women with postmenopausal osteoporosis without medications: novel findings and literature review. *J Musculoskelet Neuronal Interact*. 2016;16(3):193-203.
6. Paineiras-Domingos LL, Sa-Caputo DDC, Moreira-Marconi E, et al. Can whole body vibration exercises affect growth hormone concentration? A systematic review. *Growth Factors*. 2017;35(4-5):189-200.
7. Jepsen DB, Thomsen K, Hansen S, Jorgensen NR, Masud T, Ryg J. Effect of whole-body vibration exercise in preventing falls and fractures: a systematic review and meta-analysis. *BMJ Open*. 2017;7(12):e018342.
8. Matthews PB. Reflex activation of the soleus muscle of the decerebrate cat by vibration. *Nature*. 1966;209(5019):204-205.
9. Brown MC, Engberg I, Matthews PB. The relative sensitivity to vibration of muscle receptors of the cat. *J Physiol*. 1967;192(3):773-800.
10. Burke D, Hagbarth KE, Lofstedt L, Wallin BG. The responses of human muscle spindle endings to vibration during isometric contraction. *J Physiol*. 1976;261(3):695-711.
11. Gillies JD, Lance JW, Neilson PD, Tassinari CA. Presynaptic inhibition of the monosynaptic reflex by vibration. *J Physiol*. 1969;205(2):329-339.
12. Ritzmann R, Kramer A, Gollhofer A, Taube W. The effect of whole body vibration on the H-reflex, the stretch reflex, and the short-latency response during hopping. *Scand J Med Sci Sports*. 2013;23(3):331-339.
13. Karacan I, Cidem M, Yilmaz G, Sebik O, Cakar HI, Turker KS. Tendon reflex is suppressed during whole-body vibration. *J Electromyogr Kinesiol*. 2016;30:191-195.
14. Rittweger J. Vibration as an exercise modality: how it may work, and what its potential might be. *Eur J Appl Physiol*. 2010;108(5):877-904.
15. Park YJ, Park SW, Lee HS. Comparison of the effectiveness of whole body vibration in stroke patients: a meta-analysis. *Biomed Res Int*. 2018;2018:5083634.
16. Sharififar S, Coronado RA, Romero S, Azari H, Thigpen M. The effects of whole body vibration on mobility and balance in Parkinson disease: a systematic review. *Iran J Med Sci*. 2014;39(4):318-326.

17. Dionello CF, de Souza PL, Sa-Caputo D, et al. Do whole body vibration exercises affect lower limbs neuromuscular activity in populations with a medical condition? A systematic review. *Restor Neurol Neurosci*. 2017;35(6):667-681.
18. Krause A, Gollhofer A, Freyler K, Jablonka L, Ritzmann R. Acute corticospinal and spinal modulation after whole body vibration. *J Musculoskelet Neuronal Interact*. 2016;16(4):327-338.
19. Mileva KN, Bowtell JL, Kossev AR. Effects of low-frequency whole-body vibration on motor-evoked potentials in healthy men. *Exp Physiol*. 2009;94(1):103-116.
20. Souron R, Besson T, McNeil CJ, Lapole T, Millet GY. An acute exposure to muscle vibration decreases knee extensors force production and modulates associated central nervous system excitability. *Front Hum Neurosci*. 2017;11:519.
21. Chang S, Ryu Y, Gwak YS, et al. Spinal pathways involved in somatosensory inhibition of the psychomotor actions of cocaine. *Sci Rep*. 2017;7(1):5359.
22. Zhang N, Fard M, Bhuiyan MHU, Verhagen D, Azari MF, Robinson SR. The effects of physical vibration on heart rate variability as a measure of drowsiness. *Ergonomics*. 2018;1-19.
23. Kaut O, Becker B, Schneider C, et al. Stochastic resonance therapy induces increased movement related caudate nucleus activity. *J Rehabil Med*. 2016;48(9):815-818.
24. Satou Y, Ishitake T, Ando H, et al. Effect of short-term exposure to whole body vibration in humans: relationship between wakefulness level and vibration frequencies. *Kurume Med J*. 2009;56(1-2):17-23.
25. McLain RF, Raiszadeh K. Mechanoreceptor endings of the cervical, thoracic, and lumbar spine. *Iowa Orthop J*. 1995;15:147-155.
26. McLain RF. Mechanoreceptor endings in human cervical facet joints. *Spine (Phila Pa 1976)*. 1994;19(5):495-501.
27. Zelena J. The development of Pacinian corpuscles. *J Neurocytol*. 1978;7(1):71-91.
28. Macefield VG. Physiological characteristics of low-threshold mechanoreceptors in joints, muscle and skin in human subjects. *Clin Exp Pharmacol Physiol*. 2005;32(1-2):135-144.
29. Rowe MJ, Tracey DJ, Mahns DA, Sahai V, Ivanusic JJ. Mechanosensory perception: are there contributions from bone-associated receptors? *Clin Exp Pharmacol Physiol*. 2005;32(1-2):100-108.
30. S Coren LW, JT Enns. *Sensation and Perception*. 5th ed: Harcourt Brace and Co.; 1999.
31. Biswas A, Manivannan M, Srinivasan MA. Vibrotactile sensitivity threshold: nonlinear stochastic mechanotransduction model of the Pacinian Corpuscle. *IEEE Trans Haptics*. 2015;8(1):102-113.
32. Gottschaldt KM, Iggo A, Young DW. Functional characteristics of mechanoreceptors in sinus hair follicles of the cat. *J Physiol*. 1973;235(2):287-315.
33. Fleming MS, Luo W. The anatomy, function, and development of mammalian Abeta low-threshold mechanoreceptors. *Front Biol (Beijing)*. 2013;8(4).
34. Kim SA, Lee BH, Bae JH, et al. Peripheral afferent mechanisms underlying acupuncture inhibition of cocaine behavioral effects in rats. *PLoS One*. 2013;8(11):e81018.
35. Jin W, Kim MS, Jang EY, et al. Acupuncture reduces relapse to cocaine-seeking behavior via activation of GABA neurons in the ventral tegmental area. *Addict Biol*. 2017.
36. Yang CH, Yoon SS, Hansen DM, et al. Acupuncture inhibits GABA neuron activity in the ventral tegmental area and reduces ethanol self-administration. *Alcohol Clin Exp Res*. 2010;34(12):2137-2146.

37. Lam FM, Lau RW, Chung RC, Pang MY. The effect of whole body vibration on balance, mobility and falls in older adults: a systematic review and meta-analysis. *Maturitas*. 2012;72(3):206-213.
38. Orr R. The effect of whole body vibration exposure on balance and functional mobility in older adults: a systematic review and meta-analysis. *Maturitas*. 2015;80(4):342-358.
39. Rohlmann A, Schmidt H, Gast U, Kutzner I, Damm P, Bergmann G. In vivo measurements of the effect of whole body vibration on spinal loads. *Eur Spine J*. 2014;23(3):666-672.

Figure Legends

Figure 2.1: Vibrational motor

Figure 2.2: Motor displacement and acceleration by frequency

(A) Displacement. (B) Acceleration. The dots on the graphs represent an average of 10, test samples and the vertical lines at each data point represent one standard deviation above and below the indicated value

Figure 2.3: Circuit for micro controller driving motor

Figure 2.4: Effects of variable frequency and locale subcutaneous vibrational stimulus on GABA neuron firing rate in the VTA

(A, B) 50Hz stim given at right hindleg (A) and 115 Hz stim given at cervical spine (B) show no effect on VTA GABA neuron firing rate. C- 50 Hz stim at cervical spine causes a 52.9% reduction in GABA firing rate from 100 to 300 sec.

Figure 2.5 Group data showing average and maximal GABA neuron firing rate depression from baseline

(A) 50 Hz stim to the cervical spine produces an average depression to 69.2% of baseline. (B) 50 Hz stim to the cervical spine produces an average maximal depression to 24.8% of baseline.

CHAPTER 3: Mechanical stimulation of cervical vertebrae modulates the discharge activity of
ventral tegmental area neurons and dopamine release in the nucleus accumbens

**Mechanical stimulation of cervical vertebrae modulates the discharge activity
of ventral tegmental area neurons and dopamine release in the nucleus
accumbens**

Kyle B Bills¹, J Daniel O Bray¹, Travis Clarke¹, Mandy Parsons¹, James Brundage¹, Chae Ha
Yang², Hee Young Kim², Jordan Yorgason¹, Jonathan D Blotter³, and Scott C Steffensen^{1*}

¹ Brigham Young University, Department of Psychology/Neuroscience; Provo, Utah 84602

² College of Korean Medicine, Daegu Haany University, Daegu, South Korea 42158

³ Brigham Young University, Department of Engineering; Provo, Utah 84602

Running title: **MStim Alters Neuronal Activity in VTA and NAc**

*Corresponding Author

Scott C. Steffensen

1050 SWKT

Brigham Young University

Provo UT, 84602

Tel: 801-422-9499

Fax: 801-422-0602

Email: scott_steffensen@byu.edu

Number of pages: 32

Number of figures: 7

Abstract: 209 words

Introduction: 640 words

Discussion: 1412 words

Formatted for *The Journal of Neuroscience*

Abstract

The therapeutic benefits attributed to activation of peripheral mechanoreceptors are poorly understood. There is growing evidence that mechanical stimulation modulates substrates in the supraspinal central nervous system (CNS) that are outside the canonical somatosensory circuits. The aim of this study was to evaluate the effects of mechanical stimulation applied to the cervical spine at the C7-T1 level (termed “MStim”) on neurons and neurotransmitter release in the mesolimbic dopamine (DA) system, an area implicated in reward and motivation. Utilizing electrophysiological, pharmacological, neurochemical and immunohistochemical techniques in male Wistar rats we demonstrate that low frequency (45-80 Hz), but not higher frequency (115 Hz), MStim inhibited the firing rate of ventral tegmental area (VTA) GABA neurons (52.8% baseline; 450 sec) and concomitantly increased the firing rate of VTA DA neurons (248% baseline; 500 sec). Inactivation of the nucleus accumbens (NAc), or systemic or *in situ* antagonism of delta opioid receptors (DORs), blocked MStim inhibition of VTA GABA neuron firing rate. MStim enhanced both basal (178.4 % peak increase at 60 min) and evoked DA release in NAc (135.0 % peak increase at 40 min), which was blocked by *in situ* antagonism of DORs or acetylcholine release in the NAc. MStim enhanced the number of cells expressing c-FOS in the NAc, but inhibited total expression in the VTA, and induced translocation of DORs to neuronal membranes in the NAc. These findings suggest that MStim acts through endogenous opioids in the NAc to modulate DA release in the mesolimbic DA system. These findings demonstrate the need to explore more broadly the extra-somatosensory effects of peripheral mechanoreceptor activation and the specific role for mechanoreceptor-based therapies in the treatment of substance abuse.

Significance Statement

This research is the first to mechanistically describe a rationale for further exploration of physical medicine in the treatment of substance abuse. It is also the first to describe, mechanistically, robust and specific modulation of supraspinal brain circuits in response to targeted peripheral mechanical stimulation. It lays the groundwork for future studies to explore the effects of mechanical stimulation on other brain regions.

Introduction

The use of mechanoreceptor-based therapies in the treatment of drug-abuse disorders is a largely unexplored field. Indeed, the role of mechanoreceptors other than as canonical mediators of somato-sensation has only become relevant in recent years. Whole body vibration (WBV) has been shown to positively impact power and strength [1], flexibility [2, 3], balance [4], bone metabolism [5], hormone release [6], and falls in the elderly [7]. Notably, several complementary health care approaches are thought to have effects mediated in part by activation of mechanoreceptors, including chiropractic medicine, acupuncture, and physical therapy. Early understanding of the mechanisms underlying mechanoreceptor-based therapies such as WBV centered on peripheral neuromechanical alterations. Recent reports have included evidence of increased cortical excitability [8], increased motor evoked potentials [9], and compelling evidence demonstrating CNS changes in response to peripheral mechanical stimulation as measured with fMRI, EEG, heart rate variability, and evoked potentials [8, 10-12]. Notwithstanding these gains, our understanding of the CNS changes induced by peripheral mechanical stimulation remains understudied, and perhaps undervalued.

Midbrain dopamine (DA) neuron activity is involved in many aspects of reward seeking [13-15]. Although the prevailing dogma is that DA neurons mediate the rewarding and addictive properties of drugs of abuse [16], VTA GABA neurons have garnered much interest for their role in modulating DA neuronal activity and DA release and perhaps as independent substrates mediating reward or aversion [17-23]. We have shown previously that acute administration of ethanol, opioids, or cocaine inhibits VTA GABA neurons [17-21, 24], leading to a net disinhibition of VTA DA neurons [25-27]. In contrast, during ethanol or opioid withdrawal, VTA GABA neurons become hyperactive [17, 28] leading to decreased mesolimbic DA activity and release in the NAc [29-33]. This reduction in mesolimbic DA transmission is theorized to be the primary driver of relapse [34].

There is compelling evidence suggesting that some of the benefits ascribed to acupuncture are mediated through somatosensory neuronal pathways. We have shown in multiple reports that stimulation of the HT7 acupoint modifies drug-seeking behaviors and relapse to cocaine [35, 36], methamphetamine [37], and ethanol [38]. These effects can be attenuated with ablation of the dorsal column/medial lemniscal pathway and appear to act through endogenous opioids [39-41].

Though these studies demonstrate anatomically site-specific effects, they are suggestive that activation of primary somatosensory fibers generally may attenuate the reinforcing effects of drugs of abuse.

In this study, we hypothesized that mechanical stimulation of the cervical spine at C7-T1 (termed “MStim”) is sufficient to modulate neuronal activity in the VTA and neurotransmitter release in the NAc and that this effect is driven by activation of endogenous opioids. We have recently reported that MStim of the cervical spine modifies the activity of VTA GABA neurons [42]. Here we extend these studies to include the recording of VTA GABA and DA neurons, DA release, and mechanistic studies demonstrating the role of endogenous opioid release in mediating mechanoreceptor activation of the mesolimbic DA system.

Materials and Methods

Vibrational Motors

A 3 volt, DC coin vibration motor (10 mm x 2.7 mm, DC 3V/0.1A, Uxcell, Hong Kong, CN) was used as the source of vibrational stimulation. The motor, which was encased in a small circular disc with a 10 mm diameter and 2.7 mm width, created vibration due to off-centered weight attached to the motor's rotational shaft. The weight of the motor was 1.5 g and its specifications and performance were as previously reported [42].

Animals and MStim Motor Implantation

Male wistar rats, weighing 250-320 g, from our breeding colony at Brigham Young University were used. Rats were housed in groups of 2-3 at 21-23°C and humidity (55-65%) on a reverse light/dark cycle with *ad libitum* food and water. A 10 mm incision was made either at the C7-T1 levels posteriorly at midline or at the ipsilateral biceps femoris muscle. The fascia was dissected and muscle tissue was left intact. A DC micro coin vibration motor was implanted subcutaneously (to the right of mid-line for cervical implant) and the incision was closed with surgical adhesive tape to maintain consistent motor placement.

Single Cell Electrophysiology

For recordings of VTA GABA neurons, rats were anesthetized using isoflurane and placed in a stereotaxic apparatus. Anesthesia was maintained at 1.5% with 2.0 L of air flow from a nebulizer (Isotec 4, Avante Charolette, NC) driven by an oxygen concentrator (Pureline, Nidek Gamagori Japan). For recordings of DA neurons, 1.5 g/kg urethane was injected IP. Body temperature was maintained at $37.4 \pm 0.4^\circ\text{C}$ by a feedback-regulated heating pad. With the skull exposed, a hole was drilled for placement of a 3.0 M KCl-filled micropipette (2 to 4 M Ω ; 1-2 μm inside diameter), driven into the VTA with a piezoelectric microdrive (EXFO Burleigh 8200 controller and Inchworm, Victor, NY) based on stereotaxic coordinates [from bregma: 5.6 to 6.5 posterior (P), 0.5 to 1.0 lateral (L), 6.5 to 9.0 ventral (V)]. Potentials were amplified with an Multiclamp 700A amplifier (Axon Instruments, Molecular Devices, Union City, CA). Single-cell activity was filtered at 0.3 to 10 kHz (3 dB) with the Multiclamp 700A amplifier and displayed on Tektronix (Beaverton, OR) digital oscilloscopes. Potentials were sampled at 20 kHz (12 bit resolution) with National Instruments (Austin, TX) data acquisition boards in Macintosh computers (Apple

Computer, Cupertino, CA). Extracellularly recorded action potentials were discriminated with a World Precision Instruments WP-121 Spike Discriminator (Sarasota, FL) and converted to computer-level pulses. Single-unit potentials, discriminated spikes, and stimulation events were captured by National Instruments NB-MIO-16 digital I/O and counter / timer data acquisition boards in Macintosh computers.

Characterization of VTA GABA and DA Neurons In vivo

VTA GABA and DA neurons were identified by previously-established stereotaxic coordinates and by spontaneous electrophysiological and pharmacological criteria [43]. VTA GABA neuron discharge activity characteristics included: relatively fast firing rate ($>10\text{Hz}$), ON-OFF phasic non-bursting activity, and an initially negative spike with duration less than $200\text{ }\mu\text{sec}$. In some experiments, GABA neurons were excited by DA ($+40\text{ nA}$) ejected iontophoretically from the recording pipette [20, 21, 44]. Dopamine neurons were identified by relatively slow firing rate ($<10\text{ Hz}$) and an initially positive-going spike of duration greater than $200\text{ }\mu\text{sec}$. Most DA neurons were inhibited by iontophoretic DA from the recording pipette. We evaluated only those spikes that had greater than 5:1 signal-to-noise ratio. After positive neuron identification, baseline firing rate was measured for 5 min to ensure stability prior to MStim.

Grass Stimulator and MStim for In-vivo Recordings

Following measurement of neuronal baseline firing rate, a 60 or 120 sec MStim was introduced. The vibrating motor was controlled by a S44 Grass Stimulator (Grass Medical Instruments, West Warwick, RI). For electrophysiological recordings, the stimulator was set at 3 V for 0.1 msec duration and 0 msec delay [42]. Pulses/sec were varied to produce variations in vibrational frequency. All vibratory stimuli were 60 or 120 sec in duration and followed by 15 min of recording. Experimental groups included GABA neurons recordings following stimuli of 45, 80 and 115 Hz for both 60 and 120 sec with MStim given subcutaneously at the C7/T1 level, GABA neurons recordings following 80 Hz, 120 sec stimuli (this combination resulted in the greatest inhibition of GABA neuron firing rate and was used in all subsequent testing) given subcutaneously at the right biceps femoris muscle and DA neuron recordings after 80 Hz, 120 sec stimuli given subcutaneously at the C7/T1 level. Paired stimulation experiments were performed

with the second stimulation 60 sec after GABA neuron firing rate returned to baseline following the first stimulation.

Fast-Scan Cyclic Voltammetry

Evoked DA release in the NAc was measured by fast-scan cyclic voltammetry (FSCV) *in vivo*. A 7.0 μm diameter carbon fiber was inserted into borosilicate glass capillary tubing (1.2 mm o.d., A-M Systems, Sequim, WA, USA) under negative pressure and subsequently pulled on a vertical pipette puller (Narishige, East Meadow, NY, USA). The carbon fiber electrode (CFE) was cut under microscopic control with 150–200 μm of bare fiber protruding from the end of the glass micropipette. The CFE was back-filled with 3 M KCl. The electrode potential was linearly scanned with a triangular waveform from -0.4 V to 1.3 V and back to -0.4 V versus Ag/AgCl using a scan rate of 400 V/sec. Cyclic voltammograms were recorded at the CFE every 100 msec by means of a ChemClamp voltage clamp amplifier (Dagan Corporation, Minneapolis, MN, USA). Voltammetry recordings were performed and analyzed using customized software (Demon Voltammetry) [45]. For *in vivo* voltammetry recordings of DA signals, rats were anesthetized with 2% isoflurane and placed in a stereotaxic apparatus (David Kopf Instruments, Tujunga, CA, USA). Bipolar, coated stainless steel electrodes were stereotactically implanted into the medial forebrain bundle (MFB; -2.5 mm posterior, $+1.9\text{ mm}$ lateral from bregma, -8.0 to -8.3 mm from skull), and a capillary glass-based CFE in the NAc ($+1.6\text{ mm}$ anterior, $+1.9\text{ mm}$ lateral from bregma, -6.5 to -8.0 mm from skull). The MFB was stimulated with 60 monophasic pulses at 60 Hz (4 msec pulse width) at 2 min intervals until stable for five successive collections, defined as $<10\%$ variance. Recordings were performed in 2 min intervals, with baseline preceding the post-vibratory (80 Hz, 120 sec) recordings. Recordings were performed for 120 min or until baseline was reached, defined as 5 consecutive recordings at previously established baseline.

Microdialysis and High Performance Liquid Chromatography

Microdialysis probes (MD-2200, BASI) were stereotactically inserted into the NAc ($+1.6\text{ AP}$, $+1.9\text{ ML}$, -8.0 DV). Artificial cerebrospinal fluid (aCSF) composed of either 150 mM NaCl, 3 mM KCl, 1.4 mM CaCl_2 , and 0.8 mM MgCl_2 in 10 mM phosphate buffer alone or, additionally, with either 10 nM naltrindole or a combination of 10 μM hexamethonium and 10 μM scopolamine was perfused through the probe at a rate of 3.0 $\mu\text{l/min}$. Samples were collected every 20 min for 4 hr

with MStim occurring after the first 2 hr had elapsed. Determination of the DA concentration in microdialysis samples was performed using a HPLC pump (Ultimate 3000, Dionex, Sunnyvale, CA, USA) connected to an electrochemical detector (Coulochem III, ESA). The detector included a guard cell (5020, ESA) set at +270 mV, a screen electrode (5014B, ESA) set at -100 mV, and a detection electrode (5014B, ESA) set at +220 mV. Dopamine was separated using a C18 reverse phase column (HR-80, Thermo Fisher Scientific, Waltham, MA, USA). Mobile phase containing 75 mM $\text{H}_2\text{NaO}_4\text{P}$, 1.7 mM sodium octane sulfonate, 25 μM EDTA, 0.714 mM triethylamine, and 10% acetonitrile was pumped through the system at a flow rate of 0.5 ml/min.

Preparation of Brain Slices for Imaging and Confocal Microscopy

Rats were anesthetized using isoflurane and placed in a stereotaxic apparatus. Anesthesia was maintained at 1.5% and motor was surgically implanted as described previously. MStim animals were given 120 sec of 80 Hz stimulation. Control animals had motors surgically implanted but not activated. After 2 hours animals underwent transcardial perfusion with 4% paraformaldehyde (PFA). Once perfused, brains were carefully removed and placed in 4% PFA for 24 hrs to facilitate continued fixation. After incubation in PFA, brains were placed in a solution of 30% sucrose in 1X PBS until the density of the brain matched that of the solution and the brains dropped to the bottom of the vial (~24-48 hrs). Brains were then flash frozen in dry ice and mounted on a cold microtome stage. Targeting the VTA and NAc, brains were sliced at 30 μm on the microtome and slices were placed in cryoprotectant (30% ethylene glycol, 30% sucrose, 0.00002% sodium azide, in 0.1 M PB) and kept at -20°C until staining. Slices were washed 3 times in 1x PBS for 10 minutes on a rotator. They were then blocked with a blocking buffer comprised of 4% normal goat serum, 0.1% Triton-X 100 and 1x PBS. Slices were then washed another 3 times in 0.2% PBST on a rotator. Primary antibodies were applied and allowed to incubate for 20 hours. Following staining the slices were washed 3 times in 0.2% PBST and secondary antibodies were applied. After a 2 hr incubation period they were washed another 3 times with 0.2% PBST and once with 1x PBS. Antibodies included Mouse anti-tyrosine hydroxylase (Novus, 1:1328), Sheep anti-c-FOS (Millipore, 1:1000) and Rabbit anti-DOR (LifeSpan, 1:200) as well as secondaries Alexa Fluor 405 Donkey Anti-Sheep from (1:900), Alexa Fluor 594 Goat anti-Rabbit (1:500). To mount slides, sections were placed on microscope slides and dried ~5 min. Once dried, a drop of vectashield (Vector Laboratories) was placed on the tissue, and a cover slip was placed on the slide. Slides set

overnight, and then they were kept at 4°C until imaging. An Olympus FluoView FV1000 confocal microscope was used to image mounted slices. Brain slices were mounted on microscope slides and imaged under oil immersion at 40X. To ensure consistent readings between samples, a constant photomultiplier tube voltage and gain were set between all acquired images.

Data Collection and Statistical Analysis

For single-unit electrophysiology studies, discriminated spikes were processed with a spike analyzer, digitized with National Instruments hardware and analyzed with National Instruments LabVIEW and IGOR Pro software (Wavemetrics, Lake Oswego, OR). Extracellularly recorded single-unit action potentials were discriminated by a peak detector digital processing LabVIEW algorithm. Firing rate data was averaged across neurons at 10 sec intervals and subsequently binned in 50 sec intervals for comparisons across time points. Experimental groups, in aggregate, were compared to unstimulated neurons using a one-way ANOVA then corresponding bins were compared with a Student's t-test. Average depression or excitation in firing was calculated from the point where firing rate deviated by >10% from baseline to the time it returned to within 10% of baseline. Baseline firing rate was calculated from the average of the final 60 sec of firing rate data before vibrational stimulus and after 5 min of recording to ensure neuron stability. The results from all MStim and control groups were derived from calculations performed on ratemeter records and expressed as means \pm SEM.

For microdialysis, the area under the curve for the DA peak was extracted and a two-point calibration was used to approximate the DA concentration. All collections were normalized to the final baseline collection before the MStim occurred. Standard error for the final baseline collection was approximated using the scalar property. Dopamine release for each timepoint following MStim was then compared to the baseline control using a Dunnett's analysis. Reverse microdialysis and VTA injection experiments were compared to the MStim alone group using a Student's t-test at the 60 min time point.

For FSCV, evoked recordings were normalized to the established baseline within subjects and then averaged across subjects in corresponding time intervals. Data was then binned in 10 min intervals. Comparisons were made for each 10 min bin to control using a Dunnett's analysis. All

statistical tests were performed in JMP13 (SAS, Cary, NC). Figures were compiled using IGOR Pro Software (Wavemetrics, Lake Oswego, OR).

For brain slice imaging, images were loaded into FIJI software. Images were duplicated to preserve the original settings while color thresholding and brightness contrast adjustments were made to determine the location of cells and create ROIs. ROIs were then projected back onto the unedited images where area and mean intensity were recorded for each channel. This process was performed by three independent raters blinded to the hypothesis. To determine relative density of DORs, the ratio of mean fluorescence to area was determined.

Results

MStim Modulation of VTA Neurons

The effects of MStim on VTA GABA neuron firing rate were tested across multiple stimulus frequencies and durations (**Fig. 3.1**), as previously described[46]. MStim at 45 Hz (60 sec) significantly inhibited GABA neuron firing rate when compared to unstimulated baseline firing ($F_{(1,277)} = 24.9997$, $p < 0.0001$; **Fig. 3.1A**). GABA neuron firing rate was significantly reduced from 50 sec to 250 sec post-stimulus when compared to baseline ($n=4$; 50 sec, $p=.0216$; 100 sec, $p=.0460$; 150 and 200 sec, $p < .0001$; 250 sec, $p=.0222$). Stimulation at 80 Hz (60 sec) ($F_{(1,272)} = 10.1423$, $p=0.0016$; **Fig. 3.1B**) produced GABA inhibition similar to that produced by 45 Hz, with significant depression from 100 to 250 sec post-stimulus ($n=5$; 100 sec, $p=.0186$; 150 and 200 sec, $p < .0001$; 250 sec, $p=.0101$). MStim effects with the same frequencies at a duration of 120 sec are shown in **Fig. 3.1D-F**. A 45 Hz stimulation (120 sec) significantly inhibited VTA GABA neurons ($F_{(1,282)} = 15.2029$, $p=0.0001$; **Fig. 3.1D**) similar to that observed with 60 sec MStim ($n=5$, 250 sec, $p=.0032$; 300 sec, $p < .0001$; 350 sec, $p=.0434$). The greatest inhibition to GABA neuron firing rate occurred following application of 80 Hz (120 sec) MStim ($F_{(1,296)} = 114.0478$, $p < 0.0001$; **Fig. 3.1E**). Following this intervention, GABA neurons were significantly inhibited from 50 to 450 sec post-stimulus ($n=7$, 50-350 sec and 450 sec, $p < .0001$; 400 sec, $p=.0028$). In contrast, both 60 and 120 sec of 115 Hz stimulation (**Fig. 3.1C,F**) did not produce a significant depression to GABA neuron firing rate at any time point measured. Thus, GABA neuron firing was inhibited by MStim in a differential and frequency-dependent manner.

Somatosensory mechanoreceptor density varies by topographical location, with greatest density in the proximal joints and lower density in distal muscle [47, 48]. Therefore, to investigate differences in anatomical application of the MStim, a location with a relatively smaller concentration of mechanoreceptors was tested. Mechanical stimulation of 80 Hz (120 sec) at the belly of the right biceps femoris muscle produced only a small erratic decrease in GABA neuron firing rate when compared to the same stimulation at C7-T1 ($F_{(1,421)} = 146.4646$, $p < .0001$; **Fig. 3.2A**). The two were significantly different at 100-200 and 300 sec post-stimulus ($n=4$; 100 sec, $p=.0137$; 150 sec, $p=.0021$), suggesting that MStim-dependent inhibition of VTA GABA firing is greatest at areas of high mechanoreceptor density. Next, the effects of paired MStim was tested on VTA GABA firing rate (**Fig. 3.2B**). . Compared to the second stimulation, the first typically produced greater inhibition of VTA GABA firing rate ($F_{(1,411)} = 29.2118$, $p < .0001$). Significant differences were

noted at 100-200 sec and 300 sec (n=5; 100 sec, $p=.0137$; 150 sec, $p=.0021$; 200 sec, $p=.0078$; 300 sec, $p=.0033$). Thus, MStim-dependent inhibition of firing rate was repeatable, but sensitive to desensitization-dependent processes. The 80 Hz (120 sec) stimulation produced the greatest effect on GABA neuron firing rate and was used in all subsequent experiments.

Since the dogma is that VTA GABA neurons provide inhibitory input onto local DA neurons, the effects of MStim on VTA DA neuron firing was tested. Dopamine neuron firing rate increased significantly post-stimulus ($F_{(1,429)} = 246.4261$, $p<0.0001$; **Fig. 3.3A**) reaching an average maximum increase of 286% of baseline at 150 sec post-stimulus. Firing rate increased significantly within the first 50 sec and stayed elevated to 500 sec post-stimulus. These time points (50-500 sec post-stimulus) were all significant when compared to unstimulated baseline DA neuron firing rate over time (n=5; 50-250 and 350-400 sec, $p<.0001$; 300 sec, $p=.0026$; 450 sec, $p=.0145$; 500 sec, $p=.0389$; **Fig. 3.3B**). On average, following MStim, DA neurons increased firing rate to 247% of baseline compared to 52.8 % inhibition observed in GABA neurons (**Fig. 3.3C**). The increase in DA neuron firing rate occurred in parallel to the reported decrease in GABA neuron firing rate noted from the same stimulation paradigm, suggesting disinhibition of DA neurons from decreased GABA neuron firing.

MStim Modulation of VTA Neurons: Role of NAc Projections and Endogenous Opioids

We have previously demonstrated that stimulation of the NAc inhibits VTA GABA neurons [43], via direct pathway GABAergic medium spiny neurons, and that opiate effects on VTA GABA neuron firing rate are mediated, in part, via GABA input to the VTA from the NAc [24]. To determine if MStim modulation of VTA GABA neurons was in the VTA or via NAc input to the VTA we evaluated the effects of *in situ* administration of the sodium channel blocker lidocaine into the NAc on MStim effects on VTA GABA neuron firing rate. Inactivation of NAc neurons by perfusion of lidocaine into the NAc via reverse microdialysis was sufficient to block MStim-induced depression of VTA GABA firing ($F_{(1,416)} = 264.9918$, $p<.0001$; n=5; **Fig. 3.4A**). All time points from 50-500 sec were significantly different (80 Hz 120 sec w/ lidocaine injection in NAc, n=5; 80 Hz 120 sec, n=7; 50 sec, $p<.0001$; 100 sec, $p<.0001$; 150 sec, $p<.0001$; 200 sec, $p<.0001$; 250 sec, $p<.0001$; 300 sec, $p<.0001$; 350 sec, $p=.0005$; 400 sec, $p<.0001$; 450 sec, $p<.0001$; 500 sec, $p<.0001$). We have previously shown that stimulation of the HT7 acupoint inhibits VTA GABA neuron firing rate, which is blocked by systemic administration of the non-selective opioid

receptor (OR) antagonist naloxone and the delta OR (DOR) antagonist naltrindole [38]. To better understand the role that DORs play in the underlying mechanisms responsible for the reported mesolimbic effects of MStim, the 80 Hz (120 sec) stimulation experiments were repeated while recording from GABA neurons in the VTA. First, systemic pretreatment with naltrindole (1 mg/kg IP), 15 min prior to MStim precluded the depression of GABA neuron firing rate ($F_{(1,487)} = 190.4457$, $p < .0001$; $n=4$; **Fig. 3.4A,B**). The depression was blocked at every time point that was previously significant when comparing the 80 Hz stimulus to unstimulated baseline recordings in GABA neurons. The differences between 80 Hz w/ naltrindole and 80 Hz alone were pronounced and noted at all time points from 50-500 sec (80 Hz 120 sec w/ naltrindole, $n=4$; 80 Hz 120 sec, $n=7$; 50 sec, $p < .0001$; 100 sec, $p < .0001$; 150 sec, $p < .0001$; 200 sec, $p < .0001$; 250 sec, $p < .0001$; 300 sec, $p < .0001$; 350 sec, $p = .0017$; 400 sec, $p = .0101$; 450 sec, $p = .0002$; 500 sec, $p < .0001$).

MStim Enhancement of Dopamine Release: Role of Endogenous Opioids

To determine if MStim-induced changes in DA firing might translate to an increase in DA neurotransmission, microdialysis and voltammetry experiments were performed on basal and evoked DA release in the NAc, respectively. Microdialysis experiments revealed an increase in basal release, with greatest release occurring from 40 – 60 min ($178.43 \pm 26.24\%$ of baseline), after MStim ($n=15$; 60 min, Dunnett's, $p = .016$; **Fig. 3.5A**). From 80 to 120 min post-stimulus, DA levels returned to baseline levels and stabilized. Next, voltammetry experiments were used to measure rapid changes in electrically evoked DA release. Evoked DA release rose slightly faster than basal release with significant increases 10 min post-stimulus (**Fig. 3.5B**). Increased levels of evoked DA release were significantly maintained from 10-50 min, peaking at 40 min ($135.03 \pm 23.13\%$ of baseline), with a return to baseline levels at 60 min ($n=4$; Dunnett's 10 min, $p = .0176$; 20 min, $p = .0053$; 30 min, $p = .0781$; 40 min, $p = .0006$; 50 min, $p = .0023$). Thus, MStim produces increases in DA levels.

We then evaluated the role of endogenous opioids in mediating MStim-induced enhancement of DA release in the NAc. To determine the site specificity of the DORs involved in the effect (VTA versus NAc) we administered an ipsilateral injection of naltrindole into the VTA 15 min prior to stimulation and found unexpectedly that it did not attenuate MStim-induced DA release in the NAc ($n=15$, MStim alone; $n=4$, VTA naltrindole; $p = 0.570$). Next, to determine whether local antagonism of NAc DORs contributes to MStim induced increases in DA release, we applied

naltrindole via reverse microdialysis (10 nM) in the NAc prior to MStim at the cervical spine (**Fig. 3.6A**). Local application of naltrindole blocked the MStim-induced increase in DA release in the NAc at the 60 min time point from $178.43 \pm 26.24\%$ of baseline in the MStim alone group to $88.0 \pm 9.31\%$ of baseline ($n=15$, MStim alone; $n=8$, naltrindole NAc; $p=.0096$; **Fig. 3.6B**). As sensory-driven cholinergic interneurons (CINs) in the NAc express DORs and have been shown to influence local DA release [49, 50], a combination of hexamethonium (10 μ M) and scopolamine (10 μ M) was then administered to the NAc via reverse microdialysis to evaluate the role of local acetylcholine (ACh) release on MStim induced DA release (**Fig. 3.6A**). At the 60 min time point DA release increased to $107.62 \pm 3.4\%$ of baseline which represents significant attenuation of the MStim induced DA increase when compared to the MStim alone group ($n=15$, MStim alone; $n=8$, Hex/Scop NAc; $p=.0311$; **Fig. 3.6B**). These data suggest that the MStim-induced increase in DA release in the NAc is mediated through endogenous activation of DORs in the NAc and not the VTA and that the effect is in part influenced by local release of Ach from CINs.

MStim Activation of NAc Neurons

To further evaluate neuronal activation changes in the NAc and VTA and alterations in DOR expression in the NAc following MStim, post-MStim brain slices were stained to evaluate changes in relative expression of DORs and c-FOS. The number of cells per slide expressing DORs in the NAc was significantly increased in the MStim group when compared to control ($F_{(1,11)} = 10.6$, $p=0.008$; $n=6$; **Fig. 3.7A,B,E**). c-FOS expression in the NAc and VTA was analyzed for mean number of cell counts and mean fluorescent intensity (MFI). There was an increase in the number of cells expressing c-FOS in the NAc following MStim (53.0 ± 6.29) when compared to control (33.83 ± 6.79 ; $p=0.0314$, $n=6$), but not in the VTA (50.50 ± 2.94 vs 65.83 ± 9.36 cells; $p=0.0847$; **Fig. 3.7C**). However, when considering c-FOS MFI, there was a decrease in c-FOS expression in the VTA with MStim ($109.6 \pm 0.9\%$ vs $116.8 \pm 1.2\%$; $p=0.0071$, $n=6$; **Fig. 3.7D**), but not in the NAc. Together, these data suggest that the decrease in VTA c-FOS expression following MStim is likely due to enhanced inhibitory projections from the NAc.

Discussion

In this study, pathway specific experiments were performed to better understand the role of MStim in natural reward pathways. Low to high frequency (45-80 Hz) MStim produced robust inhibition of VTA GABA neurons. This was not surprising given our previous reports regarding mechanoreceptor-mediated inhibition of VTA GABA neurons [38, 42]. However, here we demonstrated that decreases in VTA GABA neuron firing by MStim are frequency, location, and time-dependent, and are accompanied by concomitant increases in VTA DA cell firing, increases in DA release in the NAc and mediation by endogenous opioid and local ACh release in the NAc. The three frequencies tested were chosen to target specific mechanoreceptors. Of those chosen, 45 Hz enlists mostly Meissner's corpuscles [51, 52], while 115 Hz is more selective for Pacinian corpuscles [53, 54]. Both receptors are subcutaneously located. The frequency of 80 Hz lies between the two and likely activates both receptors. Additionally, all three frequencies can activate Ruffini endings and Golgi tendon organs, two receptors that are morphologically similar to one another and are important as joint mechanoreceptors [55-57]. The 50 and 80 Hz MStim produced a transient depression of GABA neurons in the VTA, with 80 Hz (120 sec) producing the largest and longest lasting effect. Importantly, 80 Hz MStim failed to achieve a meaningful depression in VTA GABA neuron firing rate when applied at the belly of the biceps femoris muscle. This mid-muscle location was chosen because of its distance from joints and subsequent lower concentration of mechanoreceptors relative to the cervical spine [47, 48, 54]. Given that 80 Hz produced the greatest inhibition, 115 Hz failed to elicit a response and that the mid-muscle stimulation was ineffective at 80 Hz, suggesting a role for deep joint mechanoreceptors and Meissner's corpuscle dependent pathways as main mediators of the resultant GABA depression. Taken together, these data suggest that the noted effects are only anatomically specific inasmuch as anatomical location relates to the potential for mechanoreceptor recruitment. Even dorsal root ganglion cell bodies have been shown to depolarize in response to mechanical stimulation [58], perhaps enhancing the effects noted from stimulation to spine. It is also worth noting that subcutaneous stimulation provided in this study to the cervical spine is likely to have impacted most of the cervical and some of the thoracic spine, increasing the number of cutaneous and joint receptors activated. To our knowledge, this is the first evidence demonstrating that localized MStim increases DA neuron firing rate in the VTA and increases DA release in the NAc. Mechanical stimulation at 80 Hz (120 sec) elicited DA neuron firing of 247% baseline that occurred simultaneous to the average

depression of GABA neurons to 52.8% of baseline (**Fig. 3.3C**). This relationship suggests a disinhibition of DA neurons by way of GABA neuron depression.

Though previous studies have implicated DORs in the mechanoacupuncture-elicited depression of VTA GABA neurons [38], the location of DORs (spinal versus mesolimbic) has not been described. The present results suggest that mechanoreceptor stimulation results in increases in endogenous opioid release leading to transient modulation to the mesolimbic circuitry. There is a precedence for frequency-dependent release of endogenous opioids. For instance, in rats tolerant to morphine, low frequency (1-15 Hz) transcutaneous electrical nerve stimulation (TENS) was less effective than placebo controls at reducing joint inflammation, suggesting that TENS-alleviated joint inflammation is opioid dependent [59, 60]. Also, the effects of low frequency, but not high frequency, TENS stimulation are blocked by application of naloxone at doses selective for mu opioid receptors (MORs) and sparing of DORs and KORs [61]. Conversely, administration of the selective DOR antagonist naltrindole blocks the effects of high frequency TENS but spares those of a similar low frequency stimulation, though this effect appears to be isolated to spinal circuits [61]. While KORs have been shown on both cell bodies and terminals of DA neurons, MORs and DORs are absent [62]. However, DORs are located on synaptic terminals of GABA neurons in the VTA and NAc [62] and, of particular relevance to this study, on CINs in the NAc[63]. Delta opioid receptors are located in both the VTA and NAc [64, 65] and systemic (IP) administration of naltrindole blocked MStim effects on VTA neuron firing rate and DA release in the NAc. Interestingly, MStim-induced increase in NAc DA release was attenuated by selective blockade of DORs with naltrindole in the NAc but not the VTA. Corroboration of the VTA effects being driven by activity in the NAc was confirmed when MStim-induced VTA GABA neuron depression was blocked by local administration of lidocaine into the NAc. In light of the receptor distribution, the site-specific effect of DOR antagonists, the attenuation by NAc lidocaine application, the disparate expression of c-FOS in the NAc and VTA and the congruity of GABA depression and DA excitation (**Fig. 3.4C**), these data suggest that VTA effects are mainly due to NAc to VTA projections.

Voltammetry data shows a fast increase in evoked release that returns to baseline within 60 min while microdialysis shows a more gradual increase, peaking around 60 min post-stimulus (**Fig. 3.5A and 3.5B**). Interestingly, because GABA and DA neuron firing rates returned to baseline

after 464.3 and 366.7 sec post-stimulus, respectively, it is apparent that other factors influence the elevation in DA release, allowing release levels to remain elevated after VTA neuron firing rate has returned to baseline. This coupled with the fact that DA release was attenuated by blockade of both cholinergic and DORs in the NAc but not the VTA suggests that local factors related to DA terminals are the main drivers of MStim-induced DA release. One factor that needs careful consideration in the timing and mechanisms underlying MStim-induced DA increases are the multiple converging pathways onto the mesolimbic DA system (both in somatic and distal axonic regions). Dopamine terminals can be modulated independently of activity in cell body regions [49]. Specifically, sensory thalamic projections activate striatal CINs, which drive DA release through nicotinic acetylcholine (ACh) receptor activation. Further, accumbal DA release has been shown to increase with administration of DPDPE, a DOR agonist, in a dose-dependent manner with the effects lasting around 60 min *in vivo* when measured with microdialysis [66]. Therefore, it is also possible that MStim induces striatal release onto local DORs to further enhance DA release, as suggested by the near total blockage of MStim-induced DA release with NAc application of naltrindole. In the striatum, DORs exhibit increased levels of membrane translocation on CINs in response to acute cocaine administration, learning events and by activation of D1 receptors [67, 68]. This is particularly relevant considering the increased DOR translocation caused by MStim in the NAc. Activation of DORs on striatal CINs can induce hyperpolarization-activated currents that results in burst firing of CINs [67, 69], which can, in turn, lead to further release of DA by activation of ACh receptors located on DA terminals. As previously noted, MStim effects on VTA GABA neurons are likely secondary to MStim effects in the NAc and changes in DA release are likely through changes in CIN circuit effects, local activation of DORs and reciprocal projections from the NAc to VTA. It is also unknown if other non-GABA effects are contributing to MStim-induced increases in DA release.

Mechanoreceptors remain some of the least understood physiologic receptors, especially non-canonical activation effects on central processes including modulation of neurons in sub-cortical structures like the midbrain. Even some basic aspects of their methods of signal transduction and pathways recruited remain elusive. In spite of this, it is becoming increasingly evident that mechanoreceptors play a broader role than simply as somatosensory relay devices [1-4]. Here we begin exploration of their effects on mesolimbic circuitry. The mesolimbic DA system is a therapeutic target of treatments for a myriad of conditions including depression, ADHD, eating

disorders, Parkinson's and addiction and there is a pressing need for new treatments to serve as adjuncts to current pharmacological approaches. Future studies should explore the possibility that practitioners of manual medicine, chiropractic physicians, acupuncturists, and physical therapists, might play in the development and implementation of adjunctive treatments for drug-abuse disorders. It remains to be seen if specific application of MStim therapy can alter drug-seeking behavior, which we are currently pursuing. Further, though these findings are specific to neurons in one circuit, they open the possibility that translational findings in other brain regions could lead to novel applications for mechanoreceptor-based therapies.

References

1. Bosco, C., M. Cardinale, and O. Tsarpela, *Influence of vibration on mechanical power and electromyogram activity in human arm flexor muscles*. Eur J Appl Physiol Occup Physiol, 1999. **79**(4): p. 306-11.
2. Feland, J.B., et al., *Whole body vibration as an adjunct to static stretching*. Int J Sports Med, 2010. **31**(8): p. 584-9.
3. Houston, M.N., et al., *The effectiveness of whole-body-vibration training in improving hamstring flexibility in physically active adults*. J Sport Rehabil, 2015. **24**(1): p. 77-82.
4. Tseng, S.Y., et al., *Effect of two frequencies of whole-body vibration training on balance and flexibility of the elderly: a randomized controlled trial*. Am J Phys Med Rehabil, 2016. **95**(10): p. 730-7.
5. Dionello, C.F., et al., *Effects of whole body vibration exercises on bone mineral density of women with postmenopausal osteoporosis without medications: novel findings and literature review*. J Musculoskelet Neuronal Interact, 2016. **16**(3): p. 193-203.
6. Paineiras-Domingos, L.L., et al., *Can whole body vibration exercises affect growth hormone concentration? A systematic review*. Growth Factors, 2017. **35**(4-5): p. 189-200.
7. Jepsen, D.B., et al., *Effect of whole-body vibration exercise in preventing falls and fractures: a systematic review and meta-analysis*. BMJ Open, 2017. **7**(12): p. e018342.
8. Krause, A., et al., *Acute corticospinal and spinal modulation after whole body vibration*. J Musculoskelet Neuronal Interact, 2016. **16**(4): p. 327-338.
9. Mileva, K.N., J.L. Bowtell, and A.R. Kossev, *Effects of low-frequency whole-body vibration on motor-evoked potentials in healthy men*. Exp Physiol, 2009. **94**(1): p. 103-16.
10. Zhang, N., et al., *The Effects of Physical Vibration on Heart Rate Variability as a Measure of Drowsiness*. Ergonomics, 2018: p. 1-19.
11. Kaut, O., et al., *Stochastic resonance therapy induces increased movement related caudate nucleus activity*. J Rehabil Med, 2016. **48**(9): p. 815-818.
12. Satou, Y., et al., *Effect of short-term exposure to whole body vibration in humans: relationship between wakefulness level and vibration frequencies*. Kurume Med J, 2009. **56**(1-2): p. 17-23.
13. Gentry, R.N., D.R. Schuweiler, and M.R. Roesch, *Dopamine signals related to appetitive and aversive events in paradigms that manipulate reward and avoidability*. Brain Res, 2018.
14. Ranaldi, R., *Dopamine and reward seeking: the role of ventral tegmental area*. Rev Neurosci, 2014. **25**(5): p. 621-30.
15. Dalle Grave, R., S. Calugi, and G. Marchesini, *Compulsive exercise to control shape or weight in eating disorders: prevalence, associated features, and treatment outcome*. Compr Psychiatry, 2008. **49**(4): p. 346-52.
16. Wise, R.A., *Dopamine and reward: the anhedonia hypothesis 30 years on*. Neurotox Res, 2008. **14**(2-3): p. 169-83.
17. Gallegos, R.A., et al., *Adaptive responses of GABAergic neurons in the ventral tegmental area to chronic ethanol*. J. Pharmacol. Exp. Ther., 1999. **291**: p. 1045-1053.
18. Steffensen, S.C., et al., *Contingent and non-contingent effects of low-dose ethanol on GABA neuron activity in the ventral tegmental area*. Pharmacol Biochem Behav, 2009. **92**(1): p. 68-75.
19. Stobbs, S.H., et al., *Ethanol suppression of ventral tegmental area GABA neuron electrical transmission involves NMDA receptors*. J Pharmacol Exp Ther, 2004. **311**(1): p. 282-289.
20. Ludlow, K.H., et al., *Acute and chronic ethanol modulate dopamine D2-subtype receptor responses in ventral tegmental area GABA neurons*. Alcohol Clin Exp Res, 2009. **33**(5): p. 804-11.

21. Steffensen, S.C., et al., *Cocaine disinhibits dopamine neurons in the ventral tegmental area via use-dependent blockade of GABA neuron voltage-sensitive sodium channels*. Eur J Neurosci, 2008. **28**(10): p. 2028-40.
22. Brown, M.T., et al., *Ventral tegmental area GABA projections pause accumbal cholinergic interneurons to enhance associative learning*. Nature, 2012. **492**(7429): p. 452-6.
23. Tan, K.R., et al., *GABA neurons of the VTA drive conditioned place aversion*. Neuron, 2012. **73**(6): p. 1173-83.
24. Steffensen, S.C., et al., *Contingent and non-contingent effects of heroin on mu-opioid receptor-containing ventral tegmental area GABA neurons*. Exp Neurol, 2006. **202**(1): p. 139-51.
25. Carboni, E., et al., *Amphetamine, cocaine, phencyclidine and nomifensine increase extracellular dopamine concentrations preferentially in the nucleus accumbens of freely moving rats*. Neuroscience, 1989. **28**(3): p. 653-61.
26. Yoshimoto, K., et al., *Alcohol stimulates the release of dopamine and serotonin in the nucleus accumbens*. Alcohol, 1992. **9**(1): p. 17-22.
27. Bocklisch, C., et al., *Cocaine disinhibits dopamine neurons by potentiation of GABA transmission in the ventral tegmental area*. Science, 2013. **341**(6153): p. 1521-5.
28. Bonci, A. and J.T. Williams, *Increased probability of GABA release during withdrawal from morphine*. J. Neurosci., 1997. **17**: p. 796-803.
29. Koeltzow, T.E. and F.J. White, *Behavioral depression during cocaine withdrawal is associated with decreased spontaneous activity of ventral tegmental area dopamine neurons*. Behav Neurosci, 2003. **117**(4): p. 860-5.
30. Karkhanis, A.N., et al., *Switch from excitatory to inhibitory actions of ethanol on dopamine levels after chronic exposure: Role of kappa opioid receptors*. Neuropharmacology, 2016. **110**: p. 190-197.
31. Maisonneuve, I.M., A. Ho, and M.J. Kreek, *Chronic administration of a cocaine "binge" alters basal extracellular levels in male rats: an in vivo microdialysis study*. J Pharmacol Exp Ther, 1995. **272**(2): p. 652-7.
32. Rose, J.H., et al., *Supersensitive Kappa Opioid Receptors Promotes Ethanol Withdrawal-Related Behaviors and Reduce Dopamine Signaling in the Nucleus Accumbens*. Int J Neuropsychopharmacol, 2016. **19**(5).
33. Wise, R.A., *Dopamine, learning and motivation*. Nat Rev Neurosci, 2004. **5**(6): p. 483-94.
34. Lyness, W.H. and F.L. Smith, *Influence of dopaminergic and serotonergic neurons on intravenous ethanol self-administration in the rat*. Pharmacol Biochem Behav, 1992. **42**(1): p. 187-92.
35. Jin, W., et al., *Acupuncture reduces relapse to cocaine-seeking behavior via activation of GABA neurons in the ventral tegmental area*. Addict Biol, 2018. **23**(1): p. 165-181.
36. Yoon, S.S., et al., *Effects of acupuncture on stress-induced relapse to cocaine-seeking in rats*. Psychopharmacology (Berl), 2012. **222**(2): p. 303-11.
37. Kim, N.J., et al., *Acupuncture inhibition of methamphetamine-induced behaviors, dopamine release and hyperthermia in the nucleus accumbens: mediation of group II mGluR*. Addict Biol, 2019. **24**(2): p. 206-217.
38. Yang, C.H., et al., *Acupuncture inhibits GABA neuron activity in the ventral tegmental area and reduces ethanol self-administration*. Alcohol Clin Exp Res, 2010. **34**(12): p. 2137-46.
39. Kim, S.A., et al., *Peripheral afferent mechanisms underlying acupuncture inhibition of cocaine behavioral effects in rats*. PLoS One, 2013. **8**(11): p. e81018.
40. Yang, C.H., B.H. Lee, and S.H. Sohn, *A possible mechanism underlying the effectiveness of acupuncture in the treatment of drug addiction*. Evid Based Complement Alternat Med, 2008. **5**(3): p. 257-66.

41. Chang, S., et al., *Spinal pathways involved in somatosensory inhibition of the psychomotor actions of cocaine*. Sci Rep, 2017. **7**(1): p. 5359.
42. Bills, K.B., et al., *Targeted Subcutaneous Vibration With Single-Neuron Electrophysiology As a Novel Method for Understanding the Central Effects of Peripheral Vibrational Therapy in a Rodent Model*. Dose Response, 2019. **17**(1): p. 1559325818825172.
43. Steffensen, S.C., et al., *Electrophysiological characterization of GABAergic neurons in the ventral tegmental area*. J Neurosci, 1998. **18**(19): p. 8003-15.
44. Lassen, M.B., et al., *Brain stimulation reward is integrated by a network of electrically coupled GABA neurons*. Brain Res, 2007. **1156**: p. 46-58.
45. Yorgason, J.T., R.A. Espana, and S.R. Jones, *Demon voltammetry and analysis software: analysis of cocaine-induced alterations in dopamine signaling using multiple kinetic measures*. J Neurosci Methods, 2011. **202**(2): p. 158-64.
46. Bills, K., Clarke, T., Major, G., Jacobson, C., Blotter, J., Feland, J., Steffensen, S, *Targeted Subcutaneous Vibration with Single-Neuron Electrophysiology as a Novel Method for Understanding the Central Effects of Peripheral Vibrational Therapy in a*. Dose Response, 2019.
47. McLain, R.F., *Mechanoreceptor endings in human cervical facet joints*. Spine (Phila Pa 1976), 1994. **19**(5): p. 495-501.
48. McLain, R.F. and K. Raiszadeh, *Mechanoreceptor endings of the cervical, thoracic, and lumbar spine*. Iowa Orthop J, 1995. **15**: p. 147-55.
49. Yorgason, J.T., D.M. Zeppenfeld, and J.T. Williams, *Cholinergic Interneurons Underlie Spontaneous Dopamine Release in Nucleus Accumbens*. J Neurosci, 2017. **37**(8): p. 2086-2096.
50. Threlfell, S., et al., *Striatal dopamine release is triggered by synchronized activity in cholinergic interneurons*. Neuron, 2012. **75**(1): p. 58-64.
51. Fleming, M.S. and W. Luo, *The anatomy, function, and development of mammalian Abeta low-threshold mechanoreceptors*. Front Biol (Beijing), 2013. **8**(4).
52. Macefield, V.G., *Physiological characteristics of low-threshold mechanoreceptors in joints, muscle and skin in human subjects*. Clin Exp Pharmacol Physiol, 2005. **32**(1-2): p. 135-44.
53. Biswas, A., M. Manivannan, and M.A. Srinivasan, *Vibrotactile sensitivity threshold: nonlinear stochastic mechanotransduction model of the Pacinian Corpuscle*. IEEE Trans Haptics, 2015. **8**(1): p. 102-13.
54. Zelena, J., *The development of Pacinian corpuscles*. J Neurocytol, 1978. **7**(1): p. 71-91.
55. Vega, J.A., et al., *The Meissner and Pacinian sensory corpuscles revisited new data from the last decade*. Microsc Res Tech, 2009. **72**(4): p. 299-309.
56. Albuérne, M., et al., *Development of Meissner-like and Pacinian sensory corpuscles in the mouse demonstrated with specific markers for corpuscular constituents*. Anat Rec, 2000. **258**(3): p. 235-42.
57. Vega, J.A., J.J. Haro, and M.E. Del Valle, *Immunohistochemistry of human cutaneous Meissner and pacinian corpuscles*. Microsc Res Tech, 1996. **34**(4): p. 351-61.
58. Viatchenko-Karpinski, V. and J.G. Gu, *Mechanical sensitivity and electrophysiological properties of acutely dissociated dorsal root ganglion neurons of rats*. Neurosci Lett, 2016. **634**: p. 70-75.
59. Sluka, K.A., *Systemic morphine in combination with TENS produces an increased antihyperalgesia in rats with acute inflammation*. J Pain, 2000. **1**(3): p. 204-11.
60. Sluka, K.A., et al., *Low frequency TENS is less effective than high frequency TENS at reducing inflammation-induced hyperalgesia in morphine-tolerant rats*. Eur J Pain, 2000. **4**(2): p. 185-93.
61. Kalra, A., M.O. Urban, and K.A. Sluka, *Blockade of opioid receptors in rostral ventral medulla prevents antihyperalgesia produced by transcutaneous electrical nerve stimulation (TENS)*. J Pharmacol Exp Ther, 2001. **298**(1): p. 257-63.

62. Trigo, J.M., et al., *The endogenous opioid system: a common substrate in drug addiction*. Drug Alcohol Depend, 2010. **108**(3): p. 183-94.
63. Britt, J.P. and D.S. McGehee, *Presynaptic opioid and nicotinic receptor modulation of dopamine overflow in the nucleus accumbens*. J Neurosci, 2008. **28**(7): p. 1672-81.
64. Margolis, E.B., et al., *Two delta opioid receptor subtypes are functional in single ventral tegmental area neurons, and can interact with the mu opioid receptor*. Neuropharmacology, 2017. **123**: p. 420-432.
65. Hipolito, L., et al., *Shell/core differences in mu- and delta-opioid receptor modulation of dopamine efflux in nucleus accumbens*. Neuropharmacology, 2008. **55**(2): p. 183-9.
66. Hirose, N., et al., *Interactions among mu- and delta-opioid receptors, especially putative delta1- and delta2-opioid receptors, promote dopamine release in the nucleus accumbens*. Neuroscience, 2005. **135**(1): p. 213-25.
67. Bertran-Gonzalez, J., et al., *Learning-related translocation of delta-opioid receptors on ventral striatal cholinergic interneurons mediates choice between goal-directed actions*. J Neurosci, 2013. **33**(41): p. 16060-71.
68. Heath, E., et al., *Substance P and dopamine interact to modulate the distribution of delta-opioid receptors on cholinergic interneurons in the striatum*. Eur J Neurosci, 2018. **47**(10): p. 1159-1173.
69. Laurent, V., et al., *delta-opioid and dopaminergic processes in accumbens shell modulate the cholinergic control of predictive learning and choice*. J Neurosci, 2014. **34**(4): p. 1358-69.

Figure Legends

Figure 3.1 – Frequency and duration-dependent effects of MStim on VTA GABA neuron firing rate.

(A-C) Summarized time course data for 45 (A), 80 (B) and 115 Hz (C) stimulation at 60 sec duration. Representative ratemeter recordings of VTA GABA neurons are shown on the left and summarized data on the right. Note that 45 and 80 Hz MStim significantly inhibited the firing rate of VTA GABA neurons while 115 Hz had no effect. (D-F) The same set of frequency responses, but with a 120 sec stimulation. Note that 45 and 80 Hz MStim significantly inhibited VTA GABA neuron firing rate while 115 Hz had no effect, and that the inhibition was more pronounced with longer MStim durations. Asterisks *, **, *** indicate significance levels $p < 0.05$, 0.01 and 0.001, respectively.

Figure 3.2 – Spatiotemporal variation in MStim-induced effects on VTA GABA neuron firing rate.

(A) VTA GABA neuron response to MStim (80 Hz; 120 sec) at the right biceps femoris muscle belly compared to cervical spine at C7-T1. Note that MStim at the biceps femoris was without effect on VTA GABA neuron firing rate. (B) VTA GABA neuron response to MStim at the C7-T1 vertebral level by two subsequent stimuli. Note the diminution in VTA GABA neuron firing rate with the second 80 Hz, 120 sec stimulation compared to the first. Asterisks *, **, *** indicate significance levels $p < 0.05$, 0.01 and 0.001, respectively.

Figure 3.3 – Dopamine neuron response to MStim.

(A) Representative trace of DA neuron firing rate in response to MStim (80 Hz; 120 sec). Note that MStim markedly increased the firing rate of this VTA DA neuron. (B) Summarized time course comparing VTA DA neuron firing rate to MStim vs an unstimulated baseline. (C) Dopamine neuron firing rate changes compared to time-equivalent GABA neuron firing rate changes in response to MStim. (D) Summarized data comparing average firing rate changes in VTA neurons by MStim. Values in parentheses are n values. Asterisks *, **, *** indicate significance levels $p < 0.05$, 0.01 and 0.001, respectively.

Figure 3.4 – Role of NAc inputs to the VTA and endogenous opioids in MStim-induced inhibition of VTA GABA neuron firing rate.

(A,B) Local injection of lidocaine into the NAc and IP administration of the DOR antagonist naltrindole blocked MStim-induced inhibition of VTA GABA neuron firing rate (80 Hz; 120 sec). Values in parentheses are n values. Asterisks *,**,*** indicate significance levels $p<0.05$, 0.01 and 0.001, respectively.

Figure 3.5 – MStim effects on basal and evoked DA release in the NAc.

(A) MStim enhanced basal DA release in the NAc, as measured by microdialysis. (B) Representative, superimposed voltammograms showing oxidation/reduction current vs voltage plots comparing DA release during baseline vs MStim. (C) Representative, superimposed current vs time plots showing DA release associated with local electrical stimulation. Calibration bars are nA and seconds. (D) MStim also enhanced evoked DA release in the NAc, as measured by voltammetry. Asterisks *,**,*** indicate significance levels $p<0.05$, 0.01 and 0.001, respectively.

Figure 3.6 – Role of DORs and CINs in MStim-induced enhancement of DA release in the NAc.

(A) Summarized time course of in situ NAc naltrindole or hexamethonium/scopolamine effects on MStim-induced enhancement of basal DA release in the NAc (80 Hz; 120 sec). Note that naltrindole or hexamethonium/scopolamine infusion into the NAc blocked MStim-induced enhancement of basal DA release. (B) Summarized data at the 60-min time point. Values in parentheses are n values. Asterisks *,**,*** indicate significance levels $p<0.05$, 0.01, and 0.001, respectively.

Figure 3.7 – MStim activates neurons and induces translocation of DORs in the NAc.

(A,B) Increased expression of DORs (red; TH is blue) in the NAc 2-hours post MStim compared to control. Insets show magnified views at point on 40X image indicated by the *. Note the translocation of DORs to the cell membrane. (C) Increased number of neurons in the NAc, but not the VTA, expressing c-FOS 2 hrs post MStim. (D) Decreased expression of c-FOS mean fluorescent intensity (MFI) in the VTA, but not in the NAc, 2 hrs post MStim. (E) Total number of NAc cells expressing DORs 2 hrs post MStim. Values in parentheses are n values. Asterisks *,** indicate significance levels $p<0.05$ and 0.01, respectively.

Figures

Figure 3.1

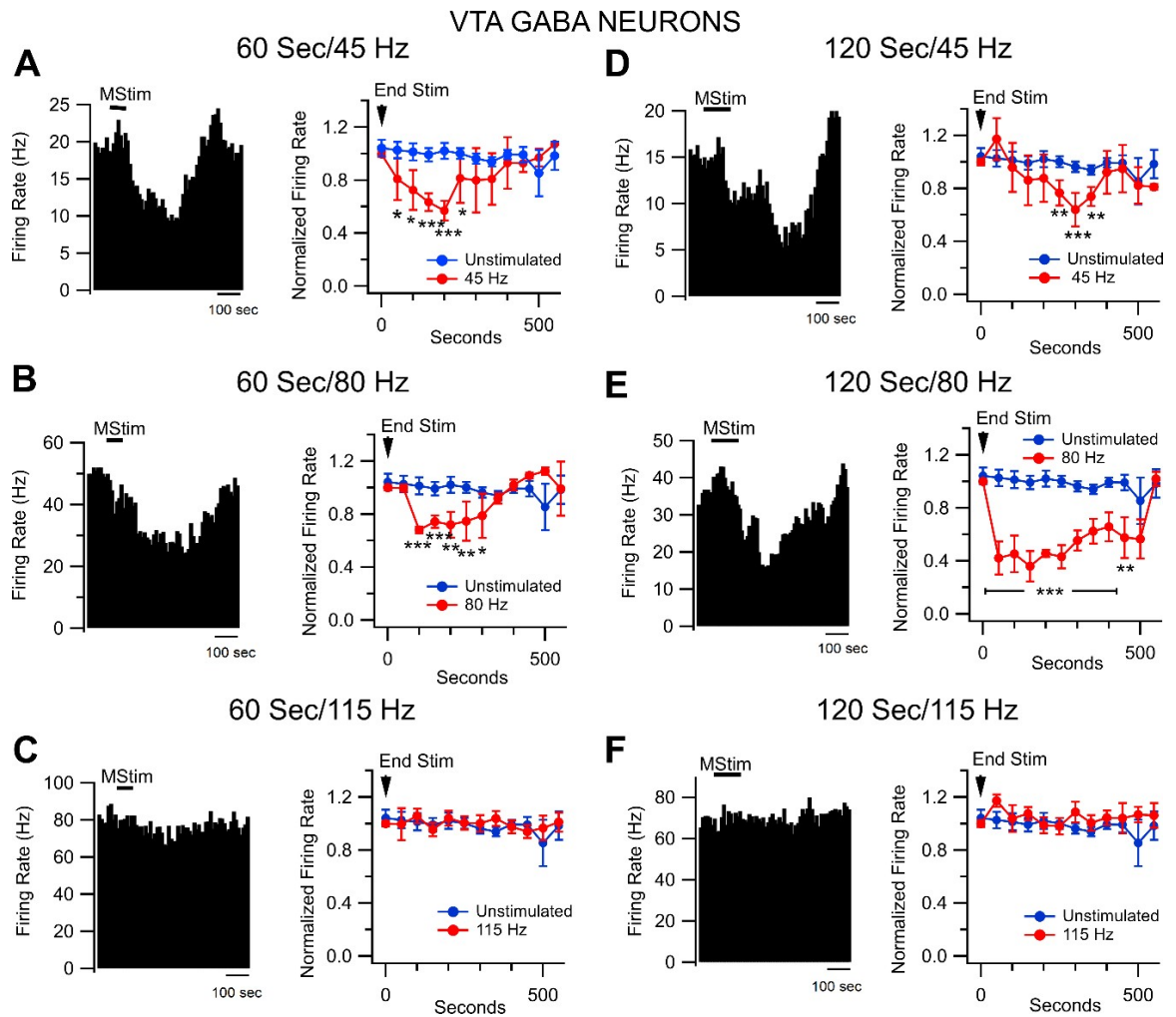


Figure 3.2

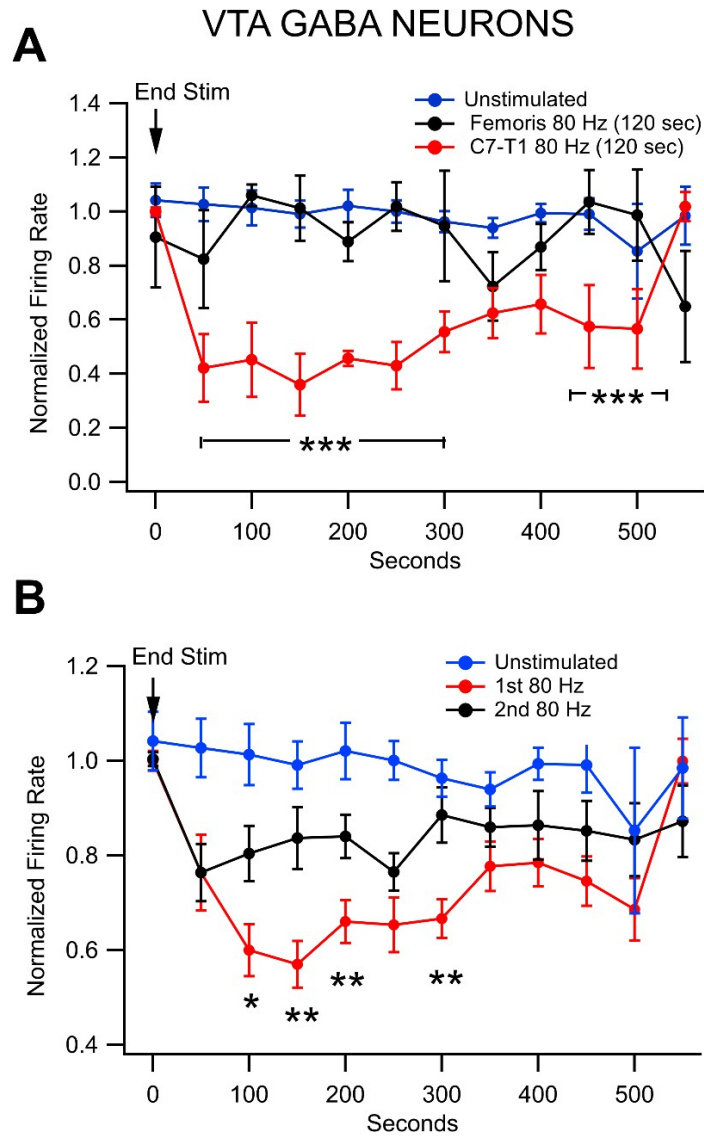


Figure 3.3

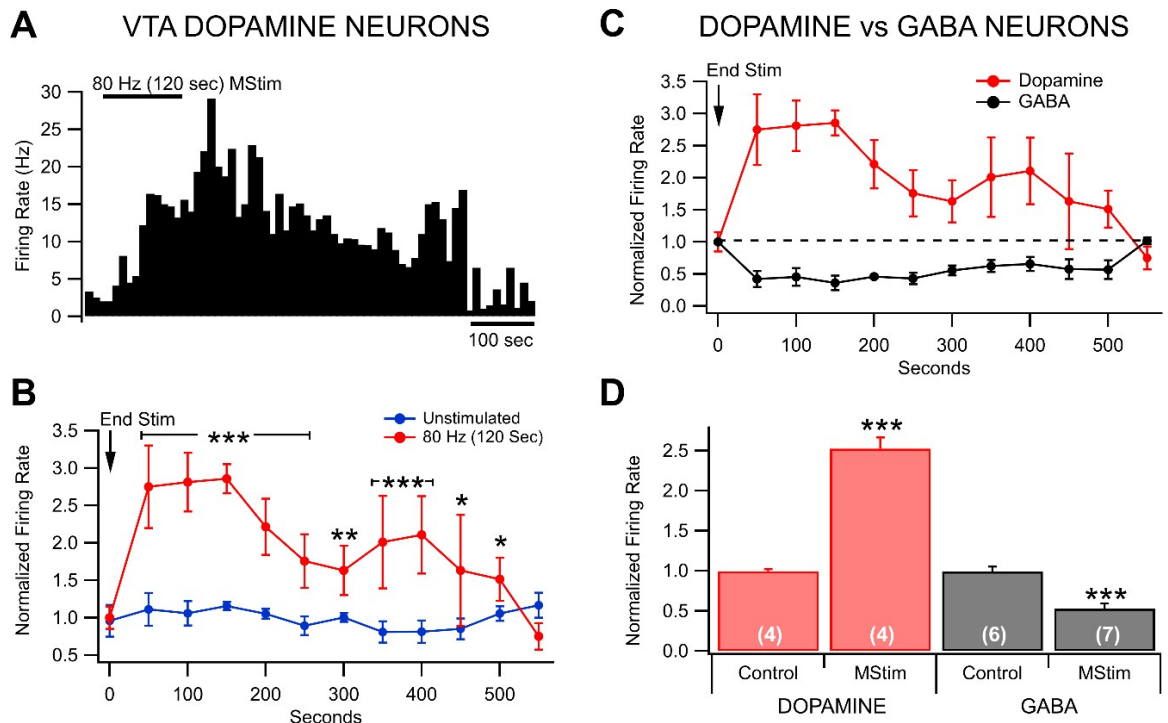


Figure 3.4

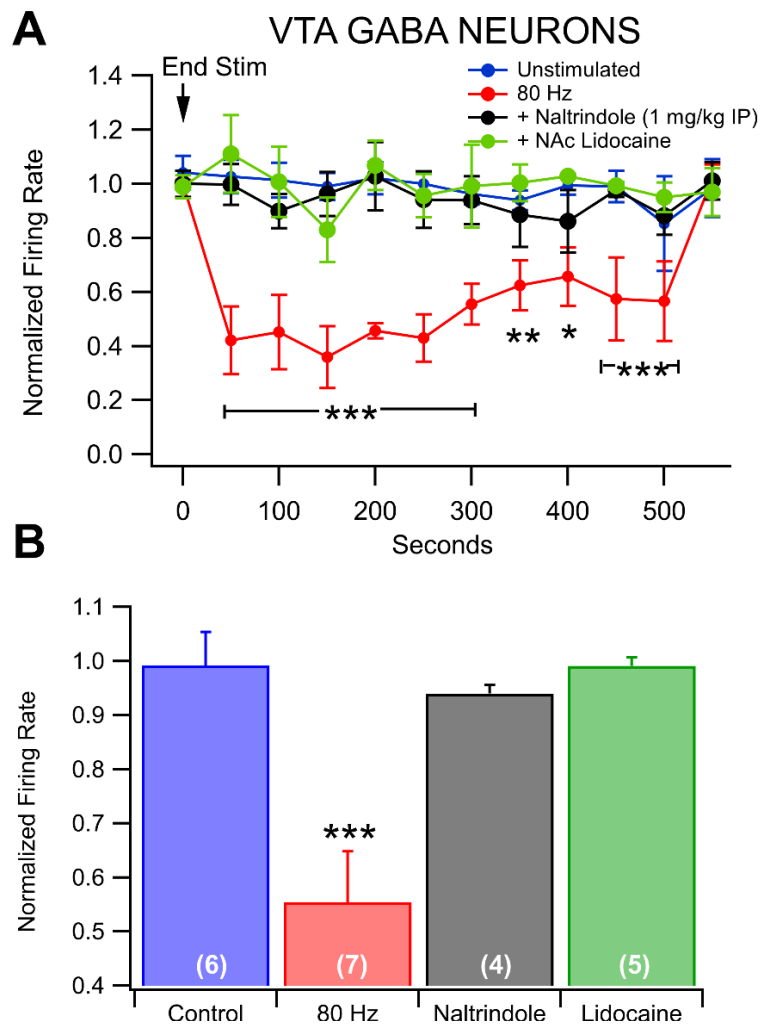


Figure 3.5

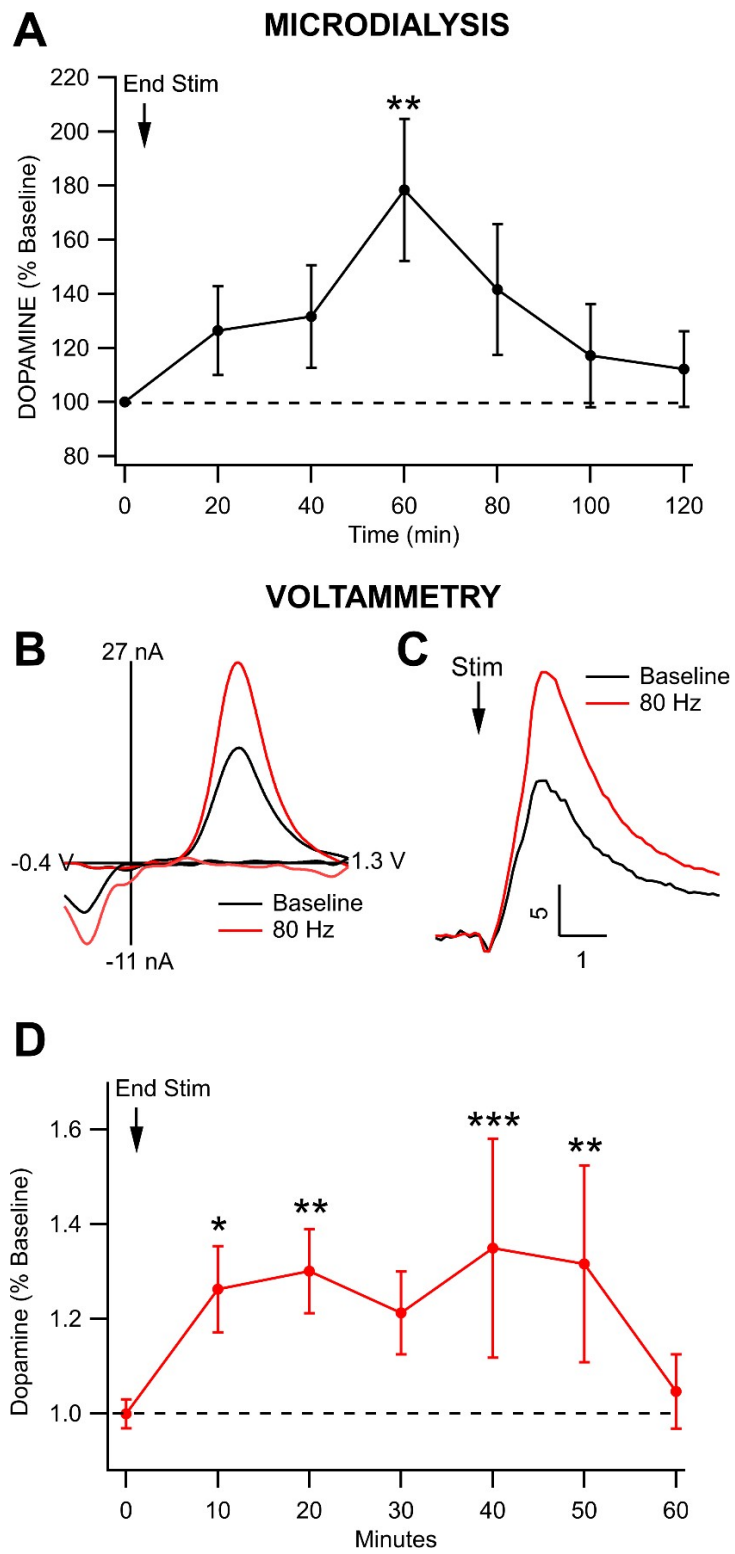


Figure 3.6

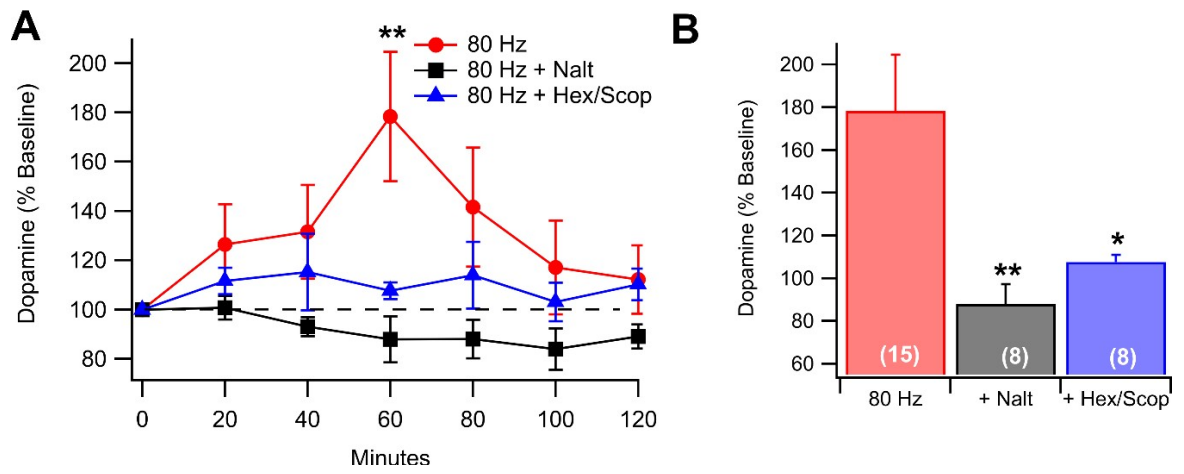
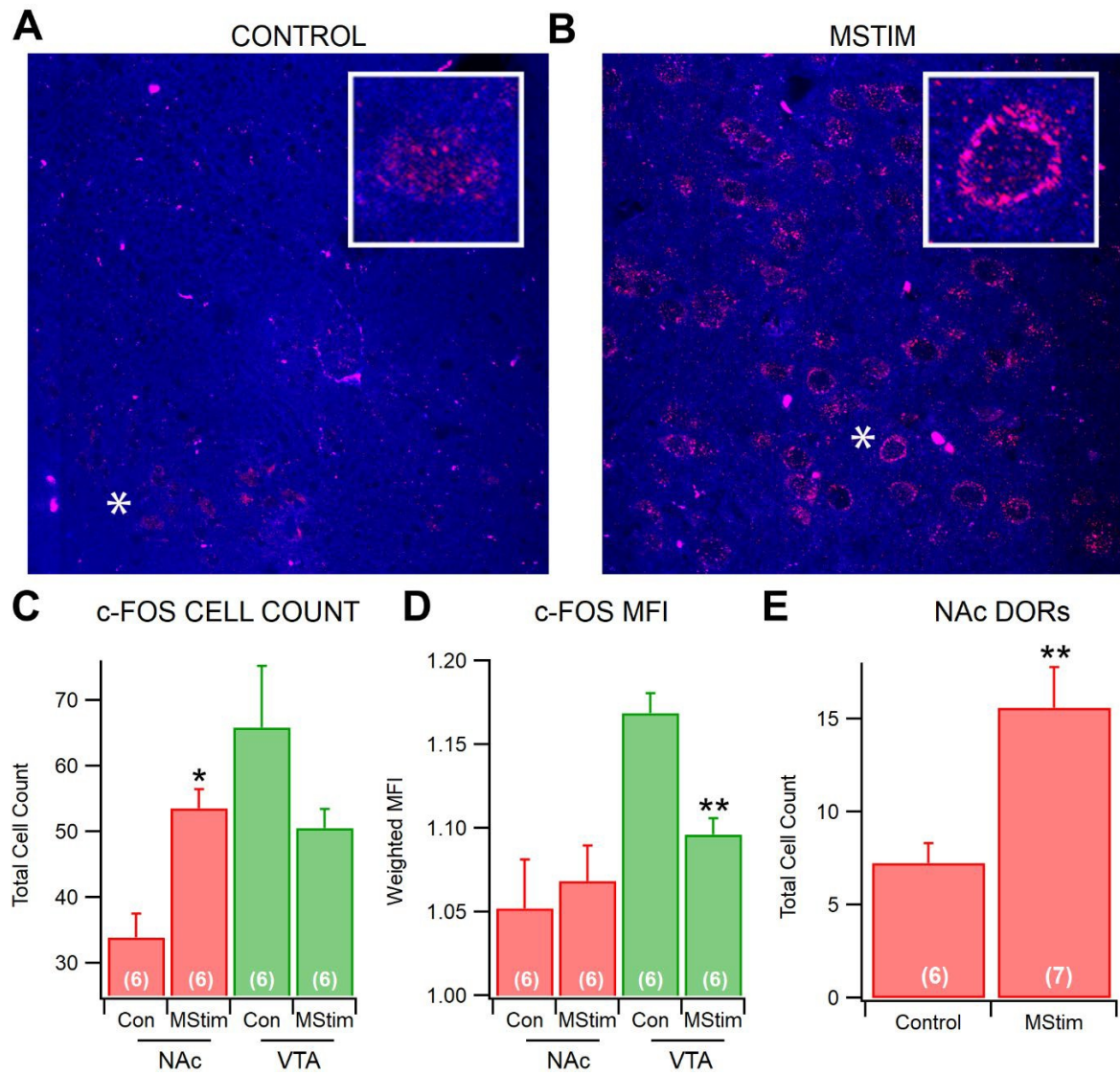


Figure 3.7



CHAPTER 4: Mechanical stimulation alters chronic ethanol-induced changes to VTA GABA
neurons, NAc DA release and measures of withdrawal

**Mechanical stimulation alters chronic ethanol-induced changes to VTA
GABA neurons, NAc DA release and measures of withdrawal**

Kyle B Bills¹, J Daniel O Bray¹, James Brundage¹, Jordan Yorgason¹, Jonathan D Blotter², and
Scott C Steffensen^{1*}

¹ Brigham Young University, Department of Psychology/Neuroscience; Provo, Utah 84602

² Brigham Young University, Department of Engineering; Provo, Utah 84602

Running title: **MStim Alters Neuronal and Behavioral Effects of Chronic Ethanol**

*Corresponding Author

Scott C. Steffensen

1050 SWKT

Brigham Young University

Provo UT, 84602

Tel: 801-422-9499

Fax: 801-422-0602

Email: scott_steffensen@byu.edu

Number of pages: 22

Number of figures: 3

Abstract: 132 words

Introduction: 768 words

Discussion: 572 words

Formatted for *The Journal of Neuroscience*

Abstract

Mechanical stimulation (MStim) has been previously shown to modulate firing rate of neurons in the ventral tegmental area (VTA) and dopamine (DA) release in the nucleus accumbens (NAc), an area of interest in alcohol-use disorder (AUD). In this study we examine the effects of MStim, during chronic alcohol dependence, on neurons in VTA and NAc and behavioral measures during withdrawal. We show that when MStim is administered concurrently with alcohol, it alters alcohol-induced desensitization of VTA GABA neuron firing rate in response to a reinstatement dose from 117.5 % of baseline to 32.3 %. Dopamine release in the NAc at 120 min post-injection is changed from 119.8 % of baseline to 70.1 %. Further, behavioral indices of withdrawal (rearing, open-field crosses, tail stiffness and gait) were substantively ameliorated with treatment with MStim

Introduction

Alcohol addiction is a chronic relapsing disease that affects more Americans than all forms of cancer combined (SAMHSA, 2016). It leads to destructive psychological, physical, social, and economic consequences. It is estimated that over 28 million Americans are currently in need of treatment for alcohol abuse, resulting in over \$249 billion in direct costs (Sacks et al., 2015). Making matters worse, only 13% of those needing intervention actually receive it. Further, in spite of the wonderful advances in our understanding of the neuropathophysiology of addiction, the success rate of treatment has not substantively changed over the last hundred years, with around 50% of those treated relapsing (Moos and Moos, 2006; White, 2012; SAMHSA, 2016). This represents approximately 6% of those suffering from the disease receiving effective treatment. A report ranking the different conditions relative to the “global burden of disease” found that ethanol ranked 3rd out of the 25 major contributors (Lim et al., 2012).

The current FDA-approved treatments for AUD are the sensitizing agent disulfiram, the mu-opioid receptor (MOR) antagonist naltrexone, and the neuromodulatory balancing agent acamprosate (Akbar et al., 2018). Many consider these pharmacological treatments to be woefully inadequate, and the public is begging for more efficacious treatments for AUD. Many are seeking alternative, non-invasive, non-pharmacological alternatives as personalized care and as adjuncts to self-help programs. Thus, more fundamental science and novel methods are needed to determine mechanisms underlying alternative approaches and improve outcomes.

The use of mechanoreceptor-based therapies (MStim) in the treatment of drug-abuse disorders is a largely unexplored field. Notably, several complementary health care approaches are thought to have effects mediated in part by activation of mechanoreceptors, including chiropractic medicine,

acupuncture, and physical therapy. There is compelling evidence suggesting that some of the benefits ascribed to acupuncture are mediated, through somatosensory neuronal pathways shared with MStim. We have shown in multiple reports that stimulation of the HT7 acupoint modifies drug-seeking behaviors and relapse to cocaine (Yoon et al., 2012; Jin et al., 2018), methamphetamine (Kim et al., 2019), and ethanol (Yang et al., 2010). These effects can be attenuated with ablation of the dorsal column/medial lemniscal pathway and appear to act through endogenous opioids (Yang et al., 2008; Kim et al., 2013; Chang et al., 2017). Though these studies demonstrate anatomically site-specific effects, they are suggestive that activation of primary somatosensory fibers generally may attenuate the reinforcing effects of drugs of abuse.

We have previously reported that MStim at 80 Hz to the cervical spine inhibits VTA GABA neuron firing, enhances VTA DA neuron firing and increases DA release in the NAc. Further, we have shown that VTA effects are driven by cholinergic interneurons (CIN) and delta opioid receptors (DOR) in the NAc. These findings are salient considering the role that the mesolimbic circuitry plays in reward, dependence and withdrawal. Midbrain dopamine (DA) neuron activity is involved in many aspects of reward seeking (Dalle Grave et al., 2008; Ranaldi, 2014; Gentry et al., 2018). Although the prevailing dogma is that DA neurons mediate the rewarding and addictive properties of drugs of abuse (Wise, 2008), VTA GABA neurons have garnered much interest for their role in modulating DA release and perhaps as independent substrates mediating reward or aversion (Gallegos et al., 1999; Stobbs et al., 2004; Steffensen et al., 2008; Ludlow et al., 2009; Steffensen et al., 2009; Brown et al., 2012; Tan et al., 2012). We have shown previously that acute administration of ethanol, opioids, or cocaine inhibits VTA GABA neurons (Gallegos et al., 1999; Stobbs et al., 2004; Steffensen et al., 2006; Steffensen et al., 2008; Ludlow et al., 2009; Steffensen et al., 2009), leading to a net disinhibition of VTA DA neurons (Carboni et al., 1989; Yoshimoto

et al., 1992; Bocklisch et al., 2013). In contrast, during ethanol or opioid withdrawal, VTA GABA neurons become hyperactive (Bonci and Williams, 1997; Gallegos et al., 1999) leading to decreased mesolimbic DA activity and release in the NAc (Maisonneuve et al., 1995; Koeltzow and White, 2003; Wise, 2004; Karkhanis et al., 2016; Rose et al., 2016). This reduction in mesolimbic DA transmission is theorized to be the primary driver of relapse (Lyness and Smith, 1992).

In this study, we investigate the role of MStim as a potential treatment for ethanol-use disorder by evaluating its ability to ameliorate chronic ethanol-induced changes to VTA GABA neuron firing, DA release in the NAc and behavioral indices related to withdrawal. We hypothesized that MStim is sufficient to block chronic ethanol-induced desensitization of VTA GABA neurons and changes in NAc DA release in response to ethanol reinstatement. Further, that MStim would block anxiety-related behaviors normally associated with chronic ethanol withdrawal.

Materials and Methods

Animals and MStim Motor Implantation

Male wistar rats, weighing 250-320 g, from our breeding colony at Brigham Young University were used. Rats were housed in groups of 2-3 at a fixed temperature (21-23°C) and humidity (55-65%) on a reverse light/dark cycle with *ad libitum* food and water. Rats were briefly anesthetized using isoflurane (4.0%) during injections to mitigate injection stress. Each received BID IP injections (9 am and 5 pm) of ethanol (2.5g/Kg; 16% w/v) or saline for 14-days. Intoxication was verified visually by noting loss of consciousness following initial injections with increasing tolerance. Immediately following injections MStim rats were placed on a LabWorks Inc ET-126

shaker device (Alpine, UT) with a sheet of 1/4 inch, 18 in x 18 in plexiglass fastened atop for 15-min. An 80 Hz, 500 mVpp sine wave was generated using a Wavetex Datron Universal Waveform Generator model 195 (San Diego, CA) and amplified using a Crown model XLi 3500 (Los Angeles, CA) amplifier. All animal received a final injection at 9am and were tested at 9am the following day. Experimental protocols were approved by the Brigham Young University Institutional Animal Care and Use Committee according to NIH guidelines.

Single Cell Electrophysiology

For recordings of VTA GABA neurons, rats were anesthetized using isoflurane and placed in a stereotaxic apparatus. Anesthesia was maintained at 1.5% with 2.0 L of air flow from a nebulizer driven by an oxygen concentrator. Body temperature was maintained at $37.4 \pm 0.4^{\circ}\text{C}$ by a feedback regulated heating pad. With the skull exposed, a hole was drilled for placement of a 3.0 M KCl-filled micropipette (2 to 4 M Ω ; 1-2 μm inside diameter), driven into the VTA with a piezoelectric microdrive (EXFO Burleigh 8200 controller and Inchworm, Victor, NY) based on stereotaxic coordinates [from bregma: 5.6 to 6.5 posterior (P), 0.5 to 1.0 lateral (L), 6.5 to 9.0 ventral (V)]. Potentials were amplified with an Axon Instruments Multiclamp 700A amplifier (Union City, CA). Single-cell activity was filtered at 0.3 to 10 kHz (3 dB) with the Multiclamp 700A amplifier and displayed on Tektronix (Beaverton, OR) digital oscilloscopes. Potentials were sampled at 20 kHz (12 bit resolution) with National Instruments (Austin, TX) data acquisition boards in Macintosh computers (Apple Computer, Cupertino, CA). Extracellularly recorded action potentials were discriminated with a World Precision Instruments WP-121 Spike Discriminator (Sarasota, FL) and converted to computer-level pulses. Single-unit potentials, discriminated spikes, and stimulation events were captured by National Instruments NB-MIO-16 digital I/O and counter / timer data acquisition boards in Macintosh computers.

Characterization of VTA GABA

VTA GABA neurons were identified by previously-established stereotaxic coordinates and by spontaneous electrophysiological and pharmacological criteria (Steffensen et al., 1998). VTA GABA neuron discharge activity characteristics included: relatively fast firing rate ($>10\text{Hz}$), ON-OFF phasic non-bursting activity, and an initially negative spike with duration less than $200\text{ }\mu\text{sec}$. GABA neurons were excited by iontophoretic DA ($+40\text{ nA}$) ejected from the recording pipette. . We evaluated only those spikes that had greater than 5:1 signal-to-noise ratio. After positive neuron identification, baseline firing rate was measured for 5 min to ensure stability prior to MStim.

Grass Stimulator and MStim for in-vivo Recordings

Following measurement of neuronal baseline firing rate, a 60 or 120 sec MStim was introduced. The vibrating motor was controlled by a S44 Grass Stimulator (Grass Medical Instruments, West Warwick, RI). For electrophysiological recordings, the stimulator was set at 3 V for 0.1 msec duration, 0 msec delay and 80 pulses/sec (Bills et al., 2019). All vibratory stimuli were 120 sec in duration and followed by 60 min of recording.

Microdialysis and High Performance Liquid Chromatography

Microdialysis probes (MD-2200, BASI) were stereotactically inserted into the NAc ($+1.6\text{ AP}$, $+1.9\text{ ML}$, -8.0 DV). Artificial cerebrospinal fluid (aCSF) composed of 150 mM NaCl, 3 mM KCl, 1.4 mM CaCl_2 , and 0.8 mM MgCl_2 in 10 mM phosphate buffer was perfused through the probe at a rate of $3.0\text{ }\mu\text{l/min}$. Samples were collected every 20 min for 4 hr with MStim occurring after the first 2 hr had elapsed. Determination of the DA concentration in microdialysis samples was

performed using a HPLC pump (Ultimate 3000, Dionex, Sunnyvale, CA, USA) connected to an electrochemical detector (Coulochem III, ESA). The detector included a guard cell (5020, ESA) set at +270 mV, a screen electrode (5014B, ESA) set at -100 mV, and a detection electrode (5014B, ESA) set at +220 mV. Dopamine was separated using a C18 reverse phase column (HR-80, Thermo Fisher Scientific, Waltham, MA, USA). Mobile phase containing 75 mM $\text{H}_2\text{NaO}_4\text{P}$, 1.7 mM sodium octane sulfonate, 25 μM EDTA, 0.714 mM triethylamine, and 10% acetonitrile was pumped through the system at a flow rate of 0.5 ml/min.

Behavioral Measures of Withdrawal

Behavioral experiments were performed in a 16 T \times 16 W \times 32 L inch light attenuating plexiglass compartment and were recorded using a camera mounted on the ceiling above the apparatus connected to a Windows 7 PC running Pinnacle Studio 16 (Corel, Menlo Park, CA, USA). On test days, withdrawal rats were placed in the center of the chamber and visually inspected and subjectively scored for gait and tail stiffness. Each rat was scored twice by different raters blinded to the rat's experimental condition to reduce bias. The two scores were averaged. Tail stiffness was scored 1-5 (1-no stiffness; 2-minor stiffness with no tail elevation with ambulation; 3-minor stiffness with elevation during ambulation; 4-moderate stiffness with elevation at rest; 5- severe stiffness with elevation at all times). Gait was scored 1-5 (1-normal movement pattern with no hunching at rest or during ambulation; 2-normal movement patterns with mild hunching at rest but not during ambulation; 3-abnormal movement patterns with mild hunching at rest but not during ambulation; 4-abnormal movement patterns with moderate to severe hunching at rest but not during ambulation; 5-abnormal movement patterns with severe hunching at rest and during ambulation). Open-field crosses were defined as the number of times the animal crossed through the middle 1/3

of the chamber and rears were defined as independent instances of both front paws leaving the ground and being elevated above resting head level.

Data Collection and Statistical Analysis

For single-unit electrophysiology studies, discriminated spikes were processed with a spike analyzer, digitized with National Instruments hardware and analyzed with National Instruments LabVIEW and IGOR Pro software (Wavemetrics, Lake Oswego, OR). Extracellularly recorded single-unit action potentials were discriminated by a peak detector digital processing LabVIEW algorithm and recorded in 10 sec intervals. Firing rate data was averaged across neurons at 10 sec intervals and subsequently binned in 50 sec intervals for comparisons across time points as previously reported (Bills, 2019). Experimental groups were averaged across bins and then compared using a one-way ANOVA then corresponding bins were compared with a Student's t-test. Average depression or excitation in firing was calculated from 10-40 min post injection. Baseline firing rate was calculated from the average of the final 60 sec of firing rate data before vibrational stimulus and after 5 min of recording to ensure neuron stability. The results from all MStim and control groups were derived from calculations performed on ratemeter records and expressed as means \pm SEM.

For microdialysis, the area under the curve for the DA peak was extracted and a two-point calibration was used to approximate the DA concentration. All collections were normalized to the final baseline collection before injection occurred. Standard error for the final baseline collection was approximated using the scalar property. Dopamine release for each time point was expressed as a percentages of baseline \pm SEM. They were compared using a one-way ANOVA after which the groups were compared using a Tukey's posthoc analysis.

For behavioral experiments, after blinded scoring, results were compared using a one-way ANOVA after which groups were compared using a Tukey's posthoc analysis.

Results

Amelioration of chronic ethanol-induced changes to VTA GABA neurons by MStim

The effects of concurrent administration of 80 Hz MStim during chronic EtOH exposure were tested on VTA GABA neuron firing rate in the context of a reinstatement dose of EtOH (2.5g/kg IP) (**Fig. 4.1**). Baseline firing rate of GABA neurons in animals chronically exposed to EtOH was significantly higher (49.59 Hz) than that of animals that received concurrent MStim or saline with MStim (30.02 Hz and 35.94 Hz respectively) ($F_{(2,11)} = 5.1149$, $p=0.0269$; **Fig. 4.1D**).

Mechanical stimulation produced altered GABA neuron response to reinstatement EtOH when compared to chronic EtOH and saline groups ($F_{(2,108)} = 1348.799$, $p<0.0001$; **Fig. 4.1E**)

Administration of 2.5g/kg IP reinstatement dose of EtOH in chronically exposed animals produced a slight increase in average GABA neuron firing to 117.52% (± 0.039 , $n=5$) of baseline. The same injection in MStim treated animals caused a decrease in firing to 32.72% (± 0.043 , $n=5$) of baseline while in saline treated rats it produced a drop to 14.71% (± 0.050 , $n=5$) of baseline. All groups were significantly different from each other (EtOH and MStim, $p<0.0001$; EtOH and Sal, $p<0.0001$; Sal and MStim, $p<0.0001$; **Fig. 4.1F**). between MStim and saline groups ($p=0.046$). Thus, MStim, when given concurrently with chronic intermittent EtOH exposure to 2.5g/kg EtOH, blocks chronic EtOH-induced desensitization of VTA GABA neurons to reinstatement exposure.

MStim effects on chronic ethanol-induced changes to NAc DA release

To determine if blockage of chronic EtOH-induced changes to VTA GABA neuron firing rate by MStim translates to alterations in DA release in the NAc, dialysate samples were collected by microdialysis canula before and after a reinstatement dose of EtOH was given to rats after 24 hours of withdrawal (**Fig. 4.2**). Groups tested included a group naïve to both MStim and EtOH, EtOH, EtOH with MStim and saline with MStim. Animals naïve to both EtOH and MStim exhibited a rise in DA levels from 20 min to 120 min post-injection and significant differences were noted between the groups at those times (20 min, $F_{(3,13)} = 6.0631$, $p=0.0082$; 40 min, $F_{(3,13)} = 3.4890$, $p=0.0471$; 60 min, $F_{(3,13)} = 3.8812$, $p=0.0368$; 80 min, $F_{(3,13)} = 5.0333$, $p=0.0157$; 100 min, $F_{(3,13)} = 7.8089$, $p=0.0023$; 120 min, $F_{(3,13)} = 5.5628$, $p=0.0091$; **Fig. 4.2A**). Specific differences between groups were noted at min 20 between naïve and MStim groups (naïve $n=8$, MStim $n=3$, $p=0.0345$), at min 100 between naïve and MStim and naïve and saline groups (naïve $n=8$, MStim $n=3$, $p=0.0071$; saline $n=3$, $p=0.0147$) and at min 120 between naïve and saline groups ($p=0.0135$). Initial responses to ethanol reinstatement was uniform between the three experimentally exposed groups with DA levels demonstrating parity from minutes 20-80. At 100 minutes post-injection the EtOH group diverged from the other two measuring 95.42 % (± 4.78) of baseline, closer to the naïve group which measured 119.99 % (± 8.77). At this same timepoint the MStim and saline groups measured 57.61 % (± 11.48) and 66.89 % (± 16.78) respectively (**Fig. 4.2B**). At 120 min post-injection dopamine levels in the EtOH group elevated past baseline levels to 120.27 % (± 10.28), which was in-line with the naïve response at 113.36 % (± 5.91). Mechanostim and saline groups remained lower at 69.48 % (± 13.16) and 47.90 % (± 11.11) respectively. This is suggestive that MStim treatment alters DA release in response to ethanol in both previously exposed and unexposed animals.

MStim blocks withdrawal symptoms in rats exposed to chronic EtOH

To assess the behavioral relevance of MStim on indices of chronic EtOH withdrawal, rats in active withdrawal (24 hours after last dose) were evaluated for open field crosses, rearing behavior, tail stiffness and gait patterns (**Fig. 4.3**). Over a 30 min period, rats were assessed for the number of times they engaged in rearing. Mechanical stimulation ameliorated the reduction in rearing that was noted by chronic EtOH exposure alone ($F_{(2,18)} = 14.8194$, $p=0.0002$; **Fig. 4.3A**). The chronic EtOH rats engaged in rearing on average 22.57 times (± 4.51). This was significantly fewer times than rats treated with concurrent MStim ($n=8$ in all groups; $p=0.0011$ for EtOH and MStim; $p=0.0003$ for EtOH and Sal). Mstim treated rats reared 46.29 times (± 3.29) while saline treated rats reared 49.86 times (± 3.65). Open-field crosses were defined as the number of times the rats crossed through the center 1/3 of the chamber in 30 min; it was also assessed. Mechanical stimulation blunted the Chronic EtOH-induced reduction in the number of times rats engaged in open-field crosses ($F_{(2,18)} = 18.8606$, $p<0.0001$; **Fig. 4.3B**). The chronic EtOH rats crossed 14.14 times (± 1.94). This was significantly fewer than the 29.86 (± 1.77) and 31.14 (± 2.71) crosses engaged in by the MStim and saline groups respectively ($n=8$ in all groups; $p=0.0002$ for EtOH and MStim; $p<0.0001$ for EtOH and Sal; **Figs. 4.3E-G**). Tail stiffness and gait were subjectively scored by two blinded assessors as further indicators of withdrawal status. Tail stiffness was increased in the chronic EtOH when compared to the MStim or saline groups ($F_{(2,18)} = 36.1579$, $p<0.0001$; **Fig. 4.3C**). Tail stiffness in the chronic EtOH group was significantly different from the other two and was scored 3.57/5 (± 0.202) while the MStim and saline groups scored 1.86/5 (± 0.261) and 1.14 (± 0.143) respectively ($n=8$ in all groups; $p<0.0001$ for EtOH and MStim; $p<0.0001$ for EtOH and Sal). Differences in gait patterns were noted between the three groups ($F_{(2,18)} = 13.5789$, $p=0.0003$; **Fig. 4.3D**). Gait scores for chronic EtOH animals were 3.43/5 (± 0.369). The MStim animals scored 1.71/5 (± 0.184) and the saline group scored 1.43 (± 0.297).

Chronic EtOH was significantly different from the other two ($n=8$ in all groups; $p=0.0004$ for EtOH and MStim; $p=0.0017$ for EtOH and Sal). Thus, MStim, when applied concurrently with chronic intermittent EtOH, is sufficient to ameliorate certain behavioral indices associated with chronic EtOH withdrawal.

Discussion

We have previously reported that MStim acts on the nucleus accumbens to increase local DA release and that this effect is mediated by activation of cholinergic and delta opioid receptors. Further, projections from the NAc then cause a depression in VTA GABA neuron firing which results in VTA DA neuron disinhibition and a subsequent increase in firing. The current study was designed to investigate if these neuromodulatory changes are sufficient to alter chronic ethanol effects on VTA GABA neurons and withdrawal behavior. In the present study, the effects of 80 Hz MStim treatment for 15 min BID given in-line with dependence-inducing chronic intermittent EtOH injections were tested on various measures of EtOH withdrawal. While acute administration of ethanol reduces VTA GABA neuron firing, chronic intermittent EtOH exposure desensitizes VTA GABA neurons during reinstatement doses (Gallegos et al., 1999). These effects are thought to occur through downregulation of D2 receptors in the VTA presumably due to EtOH-induced alterations in local VTA DA release (Ludlow et al., 2009). Concurrent administration of MStim with chronic intermittent EtOH blocks these effects and changes VTA GABA neuron response to reinstatement from 117.5% of baseline to 32.7% of baseline. The blunting of the desensitization was not sufficient to return the GABA neuron response back to a naïve state as there were significant differences between the saline group and the EtOH + MStim groups. Mechanical stimulation has been previously shown to increase DA levels in the NAc for 2 hrs post-MStim.

These increased levels activate D1 and D2 expressing medium spiny neurons in the NAc that project back to the VTA and target non-dopaminergic neurons (Xia et al., 2011). These projections could be responsible for MStim-induced changes in VTA GABA neurons response to chronic ethanol. These findings are particularly relevant as they represent a non-invasive method of blocking chronic ethanol effects.

Dopamine levels were tested in the same chronic reinstatement paradigm. Animals naïve demonstrated a characteristic increase in DA levels (Yim and Gonzales, 2000) following ethanol injection. Animals treated with EtOH alone or MStim, whether in conjunction with EtOH or not, did not exhibit the same increase in DA levels following EtOH administration. This is suggestive that MStim alone is sufficient to alter mechanistic changes normally elicited by the EtOH. Chronic EtOH administration has been shown to increase expression levels of DORs while decreasing expression of mu opioid receptors (Saland et al., 2005). As noted, we have previously shown that MStim produces increased translocation of DORs to cellular membranes, this commonality between EtOH and MStim could explain the desensitizing effects of MStim on acute EtOH administration in EtOH naïve rodents. The MStim-induced alterations to chronic ethanol effects on VTA GABA neurons and DA release in the NAc ultimately manifest in blunting of the noted markers of dependence. The behavioral studies reported here buoy that finding as all measures of withdrawal gathered for this study were substantively improved by the addition of MStim to the chronic intermittent EtOH exposure paradigm employed to induce dependence. These data, when taken as a whole suggest that MStim at 80 Hz could be a viable treatment option for the treatment of alcohol-use disorder (AUD). This study is practically limited by the fact that MStim exposure was given concurrently with EtOH exposure. It is less likely that individuals battling with AUD

will receive MStim at the time of first exposure to alcohol. Future studies need to explore the efficacy of MStim treatment in previously dependent animals.

References

- Akbar M, Egli M, Cho YE, Song BJ, Noronha A (2018) Medications for alcohol use disorders: An overview. *Pharmacol Ther* 185:64-85.
- Bills K, Clarke, T., Major, G., Jacobson, C., Blotter, J., Feland, J., Steffensen, S (2019) Targeted Subcutaneous Vibration with Single-Neuron Electrophysiology as a Novel Method for Understanding the Central Effects of Peripheral Vibrational Therapy in a. Dose Response.
- Bills KB, Clarke T, Major GH, Jacobson CB, Blotter JD, Feland JB, Steffensen SC (2019) Targeted Subcutaneous Vibration With Single-Neuron Electrophysiology As a Novel Method for Understanding the Central Effects of Peripheral Vibrational Therapy in a Rodent Model. *Dose Response* 17:1559325818825172.
- Bocklisch C, Pascoli V, Wong JC, House DR, Yvon C, de Roo M, Tan KR, Luscher C (2013) Cocaine disinhibits dopamine neurons by potentiation of GABA transmission in the ventral tegmental area. *Science* 341:1521-1525.
- Bonci A, Williams JT (1997) Increased probability of GABA release during withdrawal from morphine. *J Neurosci* 17:796-803.
- Brown MT, Tan KR, O'Connor EC, Nikonenko I, Muller D, Luscher C (2012) Ventral tegmental area GABA projections pause accumbal cholinergic interneurons to enhance associative learning. *Nature* 492:452-456.
- Carboni E, Imperato A, Perezani L, Di Chiara G (1989) Amphetamine, cocaine, phencyclidine and nomifensine increase extracellular dopamine concentrations preferentially in the nucleus accumbens of freely moving rats. *Neuroscience* 28:653-661.
- Chang S, Ryu Y, Gwak YS, Kim NJ, Kim JM, Lee JY, Kim SA, Lee BH, Steffensen SC, Jang EY, Yang CH, Kim HY (2017) Spinal pathways involved in somatosensory inhibition of the psychomotor actions of cocaine. *Sci Rep* 7:5359.
- Dalle Grave R, Calugi S, Marchesini G (2008) Compulsive exercise to control shape or weight in eating disorders: prevalence, associated features, and treatment outcome. *Compr Psychiatry* 49:346-352.
- Gallegos RA, Criado JR, Lee RS, Henriksen SJ, Steffensen SC (1999) Adaptive responses of GABAergic neurons in the ventral tegmental area to chronic ethanol. *J Pharmacol Exp Ther* 291:1045-1053.
- Gentry RN, Schuweiler DR, Roesch MR (2018) Dopamine signals related to appetitive and aversive events in paradigms that manipulate reward and avoidability. *Brain research*.
- Jin W, Kim MS, Jang EY, Lee JY, Lee JG, Kim HY, Yoon SS, Lee BH, Chang S, Kim JH, Choi KH, Koo H, Gwak YS, Steffensen SC, Ryu YH, Kim HY, Yang CH (2018) Acupuncture reduces relapse to cocaine-seeking behavior via activation of GABA neurons in the ventral tegmental area. *Addiction biology* 23:165-181.
- Karkhanis AN, Huggins KN, Rose JH, Jones SR (2016) Switch from excitatory to inhibitory actions of ethanol on dopamine levels after chronic exposure: Role of kappa opioid receptors. *Neuropharmacology* 110:190-197.
- Kim NJ, Ryu Y, Lee BH, Chang S, Fan Y, Gwak YS, Yang CH, Bills KB, Steffensen SC, Koo JS, Jang EY, Kim HY (2019) Acupuncture inhibition of methamphetamine-induced behaviors, dopamine release and hyperthermia in the nucleus accumbens: mediation of group II mGluR. *Addiction biology* 24:206-217.
- Kim SA, Lee BH, Bae JH, Kim KJ, Steffensen SC, Ryu YH, Leem JW, Yang CH, Kim HY (2013) Peripheral afferent mechanisms underlying acupuncture inhibition of cocaine behavioral effects in rats. *PLoS One* 8:e81018.

- Koeltzow TE, White FJ (2003) Behavioral depression during cocaine withdrawal is associated with decreased spontaneous activity of ventral tegmental area dopamine neurons. *Behav Neurosci* 117:860-865.
- Lim SS et al. (2012) A comparative risk assessment of burden of disease and injury attributable to 67 risk factors and risk factor clusters in 21 regions, 1990-2010: a systematic analysis for the Global Burden of Disease Study 2010. *Lancet* 380:2224-2260.
- Ludlow KH, Bradley KD, Allison DW, Taylor SR, Yorgason JT, Hansen DM, Walton CH, Sudweeks SN, Steffensen SC (2009) Acute and chronic ethanol modulate dopamine D2-subtype receptor responses in ventral tegmental area GABA neurons. *Alcohol Clin Exp Res* 33:804-811.
- Lyness WH, Smith FL (1992) Influence of dopaminergic and serotonergic neurons on intravenous ethanol self-administration in the rat. *Pharmacol Biochem Behav* 42:187-192.
- Maisonneuve IM, Ho A, Kreek MJ (1995) Chronic administration of a cocaine "binge" alters basal extracellular levels in male rats: an in vivo microdialysis study. *J Pharmacol Exp Ther* 272:652-657.
- Moos RH, Moos BS (2006) Rates and predictors of relapse after natural and treated remission from alcohol use disorders. *Addiction (Abingdon, England)* 101:212-222.
- Ranaldi R (2014) Dopamine and reward seeking: the role of ventral tegmental area. *Rev Neurosci* 25:621-630.
- Rose JH, Karkhanis AN, Chen R, Gioia D, Lopez MF, Becker HC, McCool BA, Jones SR (2016) Supersensitive Kappa Opioid Receptors Promotes Ethanol Withdrawal-Related Behaviors and Reduce Dopamine Signaling in the Nucleus Accumbens. *Int J Neuropsychopharmacol* 19.
- Sacks JJ, Gonzales KR, Bouchery EE, Tomedi LE, Brewer RD (2015) 2010 National and State Costs of Excessive Alcohol Consumption. *American journal of preventive medicine* 49:e73-79.
- Saland LC, Hastings CM, Abeyta A, Chavez JB (2005) Chronic ethanol modulates delta and mu-opioid receptor expression in rat CNS: immunohistochemical analysis with quantitative confocal microscopy. *Neuroscience letters* 381:163-168.
- SAMHSA (2016) Facing Addiction in America: The Surgeon General's Report on Alcohol, Drugs, and Health. In: US Department of Health and Human Services.
- Steffensen SC, Svingos AL, Pickel VM, Henriksen SJ (1998) Electrophysiological characterization of GABAergic neurons in the ventral tegmental area. *J Neurosci* 18:8003-8015.
- Steffensen SC, Walton CH, Hansen DM, Yorgason JT, Gallegos RA, Criado JR (2009) Contingent and non-contingent effects of low-dose ethanol on GABA neuron activity in the ventral tegmental area. *Pharmacol Biochem Behav* 92:68-75.
- Steffensen SC, Stobbs SH, Colago EE, Lee RS, Koob GF, Gallegos RA, Henriksen SJ (2006) Contingent and non-contingent effects of heroin on mu-opioid receptor-containing ventral tegmental area GABA neurons. *Exp Neurol* 202:139-151.
- Steffensen SC, Taylor SR, Horton ML, Barber EN, Lyle LT, Stobbs SH, Allison DW (2008) Cocaine disinhibits dopamine neurons in the ventral tegmental area via use-dependent blockade of GABA neuron voltage-sensitive sodium channels. *The European journal of neuroscience* 28:2028-2040.
- Stobbs SH, Ohran AJ, Lassen MB, Allison DW, Brown JE, Steffensen SC (2004) Ethanol suppression of ventral tegmental area GABA neuron electrical transmission involves NMDA receptors. *J Pharmacol Exp Ther* 311:282-289.
- Tan KR, Yvon C, Turiault M, Mirzabekov JJ, Doehner J, Labouebe G, Deisseroth K, Tye KM, Luscher C (2012) GABA neurons of the VTA drive conditioned place aversion. *Neuron* 73:1173-1183.
- White WL (2012) Recovery/Remission from Substance Use Disorders. In: Philadelphia Department of Behavioral Health and Intellectual Disability.
- Wise RA (2004) Dopamine, learning and motivation. *Nat Rev Neurosci* 5:483-494.

- Wise RA (2008) Dopamine and reward: the anhedonia hypothesis 30 years on. *Neurotox Res* 14:169-183.
- Xia Y, Driscoll JR, Wilbrecht L, Margolis EB, Fields HL, Hjelmstad GO (2011) Nucleus accumbens medium spiny neurons target non-dopaminergic neurons in the ventral tegmental area. *J Neurosci* 31:7811-7816.
- Yang CH, Lee BH, Sohn SH (2008) A possible mechanism underlying the effectiveness of acupuncture in the treatment of drug addiction. *Evid Based Complement Alternat Med* 5:257-266.
- Yang CH, Yoon SS, Hansen DM, Wilcox JD, Blumell BR, Park JJ, Steffensen SC (2010) Acupuncture inhibits GABA neuron activity in the ventral tegmental area and reduces ethanol self-administration. *Alcohol Clin Exp Res* 34:2137-2146.
- Yim HJ, Gonzales RA (2000) Ethanol-induced increases in dopamine extracellular concentration in rat nucleus accumbens are accounted for by increased release and not uptake inhibition. *Alcohol* 22:107-115.
- Yoon SS, Yang EJ, Lee BH, Jang EY, Kim HY, Choi SM, Steffensen SC, Yang CH (2012) Effects of acupuncture on stress-induced relapse to cocaine-seeking in rats. *Psychopharmacology (Berl)* 222:303-311.
- Yoshimoto K, McBride WJ, Lumeng L, Li TK (1992) Alcohol stimulates the release of dopamine and serotonin in the nucleus accumbens. *Alcohol* 9:17-22.

Figure Legends

Figure 4.1 – Effects of MStim on VTA GABA neuron firing rate after reinstatement ethanol during withdrawal.

(A-C) Representative traces for GABA neuron response for (A) EtOH alone, (B) EtOH + MStim and (C) saline + MStim. (D) Baseline firing rate differences between the three groups. Note that EtOH alone maintained a higher baseline firing rate. (E) MStim blocks chronic EtOH-induced desensitization of GABA neurons to EtOH reinstatement. (F) Time course data with 50 sec bins demonstrating disparate effects among groups.. Asterisks *, **, *** indicate significance levels $p < 0.05$, 0.01 and 0.001, respectively.

Figure 4.2 – Basal dopamine release in the NAc following EtOH injection (2.5g/kg IP).

(A) Summarized time course of EtOH enhancement of basal DA release in the NAc. Note that naïve animals show distinct differences when compared to animal that received EtOH or MStim. (B) Comparison of [DA] at 100 min post-injection. (C) Comparison of [DA] at 120 min post-injection. Asterisks *, **, *** indicate significance levels $p < 0.05$, 0.01 and 0.001, respectively.

Figure 4.3 – Blocking of EtOH-induced behavioral measures of withdrawal by MStim.

(A) Number of times the animal reared-up on hind legs in 30 min period. (B) Number of times the animal crossed through the middle third of the chamber in a 30 min period. (C) Subjective rating of tail-stiffness. (D) Subjective measure of the animal's gait. Note that all measures improved with the concurrent administration of MStim during chronic EtOH exposure. (E-G) Representative traces of the animals movement patterns during testing.. Asterisks *, **, *** indicate significance levels $p < 0.05$, 0.01 and 0.001, respectively.

Figures

Figure 4.1

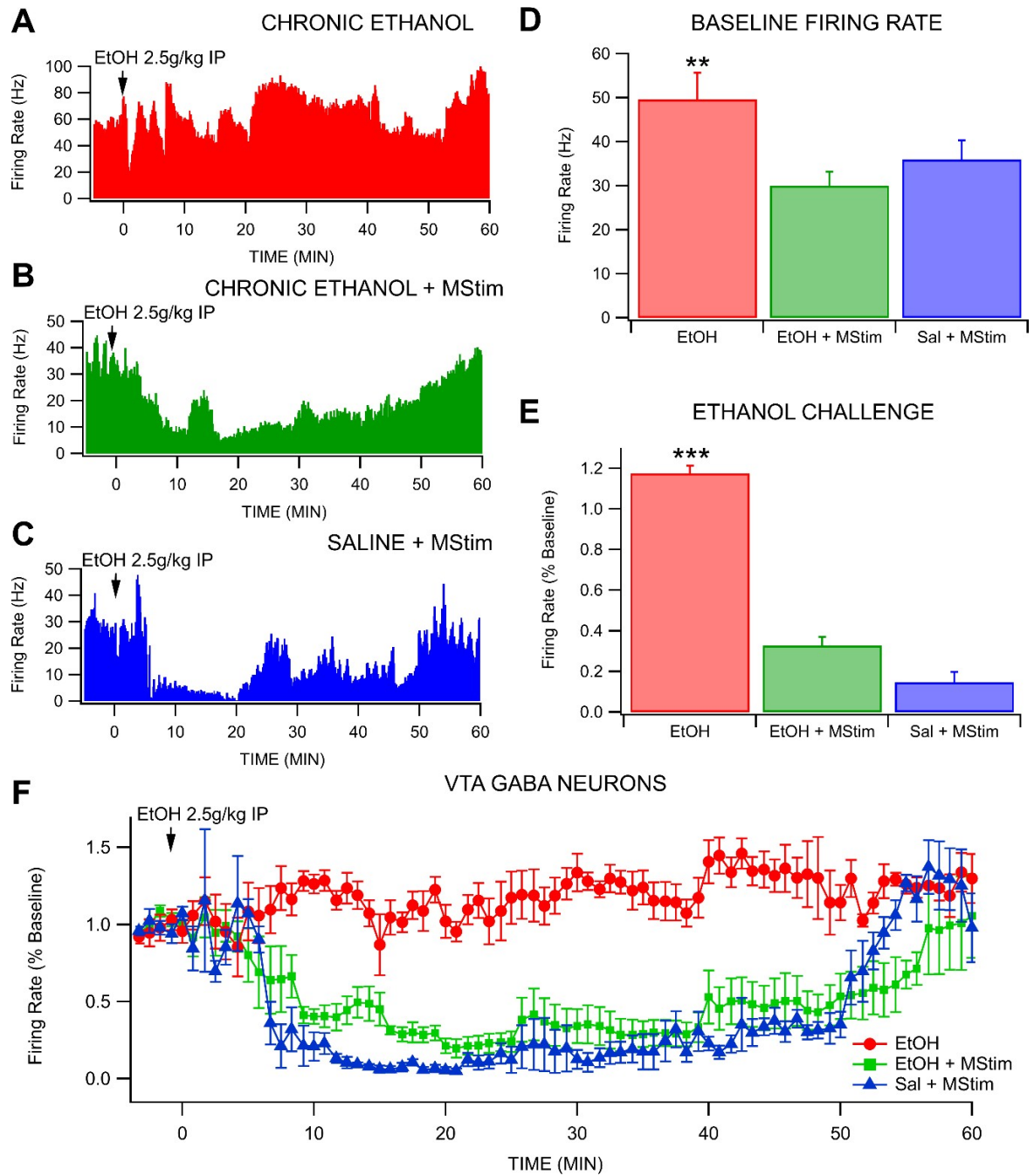


Figure 4.2

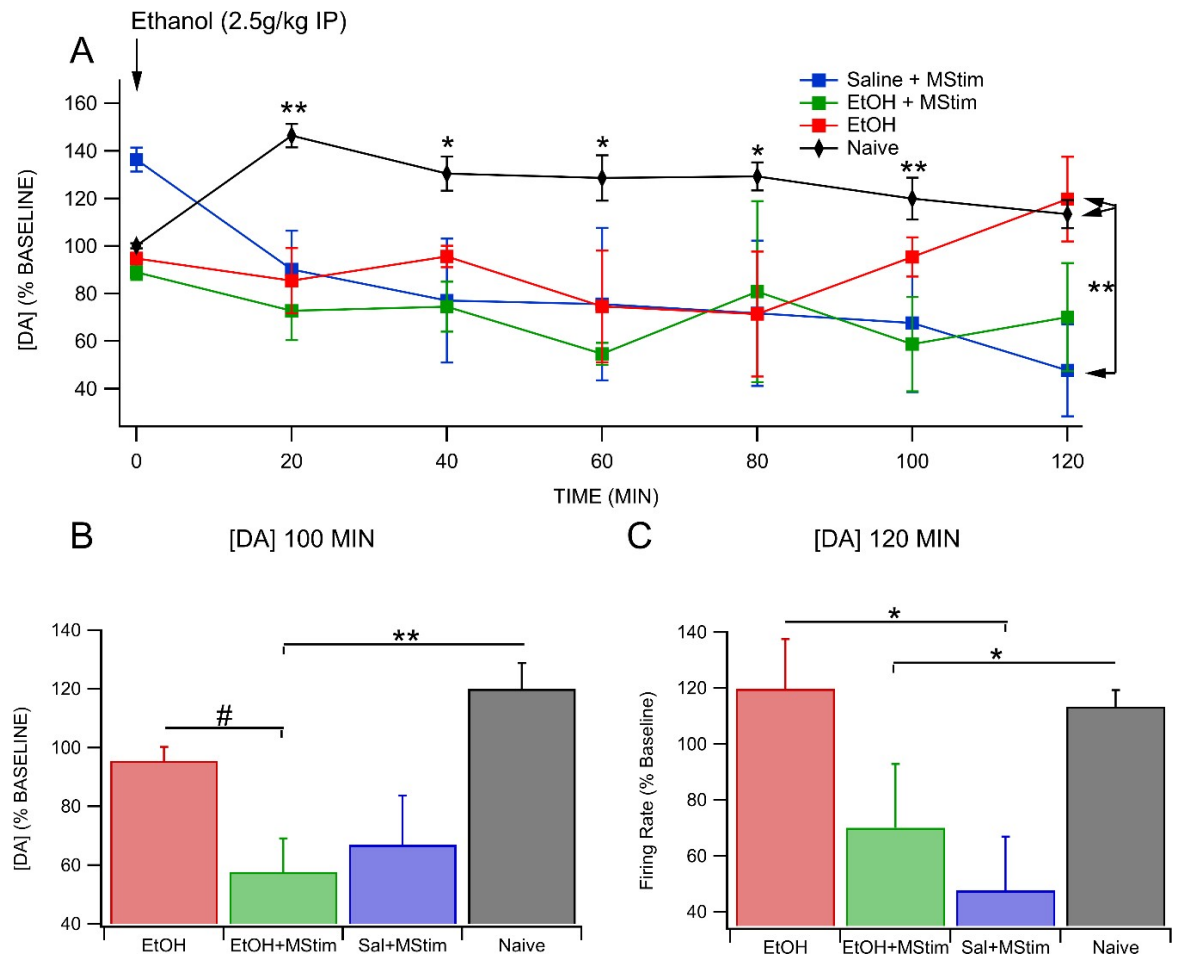
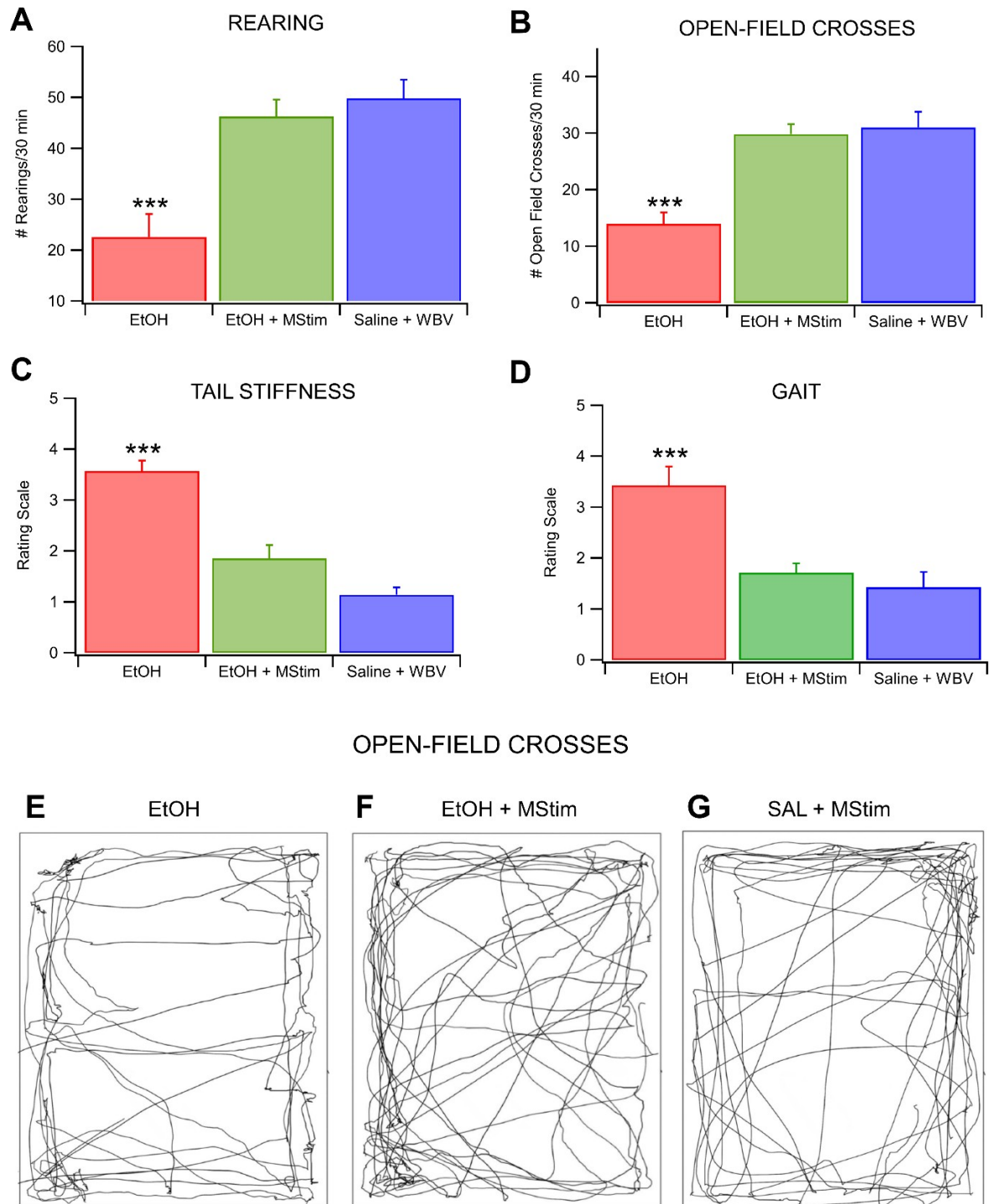


Figure 4.3



Exercise Blocks Ethanol-Induced sensitization of Kappa Opioid Receptors

Kyle B Bills¹, James Brundage¹, Jordan Yorgason¹, and Scott C Steffensen^{1*}

¹ Brigham Young University, Department of Psychology/Neuroscience; Provo, Utah 84602

Running title: **Exercise Blocks EtOH Changes to KORs**

*Corresponding Author

Scott C. Steffensen

1050 SWKT

Brigham Young University

Provo UT, 84602

Tel: 801-422-9499

Fax: 801-422-0602

Email: scott_steffensen@byu.edu

Number of pages: 15

Number of figures: 3

Abstract: 120 words

Introduction: 496 words

Discussion: 412 words

Formatted for *The Journal of Neuroscience*

Abstract

Exercise has increasingly been utilized as an adjunctive treatment for alcohol-use disorder (AUD). This is in spite of sparse mechanistic understanding of neurologic effects influencing alcohol-induced substrate adaptations in the mesolimbic circuitry or elsewhere. These limitations blunt practitioner's efficacy in developing evidence-based guidelines for exercise recommendations for AUD. Kappa opioid receptors (KORs) have been shown to increase sensitivity after chronic alcohol exposure. In this study we demonstrate that voluntary exercise alone decreases expression of KORs in the nucleus accumbens and the ventral tegmental area. These exercise-induced changes competitively alter chronic ethanol-induced changes in KOR expression in these brain regions. Curiously, we report that though voluntary exercises reduces ethanol seeking in chronically exposed mice, it potentiates drinking in saline exposed mice.

Introduction

It is estimated that over 28 million Americans are currently in need of treatment for alcohol abuse, resulting in over \$249 billion in direct costs [1]. Making matters worse, only 13% of those needing intervention actually receive it. Thus, the economic, societal, familial, and personal costs associated with AUD are staggering.

Kappa Opioid Receptors

KORs are expressed extensively in the Nucleus accumbens (NAc), both in the core and the shell [2-4], where their activation inhibits DA release [2]. Data suggests that they are synthesized in the cell bodies of DA neurons in the ventral tegmental area (VTA) where they are expressed and also subsequently transported to terminals in the NAc where they are integrated into the presynaptic membrane [5]. Activation of kappa receptors is associated with dysphoria [6].

Evidence suggests that there is an upregulation of the kappa opioid system in alcohol dependent animals that may play a role in the increased seeking behavior seen with dependence [7]. This is demonstrated by a decrease in dependent-state seeking behavior when the KOR antagonist nor-BNI is administered while having no effect on non-dependent animals [8]. Further chronic intermittent ethanol exposure has been shown to increase the effect of KORs in the NAc. These data suggest a role for KORs in the synaptic adaptations that occur in dependence [6].

Exercise and the Mesolimbic Dopamine System

There is strong evidence that aerobic exercise is a beneficial adjunct to current pharmacological and psychological treatment protocols. Exercise has been shown to produce a series of changes

with relevance to the mesolimbic system. Aerobic exercise, similar to acute ethanol consumption, has been shown to increase levels of tyrosine hydroxylase, the rate limiting enzyme in DA synthesis, in the NAc [9, 10] (Macrae 1987). It has also been associated with burst activation of DA neurons in the VTA [11](Wang and Tsien 2011). Further, 6-weeks of voluntary wheel running in rats increased D2 auto receptor density in the NAc [10]; a modification that has been associated with increased risk of addictive behavior [12-14]. However, exercise has been shown to increase D2R density in the dorsal striatum in a mouse model of Parkinson's disease [15]. Though the majority of evidence suggests an ameliorative role for exercise [16, 17], there is intriguing evidence suggesting that excessive levels of exercise can potentiate addiction [18, 19]. Currently, the causes of these outcome discrepancies has not been shown. However, as there is very little consistency in methodology, type, intensity or duration of treatment protocols, disparate recommendations might be to blame. Evidence for opioid receptor changes with exercise is less concrete, appears to be highly region dependent [20], and is lacking in the mesolimbic system. To our knowledge, no one has directly measured changes in KORs in the ventral striatum in the context of exercise and ethanol. In this study we hypothesize that voluntary wheel-running will down-regulate KORs in the NAc. We further predict that exercise will block ethanol-induced sensitization of KORs and reduce alcohol consumption in chronically exposed mice.

Material and Methods

Animals

Male C57BL/6J and DBA/2J mice (Jackson Labs; aged 6-12 weeks) were given *ad libitum* access to food and water, and were maintained on a reverse 12:12-h light/dark cycle (lights on at 15:00 h). Mice were randomly assigned to one of three cohorts, ethanol without exercise, ethanol with exercise and saline with exercise. All mice were injected BID with ethanol (2.5g/kg; 16% w/v; IP) or an equivalent volume of saline for 14 days. Exercise groups were given *ad libitum* access to a running wheel. Intoxication was visually verified with loss of consciousness which decreased visually with dependence. All protocols and animal care procedures were in accordance with the National Institutes of Health Guide for the Care and Use of Laboratory Animals and approved by the Brigham Young University Institutional Animal Care and Use Committee. All efforts were made to minimize animal suffering and number of animals used in the present study.

Brain Slice Preparation

Isoflurane (Patterson Veterinary, Devens, MA) anesthetized mice were sacrificed by decapitation and brains were rapidly removed and transferred into ice-cold, pre-oxygenated (95% O₂/5% CO₂) artificial cerebral spinal fluid (aCSF) consisting of (in mM): NaCl (126), KCl (2.5), NaH₂PO₄ (1.2), CaCl₂ (2.4), MgCl₂ (1.2), NaHCO₃ (25), glucose (11), L-ascorbic acid (0.4), pH adjusted to 7.4. Tissue was sectioned into 400 µm-thick coronal slices containing the striatum with a vibrating tissue slicer (Leica VT1000S, Vashaw Scientific, Norcross, GA). Brain slices were placed in a submersion recording chamber, and perfused at 1 ml/min at 32 °C with oxygenated aCSF.

Fast Scan Cyclic Voltammetry

Fast scan cyclic voltammetry (voltammetry) recordings of dopamine signals were performed and analyzed using Demon Voltammetry and Analysis Software [Demon Voltammetry and Analysis;

21]. The carbon fiber electrode (7 μm X ~150 μm) potential was linearly scanned as a triangular waveform from -0.4 to 1.2 V and back to -0.4 V (Ag vs Ag/Cl) at a scan rate of 400 V/s. Cyclic voltammograms were recorded at the carbon fiber electrode every 100 msec by means of a potentiostat (Dagan Corporation, Minneapolis, MN). Dopamine release was evoked every 2 min through a bipolar stimulating electrode 2. For input/output experiments examining baseline dopamine signals across increasing current stimulations, single pulse baseline dopamine signals were collected (4 ms, 350 μA) until signals were stable for across 3 collections. Baseline single pulse responses were measured followed by concentration response for U50488 at 0.3 μM and 1 μM followed by a reversal dose of 1 μM nor-BNI; all drugs were bath applied. Each response was gathered from single-pulse stimulations given 2 min apart before introduction of the next drug concentration.

Preparation of Brain Slices for Imaging and Confocal Microscopy

Mice were anesthetized using isoflurane and underwent transcardial perfusion with 4% paraformaldehyde (PFA). Once perfused, brains were carefully removed and placed in 4% PFA for 24 hrs to facilitate continued fixation. After incubation in PFA, brains were placed in a solution of 30% sucrose in 1X PBS until the density of the brain matched that of the solution and the brains dropped to the bottom of the vial (~24-48 hrs). Brains were then flash frozen in dry ice and mounted on a cold microtome stage. Targeting the VTA and NAc, brains were sliced at 30 μm on the microtome and slices were placed in cryoprotectant (30% ethylene glycol, 30% sucrose, 0.00002% sodium azide, in 0.1 M PB) and kept at -20°C until staining. Slices were washed 3 times in 1x PBS for 10 minutes on a rotator. They were then blocked with a blocking buffer comprised of 4% normal goat serum, 0.1% Triton-X 100 and 1x PBS. Slices were then washed another 3

times in 0.2% PBST on a rotator. Primary antibodies were applied and allowed to incubate for 20 hours. Following staining the slices were washed 3 times in 0.2% PBST and secondary antibodies were applied. After a 2 hr incubation period they were washed another 3 times with 0.2% PBST and once with 1x PBS. Antibodies included Mouse anti-tyrosine hydroxylase (Novus, 1:1328), and Rabbit anti-KOR (LifeSpan, 1:200) as well as secondaries Alexa Fluor 405 Donkey Anti-Sheep from (1:900), Alexa Fluor 594 Goat anti-Rabbit (1:500). To mount slides, sections were placed on microscope slides and dried ~5 min. Once dried, a drop of vectashield (Vector Laboratories) was placed on the tissue, and a cover slip was placed on the slide. Slides set overnight, and then they were kept at 4°C until imaging. An Olympus FluoView FV1000 confocal microscope was used to image mounted slices. Brain slices were mounted on microscope slides and imaged under oil immersion at 40X. To ensure consistent readings between samples, a constant photomultiplier tube voltage and gain were set between all acquired images.

Statistical Analysis

For FSCV, evoked recordings were normalized to the established baseline within subjects and then averaged across subjects in corresponding time intervals. Comparisons were made using a Dunnett's analysis. All statistical tests were performed in JMP13 (SAS, Cary, NC). Figures were compiled using IGOR Pro Software (Wavemetrics, Lake Oswego, OR).

For brain slice imaging, images were loaded into FIJI software. Images were duplicated to preserve the original settings while color thresholding and brightness contrast adjustments were made to determine the location of cells and create ROIs. ROIs were then projected back onto the unedited images where area and mean intensity were recorded for each channel. This process was

performed by three independent raters blinded to the hypothesis. To determine relative density of KORs, the ratio of mean fluorescence to area was determined.

Results

KOR effects on Dopamine Release in the Context of Exercise and Ethanol

Dopamine release was measured in each experimental group to measure changes in KOR activity with application of U50488, a KOR agonist and reversal with nor-BNI, a KOR antagonist. Significant differences were noted between the three groups at the 0.3 uM dose of U50488 ($F_{(2,12)} = 20.4619$, $p=0.0001$; **Fig. 5.1**). The ethanol no exercise group dropped to 81.4% (± 4.1) of baseline while the ethanol with exercise group only dropped to 94.5% (± 2.0). Conversely, the saline with exercise group increased evoked release to 108.3% (± 4.2) ($n=5$ in all groups; $p=0.0228$ between Eth no Ex and Eth with Ex; $p<0.0001$ between Eth no Ex and Sal with Ex; $p=0.0166$ between Eth with Ex and Sal with Ex). When 1 uM U50488 was given the differences between groups increased significantly ($F_{(2,12)} = 22.9751$, $p<0.0001$). The ethanol no exercise group dropped to 70.1% (± 2.1) of baseline and the ethanol with exercise dropped to 84.7% (± 3.8). The saline with exercise remained generally unresponsive at 98.9% (± 5.1) ($p=0.0127$ between Eth no Ex and Eth with Ex; $p<0.0001$ between Eth no Ex and Sal with Ex; $p=0.0150$ between Eth with Ex and Sal with Ex). Reversal with 1uM nor-BNI brought the ethanol no exercise, ethanol with exercise and saline with exercise groups back to 100.2% (± 5.5), 92.0% (± 4.5) and 99.7% (± 4.0) respectively. There were no significant differences between these groups. This suggests that exercise desensitizes KORs and blunts ethanol-induced sensitization of the receptors.

Immunohistochemical Analysis of KORs in the NAc and VTA

Brain slices were acquired from each of the three groups in order to analyze expression patterns of KORs in the NAc and VTA. Following analysis, significant differences were noted in average MFI of KOR expressing cells in the NAc between the three groups ($F_{(2,3162)} = 353.7626$, $p < 0.0001$; **Fig. 5.2A-C and G**). Average mean fluorescent intensity (MFI) of KOR expressing cells in the ethanol no exercise group was $7.08 (\pm 0.085)$ while the ethanol with exercise group was $3.52 (\pm 0.125)$. The saline with exercise group MFI was $3.77 (\pm 0.11)$. Notably the ethanol with exercise group expressed an MFI similar to that of saline with exercise while both were significantly different from the ethanol no exercise group ($n=6$ animals per group with 6 slices analyzed per animal with multiple cells measured per slice; $p < 0.0001$ between Eth no Ex and Eth with Ex; $p < 0.0001$ between Eth no Ex and Sal with Ex; $p = 0.4787$ between Eth with Ex and Sal with Ex). Expression patterns in the VTA followed the same trends as those in the NAc ($F_{(2,1766)} = 49.3301$, $p < 0.0001$; **Fig. 5.2D-F and H**). The ethanol no exercise group was $5.46 (\pm 0.15)$ and the MFI of the ethanol with exercise was $3.84 (\pm 0.16)$. The saline with exercise remained closely tied to the other exercise group at $3.57 (\pm 0.14)$ (n =same as in NAc; $p < 0.0001$ between Eth no Ex and Eth with Ex; $p < 0.0001$ between Eth no Ex and Sal with Ex; $p = 0.4046$ between Eth with Ex and Sal with Ex). These findings indicate that exercise is sufficient to block ethanol-induced increased expression of KORs in both the NAc and the VTA.

Effects of Exercise and Ethanol on Drink-in-the-Dark Behavior

To assess exercise and ethanol effects on drinking behavior, drinking was measured on 4 consecutive days. Significant differences were noted between the composite average of all groups for all days ($F_{(2,43)} = 11.2596$, $p = 0.0001$; **Fig. 5.3B**). The ethanol no exercise group drank on average $1.05\text{g} (\pm 0.063)$ while the ethanol with exercise group drank $0.747\text{g} (\pm 0.098)$.

Interestingly, the saline with exercise group drank more than either with an average consumption of 1.37g (± 0.089) (Eth no Ex n=6, Eth and Ex n=3, Sal and Ex n=3; $p=0.0323$ between Eth no Ex and Eth with Ex; $p=0.0124$ between Eth no Ex and Sal with Ex; $p<0.0001$ between Eth with Ex and Sal with Ex). Ethanol consumption by day was significantly different only on days two and three. On day two the ethanol with exercise and saline with exercise groups averaged 0.672g (± 0.16) and 1.51g (± 0.13) respectively ($p=0.009$; **Fig. 5.3A**). On day three the ethanol with exercise and saline with exercise groups averaged 0.575g (± 0.14) and 1.52g (± 0.14) respectively ($p=0.0035$) while the ethanol no exercise group average 0.986g (± 0.10) which was significantly different from the saline with exercise group ($p=0.0382$; **Fig. 5.3B**) Exercise significantly reduces ethanol consumption in chronically exposed mice.

Discussion

In this study, KOR expression patterns were studied in the presence of ethanol and exercise to better understand the role of exercise in the natural reward pathways. Chronic ethanol exposure increases sensitivity of KORs while downregulating MORs and DORs in the NAc [22, 23]. We have shown that activation of peripheral mechanoreceptors, potentially similar to what occurs in consistent aerobic exercise, increases translocation of DORs to cellular membranes in the NAc potentially in opposition to what occurs in after chronic ethanol exposure. Mechanosensory input mediated through the dorsal column medial lemniscal pathway, provides collateral enervation, outside the canonical somatosensory pathways that terminate in the somatosensory cortex. These collaterals have been shown to alter neuron firing rate in the VTA [24] and influence neurotransmitter release and DOR expression in the NAc. In this context we can properly examine

the neurological effects of exercise in reference to their influence on the reward circuitry. Here we find that voluntary exercise alone is sufficient to produce a reduction in KOR sensitivity to U50488, a selective receptor agonist. It is important to note that mice in their natural habitat are accustomed to consistent daily exercise and it is possible that reduction in sensitivity and expression we report is actually the more normal state that a wild mouse would express and that the abnormally sedentary lifestyle of a laboratory mouse produces alterations in KOR expression due to lack of regular exercise. Regardless, it is evident that exercise directly influences the expression of KORs in both the VTA and NAc. Additionally, exercise is capable of blunting some of the increased expression of these receptors that normally accompanies chronic ethanol exposure.

We anticipated that because of these receptor changes that exercise would produce a reduction in drinking behavior in ethanol exposed but exercised mice and certainly in saline exposed and exercised mice. Indeed, exercise reduced drinking in chronically exposed mice. However, to our surprise, saline treated mice exposed to exercise exhibited increased drinking behavior. It has been reported that excessive levels of exercise carry the potential for dependence [18, 19] though no mechanistic explanations has been proven. The dichotomous findings suggesting both that exercise might be an effective adjunctive treatment for AUD while at the same time potentially increasing risk are unexplored. Further mechanistic investigations focusing on MORs and DORs in addition to KORs and the neurological circuits responsible for the mesolimbic effects of exercise are required to fully explain exercise's potential as an adjunctive treatment modality.

References

1. Sacks, J.J., et al., *2010 National and State Costs of Excessive Alcohol Consumption*. Am J Prev Med, 2015. **49**(5): p. e73-9.
2. Spanagel, R., A. Herz, and T.S. Shippenberg, *Opposing tonically active endogenous opioid systems modulate the mesolimbic dopaminergic pathway*. Proc Natl Acad Sci U S A, 1992. **89**(6): p. 2046-50.
3. Mansour, A., et al., *Autoradiographic differentiation of mu, delta, and kappa opioid receptors in the rat forebrain and midbrain*. J Neurosci, 1987. **7**(8): p. 2445-64.
4. Mansour, A., et al., *Immunohistochemical localization of the cloned kappa 1 receptor in the rat CNS and pituitary*. Neuroscience, 1996. **71**(3): p. 671-90.
5. Mansour, A., et al., *Opioid-receptor mRNA expression in the rat CNS: anatomical and functional implications*. Trends Neurosci, 1995. **18**(1): p. 22-9.
6. Shippenberg, T.S., A. Zapata, and V.I. Chefer, *Dynorphin and the pathophysiology of drug addiction*. Pharmacol Ther, 2007. **116**(2): p. 306-21.
7. Sirohi, S., G. Bakalkin, and B.M. Walker, *Alcohol-induced plasticity in the dynorphin/kappa-opioid receptor system*. Front Mol Neurosci, 2012. **5**: p. 95.
8. Walker, B.M. and G.F. Koob, *Pharmacological evidence for a motivational role of kappa-opioid systems in ethanol dependence*. Neuropsychopharmacology, 2008. **33**(3): p. 643-52.
9. Droste, S.K., et al., *Long-term voluntary exercise and the mouse hypothalamic-pituitary-adrenocortical axis: impact of concurrent treatment with the antidepressant drug tianeptine*. J Neuroendocrinol, 2006. **18**(12): p. 915-25.
10. Greenwood, B.N., et al., *Long-term voluntary wheel running is rewarding and produces plasticity in the mesolimbic reward pathway*. Behav Brain Res, 2011. **217**(2): p. 354-62.
11. Wang, S.S., et al., *[The influence of L-glutamate and carbachol on burst firing of dopaminergic neurons in ventral tegmental area]*. Sheng Li Xue Bao, 2011. **63**(1): p. 25-30.
12. Martinez, D., et al., *Cocaine dependence and d2 receptor availability in the functional subdivisions of the striatum: relationship with cocaine-seeking behavior*. Neuropsychopharmacology, 2004. **29**(6): p. 1190-202.
13. Morgan, D., et al., *Social dominance in monkeys: dopamine D2 receptors and cocaine self-administration*. Nat Neurosci, 2002. **5**(2): p. 169-74.
14. Voisey, J., et al., *A DRD2 and ANKK1 haplotype is associated with nicotine dependence*. Psychiatry Res, 2012. **196**(2-3): p. 285-9.
15. Vuckovic, M.G., et al., *Exercise elevates dopamine D2 receptor in a mouse model of Parkinson's disease: in vivo imaging with [(1)(8)F]fallypride*. Mov Disord, 2010. **25**(16): p. 2777-84.
16. Wang, D., et al., *Impact of physical exercise on substance use disorders: a meta-analysis*. PLoS One, 2014. **9**(10): p. e110728.
17. Lipowski, M., M. Szulc, and L. Bulinski, *Physical activity among other health-related behaviors in treatment of alcoholism*. J Sports Med Phys Fitness, 2015. **55**(3): p. 231-40.
18. Piazza-Gardner, A.K. and A.E. Barry, *Examining physical activity levels and alcohol consumption: are people who drink more active?* Am J Health Promot, 2012. **26**(3): p. e95-104.
19. Dakwar, E., et al., *Exercise and Mental Illness: Results From the National Epidemiologic Survey on Alcohol and Related Conditions (NESARC)*. Journal of Clinical Psychiatry, 2012. **73**(7): p. 960-966.
20. Arida, R.M., et al., *Differential effects of exercise on brain opioid receptor binding and activation in rats*. J Neurochem, 2015. **132**(2): p. 206-17.

21. Yorgason, J.T., R.A. Espana, and S.R. Jones, *Demon voltammetry and analysis software: analysis of cocaine-induced alterations in dopamine signaling using multiple kinetic measures*. J Neurosci Methods, 2011. **202**(2): p. 158-64.
22. Melchior, J.R. and S.R. Jones, *Chronic ethanol exposure increases inhibition of optically targeted phasic dopamine release in the nucleus accumbens core and medial shell ex vivo*. Mol Cell Neurosci, 2017. **85**: p. 93-104.
23. Hynes, M.D., et al., *Chronic ethanol alters the receptor binding characteristics of the delta opioid receptor ligand, D-Ala2-D-Leu5 enkephalin in mouse brain*. Life Sci, 1983. **33**(23): p. 2331-7.
24. Bills, K., Clarke, T., Major, G., Jacobson, C., Blotter, J., Feland, J., Steffensen, S, *Targeted Subcutaneous Vibration with Single-Neuron Electrophysiology as a Novel Method for Understanding the Central Effects of Peripheral Vibrational Therapy in a Dose Response*, 2019.

Figure Legends

Figure 5.1: Exercise blocks ethanol-induced sensitivity of KORs in the NAc

Note that at concentrations of 0.03 uM U50488 and 1.0 uM U50488 there were significant differences between all groups. Asterisks *** indicate significance levels $p < 0.001$, while ## indicates $p < 0.01$.

Figure 5.2: Exercise alters ethanol-induced KOR expression in the NAc and VTA

(A-C) Representative images of KOR staining in the NAc demonstrating receptor expression differences, KORs are red. (D-F) Same as A-C but in the VTA. (G,H) Group MFI data in the NAc and VTA respectively, demonstrating that exercise decreases KOR expression in both brain regions. Asterisks *** indicate significance levels $p < 0.001$

Figure 5.3: Exercise decreases drinking in dependent but not naïve mice

(A) Time course data demonstrating per day consumption between experimental groups. (B) Group showing composite drinking from all days. Note that all groups showed significant differences. Asterisks * and *** indicate significance levels $p < 0.05$ and 0.001

Figures

Figure 5.1

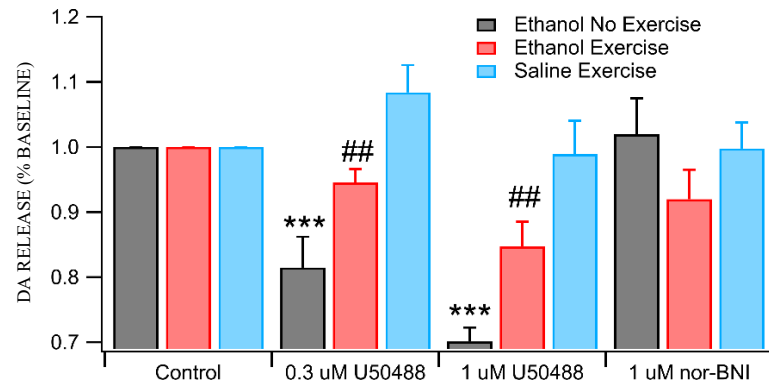


Figure 5.2

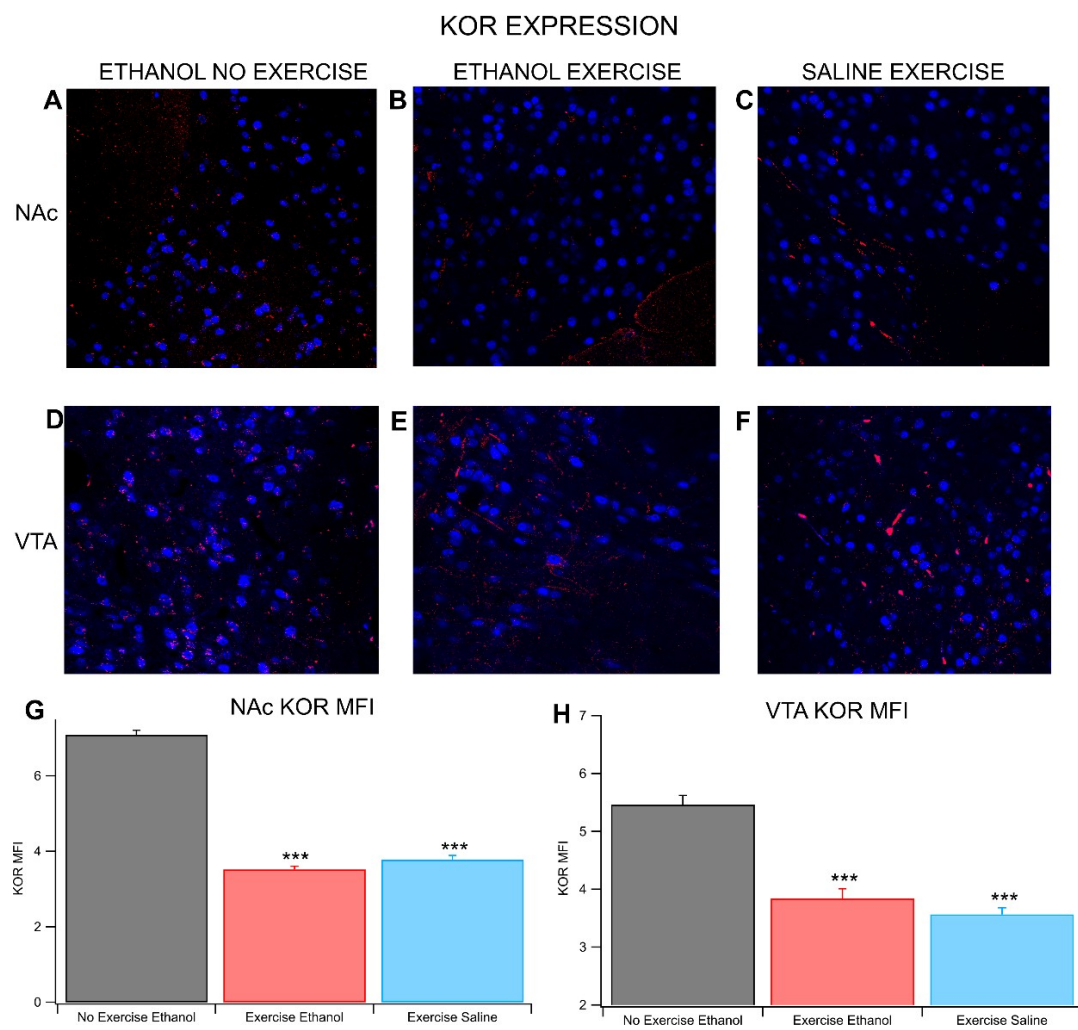
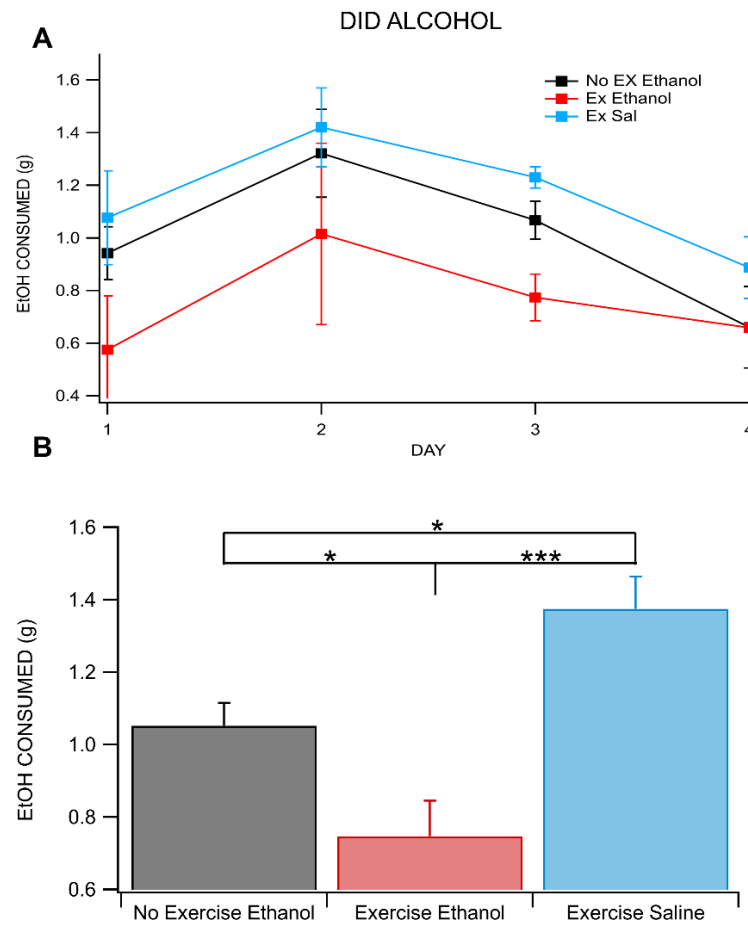


Figure 5.3



CHAPTER 6: Discussion and Conclusions

Somatosensory Pathways Involved in Acupuncture-mediated Alterations to Mesolimbic Structures

For millennia, mechanistic explanations of acupuncture's purported effects have centered on alterations to the balance of energy, or qi, meridians. These explanations have proven difficult to reconcile with modern neuroscientific investigative techniques and advances which have increasingly been used to explore the mechanistic underpinnings of an established body of positive outcome data. Acupuncture in the treatment of drug-use disorders has been an area of increasing western interest over the last decade. This interest has included hitherto unknown explanations of its neurological effects at the cellular level. Mechanoacupuncture (MA) at the HT7 acupoint, located medial to the flexor carpi ulnaris tendon at the wrist, has been shown to reduce VTA GABA neuron firing rate and decrease ethanol consumption (Yang et al., 2010). Further, the effects were shown to be mediated by delta opioid receptors (DORs) and initially driven by the dorsal column medial lemniscal pathway through the nucleus cuneatus, thalamus, and lateral habenula, not the spinothalamic tract, en route to altering firing rate in the VTA (Chang et al., 2017). This preliminary work set a foundational understanding essential to demystifying irrefutably positive outcome data that has been prejudicially discounted for generations in the West. Further, they provided a potentially unifying insight into common neurologically mechanistic explanation for the efficacy of manual therapeutics more generally; these include chiropractic medicine, physical therapy, etc...). More broadly we can refer to these disciplines as mechanoreceptor-based therapeutics. In light of these discoveries, this non-exhaustive body of work represents an attempt to further clarify, through mechanism and outcome, the potential of mechanoreceptor-based therapies to play a role in the treatment of drug-use disorders.

Mechanoreceptor Activation as the Primary Driver of Mesolimbic Alterations without Mechanoacupuncture

To determine the role of mechanoreceptors as the primary mediators of the mesolimbic responses noted, a novel technique was needed to selectively activate peripheral mechanoreceptors at a site distinct from HT7. We tested implantation of small vibrating motors next to the C7-T1 vertebrae, at the laminae (**Chapter 2**) as a means of providing direct stimulation to the DCML. These tests were successful in reducing VTA GABA neuron firing purely through mechanical stimulation (MStim), without MA. This method also represents a breakthrough in the studying of peripheral mechanoreceptor-based therapies. Previously, only direct mechanistic data from the peripheral nervous system or indirect measures of central nervous system effects had been reported.

Specificity of Effects relate to Mechanoreceptor Density and Type

Acupuncture stimulation at the wrist (HT7) or MStim at the cervical spine both represent areas of high mechanoreceptor density. In order to determine the importance of mechanoreceptors generally, we first tested the effects of MStim to an area relatively low in receptors density, the mid-thigh. We found that an 80 HZ (120 sec) MStim to the belly of the biceps femoris muscle was insufficient when compared to the effects noted by stimulation of the cervical spine at the same intensity and duration (**Fig 3.2A**).

Because different subtypes of mechanoreceptors respond to different frequencies of stimulation. Three frequencies were chosen to target specific mechanoreceptors and each was tested for 60 and 120 sec of stimulation. Of those chosen, 45 Hz enlists mostly Meissner's corpuscles (Macefield, 2005; Fleming and Luo, 2013), while 115 Hz is more selective for Pacinian corpuscles (Zelena, 1978; Biswas et al., 2015). Both receptors are subcutaneously located. The frequency of 80 Hz lies between the two and likely activates both receptors. Additionally, all

three frequencies can activate Ruffini endings and Golgi tendon organs, two receptors that are morphologically similar to one another and are important as joint mechanoreceptors (Vega et al., 1996; Albuerne et al., 2000; Vega et al., 2009). The 50 and 80 Hz MStim produced a transient depression of GABA neurons in the VTA, with 80 Hz (120 sec) producing the largest and longest lasting effect. The 115 Hz stimulation failed to achieve VTA GABA neuron effects (**Fig. 3.1**). These data suggest that the effects of the MStim are likely mediated through Meissner's corpuscles, Merkel cells and Ruffini endings rather than Pacinian corpuscles. Further simultaneous recordings from VTA DA neurons revealed that DA neuron firing increases, following MStim, transiently for an average of 500 sec. This time course is inversely mirrored by the described VTA GABA neuron depression. This is suggestive that the DA neuron firing is due to disinhibition from GABAergic input locally in the VTA. More experiments are required to fully determine the peripheral mechanoreceptors responsible for the described effects. One potential method of exploration could include the use of the ChR2-*Venus* (ChR2V+) transgenic rat line for optogenetic stimulation studies (National BioResource Project). The ChR2V+ line uses the Thy 1.2 promotor to express the channelrhodopsin-2 (ChR2) transgene in myelinated dorsal root ganglion neurons (Tomita et al., 2009; Honjoh et al., 2014). This line has been shown to express ChR2 specifically in large diameter proprioceptive neurons, mainly Merkel Cells and Meissner's corpuscles, rather than small diameter, nociceptive neurons (Ji et al., 2012). This is essential in the targeting of the DCML pathway and not the lateral spinothalamic tract. These neurons will then be selectively stimulated with transcutaneous light. To date, optogenetic stimulation has never been used to study mechanosensory modalities.

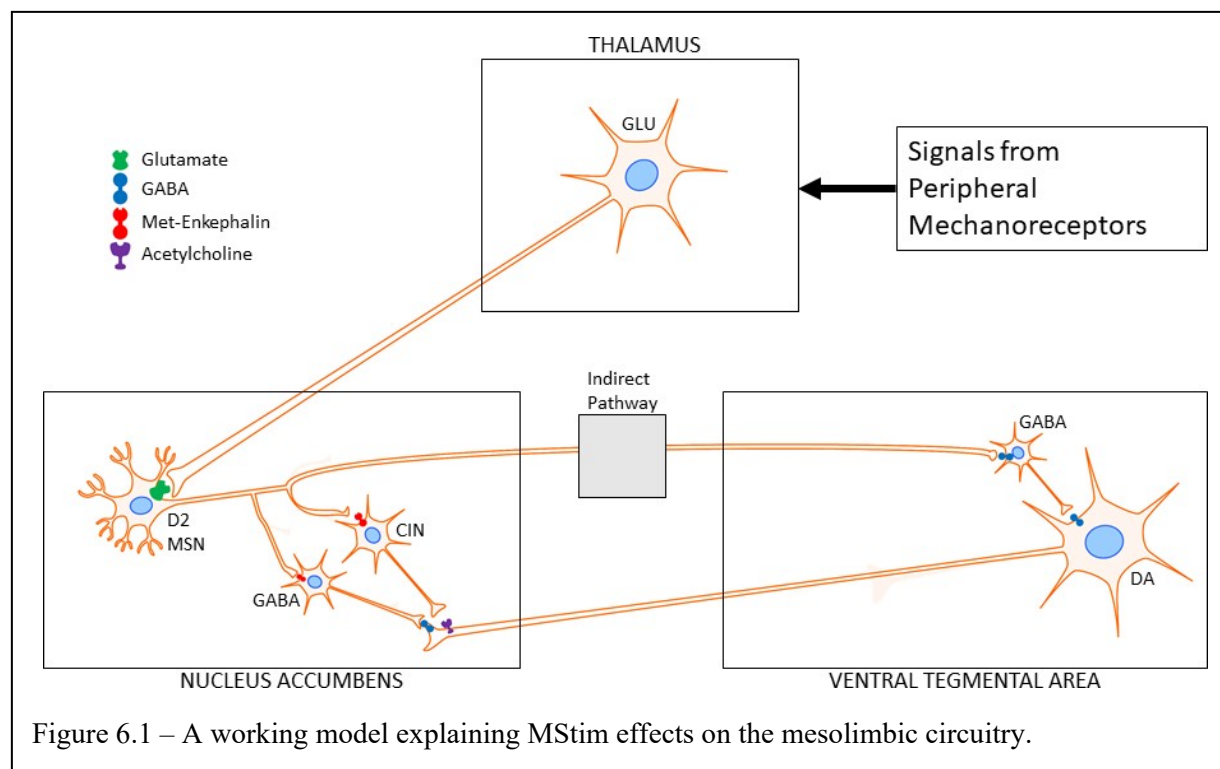
MStim Effects on NAc DA Levels are Locally Mediated by DORs and Acetylcholine Release

Increased firing from VTA DA neurons, in the context of drug-abuse disorders, is most relevant if it translates to increase DA release in the NAc. We performed microdialysis experiments to measure changes in DA release following MStim. We anticipated that DA levels would demonstrate a sharp increase immediately following the treatment and then return to baseline. We were surprised to find that not only did MStim increase DA levels, the increase peaked at 60 min post-stimulation and didn't return to baseline 120 min post-stimulation. These disparate effects in DA neuron firing and DA release were suggestive of two different etiologies. We found that MStim-induced increases in NAc DA levels can be blocked by antagonizing DORs in the NAc but not the VTA. Additionally, blockage of nicotinic and muscarinic acetylcholine receptors in the NAc also blocks DA increases (**Fig. 3.6**). Delta opioid receptors are located on local and projecting GABA neurons and cholinergic interneurons (CINs) in the NAc. Cholinergic interneuron activity increases DA release by activation of nicotinic receptors located on DA terminals. Activation of DORs in the NAc have been shown to increase DA and we show that MStim increases translocation of DOR to cell membranes in the NAc. Two theories could explain the DOR dependent increase of DA by MStim. First, increased release could be through disinhibition of CINs and DA terminals, both of which receive GABAergic input that is DOR dependent. Second, it is possible that direct activation of DORs on CINs could cause increased firing even though DORs are known to be G_i coupled GPCRs. This could occur through increased I_h or hyperpolarization currents which produce increased burst firing of CINs. To better isolate the role of disinhibition of DA terminals via GABA neuron inactivation versus increased I_h firing of CINs we could perform loose patch electrophysiological experiments on CINs in the presence of DPDPE, a DOR agonist in the genetically modified VGAT-CRE mouse strain. This strain marks VGAT expressing cells like GABA neurons with

CRE which would allow us to virally inactivate them without effecting the CINs. This would allow us to isolate the CINs and their specific responses to DOR activation and determine if burst firing occurs. Further, exploration with fast-scan cyclic voltammetry would allow us to measure evoked DA release response to DOR activation without the interference of DOR expressing GABA neurons. These experiments would allow us to more fully understand the interplay between DORs on CINs and those on GABA neurons in the MStim-induced DA increases.

A Working Model of MStim Effects in the Mesolimbic Circuitry

We developed a working model of a proposed mechanism by which MStim effects the VTA and NAc (**Fig. 6.1**). We propose that signals from peripheral mechanoreceptors are transduced through the DCML to the VPL thalamus. From there signals pass to the lateral habenula which sends glutamatergic projections to the NAc. Glutamate receptors on D2 expressing medium spiny neurons (D2 MSNs) increase their activity. These D2 MSNs release



met-Enkephalin, an endogenous ligand to the DOR. They also project back to the VTA via the indirect pathway and ultimately inhibit firing of local VTA GABA neurons, which results in a transient inhibition of VTA DA neuron firing. The importance of this NAc to VTA projection was verified by local lidocaine injection into the NAc; it blocked MStim-induced depression of VTA GABA neuron firing. Local NAc collaterals from D2 MSNs activate DORs on local GABA interneurons which cause CIN and DA terminal disinhibition; both of which result in increased DA release. Several important factors remain unknown in this process. The effects of mechanoacupuncture have been shown to be glutamate dependent in the NAc (Kim et al., 2018). The precise origin of these fibers is not known. This could be determined experimentally using dual single unit recording. One potential target for these studies is the rhomboid nucleus of the thalamus. It contains efferent projections that enervate the NAc and the other limbic structure (Vertes et al., 2006). These studies would provide direct evidence that neurons in the thalamus fire in tandem with neurons in the NAc or in the VTA.

MStim Blockage of Markers of Chronic Ethanol Dependence

Normally, a reinstatement dose of ethanol after 24 hours of withdrawal in the dependent animal will not cause a depression in VTA GABA neuron firing rate. This demonstrates the desensitization that occurs because a naïve animal will show a massive decrease in the presence of ethanol. Animals received MStim, via whole-body vibration at 80 HZ for 15 min BID, reacted to reinstatement ethanol in a manner that more closely resembles a saline treated animal (**Chapter 5**). Further, behavioral measures of dependence are largely mitigated with the addition of MStim to the process of dependence. Several possible explanations exist for this observed phenomenon. First, chronic ethanol has been shown to decrease DOR affinity in the NAc. We have shown that MStim significantly increases translocation of DORs to cellular membranes in

the NAc 2 hours post-MStim. These competing effects could be responsible for the protective influence of MStim over the normal adaptations resultant from chronic ethanol exposure. To further understand how MStim blocks measures of dependence after chronic ethanol exposure more study will be required. Evidence suggests that kappa opioid receptors (KORs) and mu opioid receptors (MORs) are important in chronic ethanol-induced mesolimbic adaptations with KORs increasing expression and MOR decreasing expression after chronic ethanol exposure. Both KORs and MORs need to be studied to determine if MStim alters their expression. Immunohistochemistry analysis of their expression patterns after MStim and colocalization with tyrosine hydroxylase and D2 receptors would help us isolate expression patterns on DA terminals, GABA neurons and CINs in the NAc.

Exercise and Ethanol Dependence

In chapter 5 we demonstrate that voluntary wheel running is sufficient to alter expression of KORs in the NAc and the VTA and their influence on evoked DA release in the NAc. These changes hold after chronic ethanol exposure. Further, ethanol drinking behavior was substantially reduced with exercise. Paradoxically, exercise without chronic ethanol increased drinking behavior even while decreasing expression of KORs, opposite to the effect elicited by chronic ethanol. It is noted that previous studies have reported conflicting results related to exercise as a treatment for drug-use disorders. Some reporting positively and some even showing potentiation of the condition (Ehringer et al., 2009; Berczik et al., 2012; Wang et al., 2014; Leasure et al., 2015). The direct connection between exercise and MStim is unknown. Interestingly, no one has ever published a direct mechanistic explanation of how exercise exerts its effects on the mesolimbic system. It remains unstudied whether these effects are mediated by cardiovascular means or in a more neurologically direct pathway similar to MStim. However,

logically, exercise activates mechanoreceptors. To date, no has reported real-time changes in neuron firing in connection with exercise. Such studies could be performed with an anesthetized rat whose head is stereotactically stationary being placed on a treadmill. Natural reflexive responses would allow the rat to engage in treadmill running while electrophysiological measurements of neurons are taken. Additionally, these results could be compared to changes induced by passive motion of limbs versus pharmacological cardiovascular stress testing. Obviously, DOR and MOR changes with exercise would provide needed mechanistic understanding as well. Finally, intensity of exercise could be a major player in the explanation of disparate outcomes related to exercise as a treatment modality (Ni et al., 2012).

Conclusions and Future Directions

Mechanical stimulation holds great promise as an adjunctive treatment approach during acute medical detox, residential and outpatient addiction recovery programs. The non-pharmacological ability to alter GABA firing rate in the VTA and increase local DA release in the NAc is an astounding finding that warrants more exploration. Because of the high level of safety associated with this type of therapy, it holds the potential to provide a step forward in light of the low levels of efficacy of current treatment approaches. It creates the possibility to collaborations with alternative health-care providers including doctors of chiropractic, acupuncture and physical therapy. Future studies should continue to explore the mechanistic science behind MStim effects including, thalamic to NAc connections and the involvement of MORs and KORs. Future testing should also include testing in animals that have become dependent before MStim has been introduced to test its efficacy as a recovery modality. Obviously, translational studies in humans are required to test these effects in the human population. Optimal durations and frequency of treatments must to be explored to maximize

changes to the neuronal substrates discussed and to maximally alter behavioral outcomes. It is hoped that this work will lay a foundation to for a new treatment to improve outcomes for those struggling to overcome drug-use disorders.

References

- Albuérne M, De Lavallina J, Esteban I, Naves FJ, Silos-Santiago I, Vega JA (2000) Development of Meissner-like and Pacinian sensory corpuscles in the mouse demonstrated with specific markers for corpuscular constituents. *Anat Rec* 258:235-242.
- Berczik K, Szabo A, Griffiths MD, Kurimay T, Kun B, Urban R, Demetrovics Z (2012) Exercise addiction: symptoms, diagnosis, epidemiology, and etiology. *Subst Use Misuse* 47:403-417.
- Biswas A, Manivannan M, Srinivasan MA (2015) Vibrotactile sensitivity threshold: nonlinear stochastic mechanotransduction model of the Pacinian Corpuscle. *IEEE Trans Haptics* 8:102-113.
- Chang S, Ryu Y, Gwak YS, Kim NJ, Kim JM, Lee JY, Kim SA, Lee BH, Steffensen SC, Jang EY, Yang CH, Kim HY (2017) Spinal pathways involved in somatosensory inhibition of the psychomotor actions of cocaine. *Sci Rep* 7:5359.
- Ehringer MA, Hoft NR, Zunhammer M (2009) Reduced alcohol consumption in mice with access to a running wheel. *Alcohol* 43:443-452.
- Fleming MS, Luo W (2013) The anatomy, function, and development of mammalian Abeta low-threshold mechanoreceptors. *Front Biol (Beijing)* 8.

- Honjoh T, Ji ZG, Yokoyama Y, Sumiyoshi A, Shibuya Y, Matsuzaka Y, Kawashima R, Mushiake H, Ishizuka T, Yawo H (2014) Optogenetic patterning of whisker-barrel cortical system in transgenic rat expressing channelrhodopsin-2. *PLoS One* 9:e93706.
- Ji ZG, Ito S, Honjoh T, Ohta H, Ishizuka T, Fukazawa Y, Yawo H (2012) Light-evoked somatosensory perception of transgenic rats that express channelrhodopsin-2 in dorsal root ganglion cells. *PLoS One* 7:e32699.
- Kim NJ, Ryu Y, Lee BH, Chang S, Fan Y, Gwak YS, Yang CH, Bills KB, Steffensen SC, Koo JS, Jang EY, Kim HY (2018) Acupuncture inhibition of methamphetamine-induced behaviors, dopamine release and hyperthermia in the nucleus accumbens: mediation of group II mGluR. *Addict Biol*.
- Leasure JL, Neighbors C, Henderson CE, Young CM (2015) Exercise and Alcohol Consumption: What We Know, What We Need to Know, and Why it is Important. *Front Psychiatry* 6:156.
- Macefield VG (2005) Physiological characteristics of low-threshold mechanoreceptors in joints, muscle and skin in human subjects. *Clin Exp Pharmacol Physiol* 32:135-144.
- Ni GX, Lei L, Zhou YZ (2012) Intensity-dependent effect of treadmill running on lubricin metabolism of rat articular cartilage. *Arthritis Res Ther* 14:R256.
- Tomita H, Sugano E, Fukazawa Y, Isago H, Sugiyama Y, Hiroi T, Ishizuka T, Mushiake H, Kato M, Hirabayashi M, Shigemoto R, Yawo H, Tamai M (2009) Visual properties of transgenic rats harboring the channelrhodopsin-2 gene regulated by the thy-1.2 promoter. *PLoS One* 4:e7679.
- Vega JA, Haro JJ, Del Valle ME (1996) Immunohistochemistry of human cutaneous Meissner and pacinian corpuscles. *Microsc Res Tech* 34:351-361.

- Vega JA, Garcia-Suarez O, Montano JA, Pardo B, Cobo JM (2009) The Meissner and Pacinian sensory corpuscles revisited new data from the last decade. *Microsc Res Tech* 72:299-309.
- Vertes RP, Hoover WB, Do Valle AC, Sherman A, Rodriguez JJ (2006) Efferent projections of reuniens and rhomboid nuclei of the thalamus in the rat. *J Comp Neurol* 499:768-796.
- Wang D, Wang Y, Wang Y, Li R, Zhou C (2014) Impact of physical exercise on substance use disorders: a meta-analysis. *PLoS One* 9:e110728.
- Yang CH, Yoon SS, Hansen DM, Wilcox JD, Blumell BR, Park JJ, Steffensen SC (2010) Acupuncture inhibits GABA neuron activity in the ventral tegmental area and reduces ethanol self-administration. *Alcohol Clin Exp Res* 34:2137-2146.
- Zelena J (1978) The development of Pacinian corpuscles. *J Neurocytol* 7:71-91.

Kyle Bills, DC, IDE, QME, MUA – *Curriculum Vitae*

Education

Brigham Young University
Ph.D. Candidate – Neuroscience
2016-2019

Parker University
DC - Doctor of Chiropractic
Summa Cum Laude
Salutatorian
2009

Brigham Young University
BS - Exercise Science
Magna Cum Laude
2005

Licensures

State of California
License to practice Chiropractic
2009 – current

State of Utah
License to practice Chiropractic Medicine
2016 – current

State of California
Radiology operator and supervisor License
Licensed to perform diagnostic radiographs and supervise licensed radiology technicians
2011 – current

Publications

Bills KB, Clarke T, Major G, Blotter J, Feland B, Steffensen S, Targeted subcutaneous vibration with single-neuron electrophysiology as a novel method for understanding the central effects of peripheral vibrational therapy in a rodent model. *Dose Response* (2019) doi:10.1177/1559325818825172

Kim, N.J., Ryu, Y., Lee, B.H., Chang, S., Fan, Y, Gwak, Y.S., Yang, C.H., **Bills, K.B.**, Steffensen, S.C., Koo, J.S., Kim, H.Y. Acupuncture inhibition of methamphetamine-induced behaviors, dopamine release and hyperthermia in the nucleus accumbens: mediation of group II mGluR. *Addiction Biology* (2018) doi: 10.1111/adb.12587. PMID: 29363229

Bills, KB, Steffensen, SC, Neuroscience 101: Understanding Opioid Addiction and how Chiropractic Can Help, *Dynamic Chiropractic* (2019) February (Volume 37, Issue 02, Page 44)

Lee BH, Yang CH, Kim HY, Jang EY, Chang S, Kim NJ, Ryu Y, Fan Y, Gwak Y, **Bills KB**, Steffensen S, Acupuncture at HT7 Inhibits Reinforcing Effects of Methamphetamine. *Journal of Acupuncture and Meridian Studies* (2018) doi:10.1016/j.jams.2018.08.059

Bills, K.B., Payne, A., Steffensen, S.C. Teaching Neuroscience through landmark primary literature: Novel method of teaching synaptic transmission. *Journal of Undergraduate Neuroscience* (2019) submitted.

Yorgason JT, Hedges D, Obray JD, **Bills KB**, Woodbury M, Williams B, Torres D, Bellinger FP, Andres MA, and Steffensen SC, Methamphetamine increases nucleus accumbens dopamine release through intracellular and extracellular calcium dependent processes. *Neuropsychopharmacology* (2019) Submitted

Bills KB, Obray JD, Clarke T, Brundage J, Yang CH, Kim HY, Yorgason JT, Blotter J, Steffensen S, Mechanical stimulation of cervical vertebrae modulates the discharge activity of ventral tegmental area neurons and dopamine release in the nucleus accumbens. *Science Advances* (2019) Submitted

Abstracts

Bills K, Fong A, Brundage J, Steffensen S, Ketogenic Diet: Improves Residual Headaches in PCS Patients. 13th World Congress on Brain Injury (2019) Toronto, Canada

Bills K, Clarke T, Ney Z, Steffensen S, Peripheral mechanoreceptor activation modulates mesolimbic GABA and DA neurons and DA release in the NAc via delta opioid receptors. *Soc. Neurosci. Absts* 43 (2018) 418.09

Bills K, Payne A, Steffensen S, Teaching synaptic transmission using primary literature: a skills based approach to student engagement. *Soc. Neurosci. Absts* 43 (2018) 024.22SU

Payne A, **Bills K**, Steffensen S, An innovative approach to a neuroscience capstone learning experience. *Soc. Neurosci. Absts* 43 (2018) 024.23SU

Bills, K, Clarke, T, Steffensen, SC, Mechanisms and neuroanatomical pathway underlying acupuncture's effects on the mesolimbic circuitry. *Oriental Medicine and Acupuncture*. (2018) *Las Vegas, NV*.

Bills, K., Yorgason, J.T., McCarthy, S., Woodbury, M., and Steffensen, S.C. Exercise-induced down-regulation of D2 autoreceptors in the nucleus accumbens. *Soc. Neurosci. Absts* 42 (2017) 515.06

K. Bills, T. Clarke, J. Brundage, S.C. Steffensen "Peripheral mechanoreceptors mediate changes in mesolimbic GABA and DA neurons via activation of delta opioid receptors," Society for Neuroscience, Salt Lake City, Utah (2017)

J.T. Yorgason, S.S. Pistorius, **K. Bills**, S.C. Steffensen "Ethanol-mediated inhibition of ventral tegmental area gabaergic neurons, and involvement of connexin-36 mediated electrical coupling," Research Society on Alcoholism, Denver, CO (2017)

K. Bills, J.T. Yorgason, M. Woodbury, G. Major, S.C. Steffensen "D2 Receptor density increases on dopaminergic terminal in the nucleus accumbens with 6-weeks moderate intensity aerobic exercise," Mar Lou Fulton Conference, Brigham Young University, Provo, UT (2017)

J.T. Yorgason, S.S. Pistorius, **K. Bills**, S.C. Steffensen "Ethanol-mediated inhibition of ventral tegmental area gabaergic neurons, and involvement of connexin-36 mediated electrical coupling," Research Society on Alcoholism, Park City, UT (2016)

Presentations

“Mechanoreceptor-based therapeutics and their role in the treating drug-use disorders” Parker University, Dallas TX (2019)

“Vibratory stimulation of cervical vertebrae modulates the discharge activity of ventral tegmental area neurons and dopamine release in the nucleus accumbens,” ACC-RAC Baltimore, MD (2019)

“Mechanisms underlying acupuncture as an adjunctive treatment in drug-use disorders” International Oriental Medicine and Acupuncture, Las Vegas, NV (2018)

“Frequency dependent modulation of the mesolimbic system through peripheral mechanoreceptors,” Brigham Young University, (2018)

“Effects of Aerobic Exercise Intensity on Dopamine Release in the Nucleus Accumbens” Graduate Research Fair, Brigham Young University (2017)

“Changes in evoked dopamine release in the nucleus accumbens with moderate exercise” Grad Expo, Brigham Young University, Provo, UT (2017)

“Exercise induced down regulation of kappa opioid receptors in the nucleus accumbens” Grad Fad, Brigham Young University, Provo, UT (2017)

External Funding

PI: F32 PHS NIH NCCIH (AT009945)

Novel methods of acupuncture delivery in the treatment of drug-abuse disorders (2019-2022) Total 3 yrs = \$229,974

PI: NCMIC Post-doctoral Fellowship

Awarded to scholars the board believes can positively and substantially impact the future of chiropractic medicine through advances in research. (2016-2020) Total 4 yrs = \$20,000

PI: Activator Methods International

Research Equipment Grant – Activator V (2017) - \$2000

Internal Funding

BYU Interdisciplinary Research Grant

Marjorie Hinckley Endowed Chair Award - \$500

Grant to present research at the Society for Neuroscience 2017, Washington DC

Parker University

President's Scholarship - \$10,000

Highest scholarship awarded for academic attainment

Brigham Young University

Half or Full Academic Scholarship

All years of attendance

Patents

US Patent Application Number - 62/837,638

A device and method to induce interferential beat vibrations and frequencies into the body for treatment of pain, anxiety, depression, addiction, and sleep disorders

Pedagogical Experience

Teaching

Neuroscience 205 – Neurobiology
Brigham Young University – Winter 2017, Spring 2018, Winter 2019
Instructor of Record

Neuroscience 380 – Neuroanatomy
Brigham Young University – Winter 2018
Graduate Instructor

Physiology 363 – Advanced Physiology Lab
Brigham Young University – Winter 2017
Graduate Instructor

Courses Developed

Curriculum Redesign
Neuroscience 205 – Neurobiology and Physiology 363 – Advanced Physiology Lab
Brigham Young University

Functional Neurology in the Practice of Manual Medicine
InnerCalm and Associates, course for continuing medical education credits. This is a *web-based course* I was asked to develop as a distance learning tool for practicing physicians.
On-line Course Developer

Appointments

State of California
Qualified Medical Evaluator (QME) appointment
Designated to perform independent medical evaluations for the Department of Workers' Compensation Medical Unit. Purpose is to provide substantial medical evidence pertaining to injured workers that can be used by workers' compensation judges to determine outcomes.
2011 - current

State of California
Subject Matter Expert – Physical Medicine and Rehabilitation
Ask to consult for the ongoing improvement of the State of California Qualified Medical Evaluator certification exam.
2014 – current

Certifications and Boards

National Board of Chiropractic Examiners
General practice of chiropractic
2008 – Parts 1-4

National Board of Chiropractic Examiners
Physiotherapy
2008

Industrial Disability Evaluator (IDE) certification
50 hours in the use of the American Medical Associations Guide to the Rating of Permanent Impairment. Extensive time given to medical legal report writing techniques.
Dr. Jim Platto, DC, MPH

Manipulation Under Anesthesia (MUA)

Certification to perform manipulation assisted by general anesthesia.
Innercalm and Associates, Edward Cremata, DC, RN

Awards, Achievements, Associations

Ruth L. Kirchstein National Research Service Award
NIH - NCCIH - Post-Doctoral Fellow (2019-2022)

Research Presentation Award
Oriental Medicine and Acupuncture (2018)

Outstanding Research Presentation Award
GS Society - 2017

Parker University
Academic awards for achievement in anatomy and biochemistry
Top student in each series of classes

Parker University
James W. Parker Philosophy Award
“This award is given to one graduate, who, to an outstanding degree, has demonstrated the Parker principles of friendship, love of mankind, and the compassion to serve in the practice of chiropractic.” – Parker University

Parker University
Salutatorian

American Botanical Council
Member

Society for Neuroscience
Member

Positions Held

Brigham Young University
Post-Doctoral Fellow
Department of Psychology and Neuroscience
Sept 2019

The Migraine and Neurological Rehabilitation Center
Owner
2018 - current

Brigham Young University
Neuroscience Graduate Researcher
Scott Steffensen Lab
Aug 2016 - 2019

Christopher Place Healthcare Review
Medical Necessity Review Physician
Sep 2016 – Present

State of California
Subject Matter Expert – Physical Medicine and Rehabilitation
2014 - present

Restoration Chiropractic

Owner

Aug 2012 - 2019

Restoration Chiropractic

Seminar Instructor

Spinal and Extremity Adjusting

for students from Life West and Palmer West Chiropractic Colleges

Jan 2010 – 2019

Dallas VA Medical Center

Intern/Resident

Examination and Treatment of Patients

2008 - 2009

Alexander Chiropractic

Treating Physician

Jan 2009 - Aug 2012

Parker University Health Clinics

Intern

Examination and Treatment of Patients

Jan 2007 - Jun 2008

Brigham Young University

Dr. Bruce Woolley, PharmD

Teaching Assistant

Anatomy, Physiology, and Pharmacology

Jan 2004 – Dec 2004

Brigham Young University

Laboratory of Dr. Bruce Woolley, PharmD

Research Assistant

Nutraceutical protocols to maximize bone density in women of child-bearing years

Jan 2004 – Dec 2004